©[2012]

Edith Natalia Castro de Cruz

ALL RIGHTS RESERVED

Development and characterization of edible films based on cassava starch-glycerol blends to incorporate nutraceuticals

By

EDITH NATALIA CASTRO DE CRUZ

A thesis submitted to the

Graduate School-New Brunswick

Rutgers, The State University of New Jersey

in partial fulfillment of the requirements

for the degree of

Master of Science

Graduate Program in Food Science

Written under the direction of

Professor Paul Takhistov

And approved by

_____

_____

_____

_____

New Brunswick, New Jersey

January 2012

ABSTRACT OF THE THESIS

Development and characterization of edible films based on cassava starch-glycerol blends to incorporate nutraceuticals

EDITH NATALIA CASTRO DE CRUZ

Thesis Director: Prof. Paul Takhistov, Ph.D.

Edible films are thin layers made of materials such as starch and proteins. Starch is a polysaccharide that could be interesting in the edible film technology. An important starch source is cassava, produced abundantly, inexpensive, and is able to form films. However, for the production of edible film with good flexibility, a plasticizer such as glycerol is usually utilized and it can affect film physical properties. In addition, the current research on edible films is focused on the addition of active compounds that improve the food packaging and/or bring health benefits to consumers. One of those active compounds are nutraceuticals, diet supplements necessary for metabolism and to prevent diseases. Iron is one of the minerals that people do not consume in enough amounts and its deficiency may cause anemia. Therefore, the objectives of this research were: (1) Formulate a solution of cassava starch-glycerol that can effectively carry nutraceuticals into the matrix; and (2) Investigate the impacts of iron gluconate on properties and functionalities of the films.

Results obtained from gloss values, morphology and rheology of starch concentrations, it was determined that 3% cassava starch produced

homogeneous and transparent films. Also, the results obtained with the addition of glycerol exhibited increased the gelatinization temperature, gelatinization enthalpy, and drying time. The tensile strength decreased with the glycerol content and Elongation at break decreased between 0 to 20% glycerol. It appears that glycerol can exert an antiplasticizing effect because glycerol did not affect the extensibility of plasticized films when it is introduced at low levels. Data from moisture sorption isotherms found that the more appropriate models to fit the experimental data were GAB (R^2=0.85) and BET (R^2=0.9). Also, was detected the retrogradation of films during drying and films with glycerol needs the double of time to start retrogradation than films with no glycerol. Based on these results, the best formulation with good properties is 3% cassava and 30% glycerol.

Lastly, the results obtained with the incorporation of iron gluconate (IG) showed that apparent viscosity of solutions increased as IG concentration increased. Color of films were affected by IG, especially b* values due to its yellowish appearance. The GAB and BET model determined that allowed to determine the water adsorption values at the monolayer level (m_o), and all films with IG adsorbed less water than films with no IG. Also, the addition of IG increased tensile strength and elongation at break. From the release kinetics of IG, no definitive conclusion could be drawn concerning the dominating release mechanism. This study demonstrated the capability of cassava-glycerol blends to carry iron gluconate.

ACKNOWLEDGEMENTS

It is a pleasure to thank many people who in some way contributed to this thesis.

I would like to thank my advisor, Dr Paul Takhistov for his guidance and the opportunity to work in his Laboratory.

Also, I am grateful to Dr Kit., Dr K. Yam and Dr. M.V. Karwe, for serving on my thesis committee. Their suggestions and comments have enriched this work.

I wish to thank my student colleagues Marlena Brown, YangYang Jin, Phong T. Huynh, Abishek Sahay, Maha Alshehab and Duechao Yu for their support and continuous preoccupation in this thesis.

Of course I wish to say my family; Pa, Mami, Li, Marcia, Sebastian, and JJ thanks a lot for their enormous love and patience. I love you so much guys.

Additionally, I want to thank Solano Family for their kindness to give me a place in your family during the last part of this work.

Finally, my lovely husband, who inspired me all the time and taught me that, was a step in our life together. Te quiero mucho, Luki.

Table of Contents

Abstract of the thesis..... ii

Acknowledgments..... iv

Table of contents..... v

List of tables..... viii

List of figures..... ix

1 Introduction**.....1**

1.1 Food Packaging and classification.....2

1.2 Biopolymers for food packaging.....3

1.3 Definition of Edible films.....3

1.4 Sources of materials to manufacture edible films.....4

1.4.1 Proteins.....*5*

1.4.2 Lipids.....*5*

1.4.3 Polysaccharides.....*6*

1.4.4 Plasticizers.....*12*

1.4.5 Additives.....*13*

1.5 Film formation and drying process.....17

1.6 Characterization of film forming solutions.....18

1.6.1 Rheological measurements.....*18*

1.6.2 Drying Kinetics.....*20*

1.6.3 Raman Spectroscopy.....*21*

1.7 Characterization of films.....22

1.7.1 Physical Appearance of films 22

1.7.2 Water Sorption 24

1.7.3 Thermal properties 26

1.7.4 Mechanical Properties 27

1.8 Water – starch – plasticizer interactions using Flory-Huggins theory 28

1.9 In-vitro nutraceutical release kinetics 29

1.10 Research problem statements 30

1.11 Rationale 30

1.12 Objectives of the study 31

***2 Materials and methods* 33**

2.1 Materials 33

2.2 Methods 33

2.2.1 Film forming process and film casting 33

2.2.2 Characterization of film forming solutions 35

2.2.3 Characterization of films 38

***3 Results and Discussion* 45**

3.1 Characterization and formulation of cassava starch films with glycerol. .. 45

3.1.1 Rheology of film forming solutions 45

3.1.2 Comparison of time evolution of water loss of cassava starch solutions with different concentrations of glycerol 55

3.1.3 Conformational changes during drying of cassava starch solutions .. 59

3.1.4 Basic physical properties of stand alone films 63

3.1.5 Optical properties and morphology of films. 64

3.1.6 Sorption isotherms studies 67

3.1.7 Changes of thermal properties of cassava starch films with the addition of glycerol 73

3.1.8 Mechanical properties of cassava starch films 77

3.1.9 Interaction between water-starch-glycerol 81

3.1.10 Conclusion 84

3.2 Characterization of cassava starch films with glycerol enriched with Iron gluconate. 88

3.2.1 Effects of Iron gluconate in flow behavior of cassava starch films plasticized with glycerol 89

3.2.2 Film color and appearance 93

3.2.3 Water sorption 94

3.2.4 Thermal properties 97

3.2.5 Mechanical properties 99

3.2.6 IG release kinetics 100

3.2.7 Conclusion 102

4 General conclusion and recommendations 105

5 References 106

List of tables

Table No.	*Title*	*Page No.*
Table 1.1	*Dietary Reference Intakes (DRIs) for Iron*	*16*
Table 2.1	*Description of the parameters of drying kinetics of film forming solutions.*	*38*
Table 2.2.	*Relative humidity of saturated salt solutions at room.*	*40*
Table 3.1	*Comparison of different models for the flow behavior of cassava starch solutions with different concentrations and temperature*	*49*
Table 3.2	*Comparison of different models for the Rheology of cassava starch film forming solutions at different temperatures (35°C and 85°C), and glycerol content (0,10,20,30,40,50 g/100g of starch).*	*52*
Table 3.3	*Parameters obtained during constant drying rate for three different concentrations of glycerol in cassava starch films.*	*59*
Table 3.4	*Sorption isotherm model constants and confidence fit (R2) of cassava starch films (3%Cassava) with different glycerol contents.*	*70*
Table 3.5	*Flory-Huggins parameters to water-starch-glycerol*	*82*
Table 3.6	*Mass fraction of water, cassava starch and glycerol during drying process.*	*83*
Table 3.7	*Sorption isotherm model constants and confidence fit (R2) of cassava starch films (3%Cassava) with different iron contents.*	*96*
Table 3.8	*Mechanical properties of cassava-starch film incorporated with Iron gluconate*	*100*
Table 3.9	*Dissolution parameters for IG concentration between 40 and 100% IG*	*102*

List of Figures

Figure No.	*Title*	*Page No.*
Figure 1.1	*Schematic division of edible biopolymers.*	*6*
Figure 1.2	*Chemical structure of amylose and amylopectin.*	*9*
Figure 1.3 (A)	*Cassava tree.*	*12*
Figure 1.3 (B)	*Cassava root.*	*12*
Figure 1.3 (C)	*Cassava starch.*	*12*
Figure 1.4	*Structure of glycerol*	*13*
Figure 1.5	*Structure of iron gluconate dehydrate.*	*17*
Figure 1.6 (A)	*Typical Drying curve.*	*20*
Figure 1.6 (B)	*Typical Drying rate curve.*	*20*
Figure 1.7	*Water sorption isotherm*	*26*
Figure 2.1	*Film forming process and film casting.*	*34*
Figure 2.2	*Brookfield DV-III Ultra Rheometer with small adapter.*	*36*
Figure 2.3.	*DSC-7 Perkin-Elmer.*	*42*
Figure 2.4	*Texture Analyzer (TA-XT2) with tensile grips.*	*43*
Figure 3.1	*Apparent viscosity of 1, 2, 3 and 4% of cassava starch solutions at 35°C.*	*47*
Figure 3.2	*Apparent viscosity of 4% of cassava starch solutions at different temperatures (35, 45, 55, 65, 75, 85°C).*	*48*
Figure 3.3	*Apparent viscosity of 3% of cassava starch solutions with different glycerol content (0, 10, 20, 30, 40, 50 g/100 g of starch) at 35°C.*	*51*
Figure 3.4	*Effects of concentration and temperature on viscosity of cassava starch solutions with glycerol.*	*53*

Figure 3.5 *Effects of concentration and temperature on flow index of cassava starch solutions with glycerol.* *54*

Figure 3.6 *Drying time curve of cassava starch films with different concentrations of glycerol at 25°C. The dashed lines represent the constant drying rate trendline.* *56*

Figure 3.7 *Mass flux of water in cassava starch films with different amounts of glycerol during drying at room temperature.* *57*

Figure 3.8 *Series of Raman spectra taken after casting the cassava starch films with different glycerol contents.* *60*

Figure 3.9 *Raman band at 480 cm^{-1} for 0, 20 and 30% Glycerol with time (24 hours).* *62*

Figure 3.10 *Ternary Diagram of the Appearance of cassava starch films.* *64*

Figure 3.11 *Gloss values at 60° angle for films with different content of starch and glycerol.* *65*

Figure 3.12 *Stereomicroscopic images of unplasticized films with different cassava starch concentration.* *66*

Figure 3.13 *Stereomicroscopic images of plasticized films (3% Cassava w/w)with different glycerol concentration (0, 10, 20, 30, 40 g/100 g starch).* *66*

Figure 3.14 *Sorption Isotherms of cassava starch films without plasticizer as a function of relative humidity (RH).* *68*

Figure 3.15 *Moisture content of 3% cassava starch films as a function of glycerol content and relative humidity.* *69*

Figure 3.16 *Water activity as a function of Relative Humidity of the environment (different glycerol content)* *72*

Figure 3.17 *DSC thermogram for cassava starch films with different contents of glycerol.* *74*

Figure 3.18 *Starch gelatinization temperature and enthalpy for films with different glycerol concentrations (0-50%) Blue line*

(peak temperature) and Red line (Enthalpy). *77*

Figure 3.19 *Effect of starch concentration on tensile strength and elongation at break of films.* *78*

Figure 3.20 *Force Vs Distance curves of cassava starch films with different amount of glycerol.* *79*

Figure 3.21 *Effect of glycerol concentration on tensile strength and elongation at break of 3% cassava starch films.* *81*

Figure 3.22 *Plot of Gibbs free energy as a function of cassava composition* *83*

Figure 3.23 *Apparent viscosity of cassava starch solutions with different IG content (0, 20, 40, 60, 80, 100%) at 35°C.* *91*

Figure 3.24 *Evolution of apparent viscosity and flow index with Iron concentration. Blue line is the flow index and red line is the consistency index* *91*

Figure 3.25 *Effects of temperature on viscosity of cassava starch solutions with iron (0 and 100%).* *92*

Figure 3.26 *L*, a* and b* values of cassava films incorporated with Iron.* *94*

Figure 3.27 *Sorption isotherm of cassava starch films with different IG concentration. (0 to 100%)* *96*

Figure 3.28 *DSC thermograms of cassava-based films incorporated with Iron gluconate.* *97*

Figure 3.29 *Starch gelatinization temperature and enthalpy for films with different Iron gluconate (0-100%) Blue line (Peak temperature), Red line (Enthalpy)* *99*

Figure 3.30 *Iron gluconate release profile from cassava-glycerol films.* *101*

1 Introduction

Edible films and coatings have received special attention in recent years due to their advantages over synthetic films. The main advantage of edible films over traditional films that they are biodegradable and can be consumed with the packaged products. Consumer interest in convenience, food quality and health continue increase, every day food industry should find new challenges to overcome these facts, and edible films might be possible solutions to the industry. Consequently, there is a needed to find new materials and explore new techniques to develop edible films.

The biopolymer studied in this work to produce edible films was cassava starch. There is an important root crop in many tropical countries. It is considered a high nutritional food and one the most economical sources of energy; since carbohydrate yield is 40% greater than rice and 20% greater than in corn [1]. Argentina, Brazil and Thailand have been investigated the possible use of cassava starch to produce edible films. Nevertheless, in the U.S there is not much information about this topic. In the other hand, the actual interest in nutraceuticals, as natural components to prevent certain disease, has been gaining space in the public eye and the consumers press the industry to incorporate these elements to enhance nutritional value of foods. The nutraceutical studied in this project was iron. Iron is an essential mineral for

energy metabolism and structural component of many enzymes. Iron deficiency can cause anemia that is a global problem affecting the health, quality of life, and productivity of millions of people worldwide. Actually, there are a few investigations approaching the possibility to incorporate nutraceuticals in edible films. Therefore, there is a research gap to combine these two topics. Essentially, this project is focused in develop a formulation with cassava starch as film matrix and glycerol as plasticizer as a possible carrier of iron as nutraceutical.

1.1 Food Packaging and classification

Packaging is one of the most important processes to preserve the quality and safety of the food it contains from the time of manufacture to the time it is used by the consumer. An equally important function of packaging is to protect the product from physical, chemical, and biological damage [2]. To manufacture food and beverage packaging the materials most common used can be classified as follow: metal, glass, plastic, paper and cardboard. In the selection of suitable packaging materials for specific food is required to know the barrier properties of those. For instance, metal and glass packages are essentially impermeable to any gas and vapor. During the last 50 years, food industry has been using materials as polyethylene or copolymer based materials to come up with new packaging innovations to respond to consumer needs. All these major packaging materials are non-renewable products, with the exception of paper. Consequently, materials based on renewable resources have been found to avoid

problems concerning waste disposal [3]

1.2 Biopolymers for food packaging

Biopolymer based packaging is defined as packaging made from renewable resources of agriculture or marine origin. *Weber and Haugaard [3]* have suggested a division for biobased polymers based on their origin and productions that includes:

- Category 1: Natural extracted biopolymers from raw materials (e.g. starch, cellulose, protein, alginate);
- Category 2: Chemically synthesized polymers from biobased monomers (e.g. polylactic acid - PLA);
- Category 3: Microbial polymers (e.g. polyhydroxyalkanoates, polyhydroxybutyrates).

Within this context of packaging, edible films and coatings are considered biopolymers with biodegradable properties.

1.3 Definition of Edible films

Edible films generally can be defined as thin layers of edible material applied on foods, or between food components, by wrapping, brushing, immersing or spraying in order to control mass transfer, provide mechanical protection or add sensory appeal to food products *[4].* Films usually, consist of biopolymers able to provide mechanical strength to the stand-alone thin structure. Such films can be used as covers, wraps or separation layers. Edible films can carry food

ingredients; pharmaceuticals and agrochemicals in different forms (hard capsules, microcapsules, soluble strips, etc), providing active substances can be incorporated into film-forming materials. Such active substances are: antimicrobials, pharmaceuticals, bioactive nutraceuticals, antioxidants, flavors, and medical/biotechnology diagnostic agents [5]. Therefore some advantages [6] found for edible films over traditional packaging materials are:

- The films can be consumed directly with the packaged product representing ideal package for environment. Even if the films are not consumed, they could still contribute to the reduction of environmental pollution. The films are produced from renewable edible ingredients and therefore, are anticipated to degrade more rapidly than polymeric materials.
- The films can enhance the organoleptic properties or supplement the nutritional value of food, providing various components (flavors, colors, and nutraceuticals) that are incorporated to them.
- The films can be used at the surface or internal layers of foods to control the diffusion rate of preservative substances (antioxidants or antimicrobials) from the surface to the interior of the food and prevent the moisture loss.

1.4 Sources of materials to manufacture edible films

Edible films are a mixture of a high molecular weight polymer, solvent and a plasticizer. Edible films and coatings are produced from edible biopolymers and

food-grade additives. These materials could be classified in three categories: proteins, polysaccharides, and lipids (Figure 1.1). During manufacturing, film materials must be dispersed and dissolved in a solvent such as water, alcohol or mixture of water and alcohol or a mixture of other solvents. Plasticizers and other additives are combined with the biopolymers solutions to modify the physical properties or functionality of films. The choice of what material is better to get the precise edible film depends on the characteristic of the product, storage conditions and protection.

1.4.1 Proteins

Proteins for edible films can be derived from animal or plant sources. Protein materials derived from animal sources include collagen, gelatin, fish myofibrillar protein, keratin, egg white protein, caseins and whey protein. Protein materials derived form plant sources included corn Zein, wheat gluten, soy protein, and cottonseed protein. Advantages of protein films include good oxygen, aroma and oil barriers films at low to intermediate relative humidity.

1.4.2 Lipids

Because lipid and resin materials are not polymer, they do not generally form cohesive stand-alone films. However, lipids give desirable gloss to food products and provide the best moisture barrier, these are used in composite films supported by a protein or polysaccharide matrix *[5].* Edible lipids include: beeswax, candelilla wax, carnauba wax, triglycerides, acetylated monoglycerides, fatty acids, shellac and terpene resin.

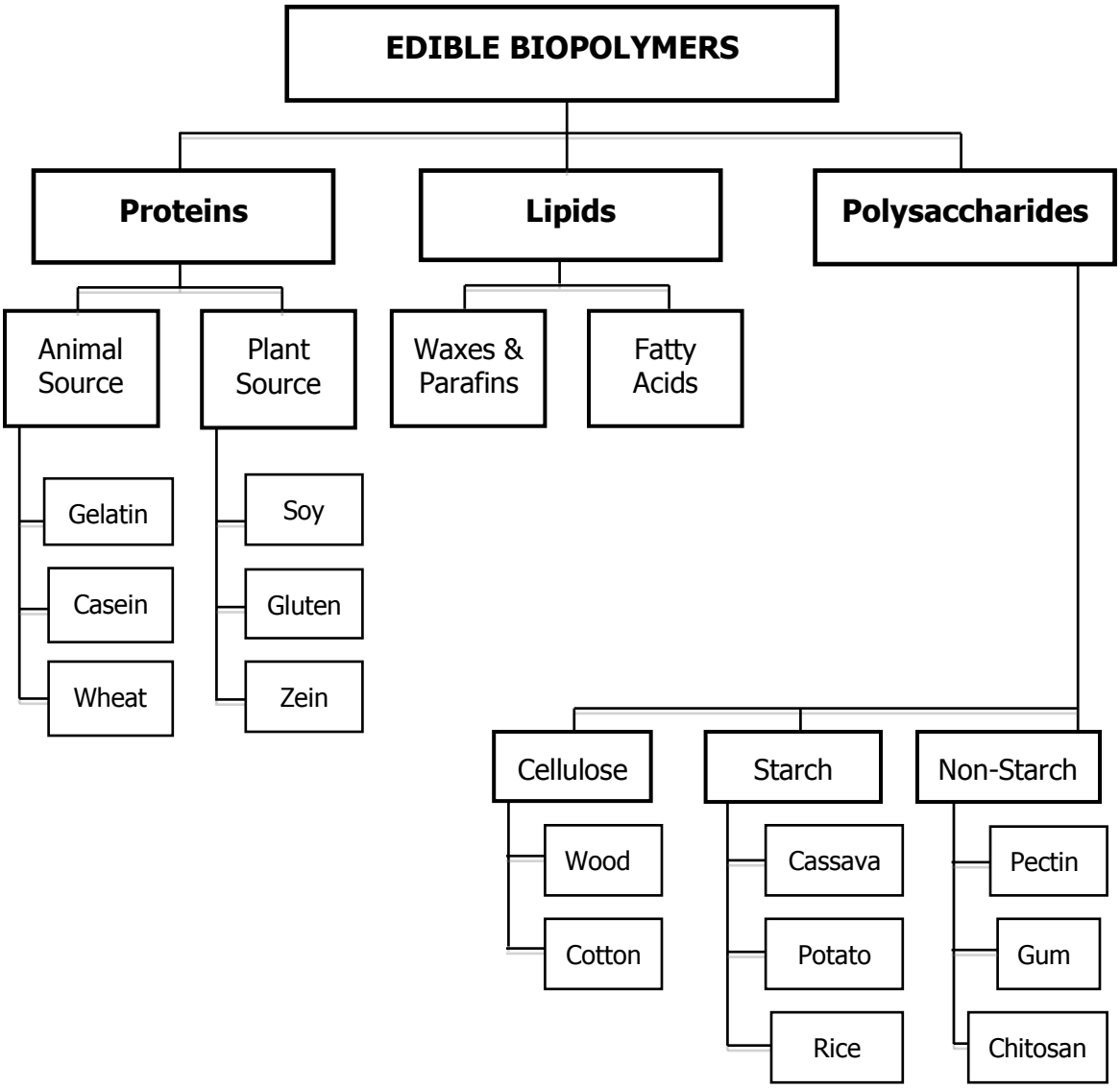


Figure 1.1 Schematic division of edible biopolymers [7]

1.4.3 Polysaccharides

Polysaccharides used for edible films include cellulose derivatives, non-starch materials and starch materials. The sequence of polysaccharides is simple compared to proteins, which have 20 common amino acids. However, the conformation of polysaccharide structure is more complicated and unpredictable,

resulting in much larger molecular weights than proteins *[5].* Polysaccharides are generally very hydrophilic resulting in poor water vapor and gas barrier properties. Although coatings by polysaccharide polymers may not provide a good water vapor barrier, these coatings can act as sacrificing agents retarding moisture loss from food products *[8]*.

1.4.3.1 Cellulose derivatives

Cellulose is composed of repeating D-glucose units linked together by ß(1-4) glucosidic bonds with methyl, hydroxypropyl or carboxyl substituents. The commons cellulose derivatives used to manufacture edible films are: Carboxymethylcellulose (CMC), Methylcellulose (MC), Hydroxypropyl methylcellulose (HPMC) and Hydroxypropyl cellulose (HPC). CMC, MC, HPMC, and HPC film possess good film-forming characteristic; films are generally odorless and tasteless, flexible and are of moderate strength, transparent, resistance to oil and fats, water-soluble, moderate to moisture and oxygen transmission *[9]*.

1.4.3.2 Non-Starch Materials

Non-starch polysaccharides are obtained from a variety of sources, such as seaweed extracts (Agar, Alginate, Carragenans), microbial gums (Arabic, Locust bean, Xanthan, Pullulan), tissue extracts (Chitin and Chitosan), and Pectins.

1.4.3.3 Starch Materials

Starch is a naturally occurring polymer that is inexpensive and abundantly available. It is the main storage of carbohydrate in most plants and is also widely consumed polysaccharide in the human diet. Depending on the botanical source, starch is formed in different parts of the plant, e.g., grain, tuber or root. Native starch, which occurs in a granular form, is one of the main carbohydrate resources found in cereal and tuber plants, such as maize and potato, respectively. The largest source of starch is corn with other commonly used sources being wheat, potato, cassava and rice.

The main components of starch are linear amylose and highly branched amylopectin composed of glucose units via α(1-4) bonds[10]. Amylopectin contains also 2–4% branching points [11] formed by α (1-6) bonds on the main backbone and other branches *[10]* (Figure 1.2).

Amylose and amylopectin do not exist free in nature, but as components of discrete, semicrystalline aggregates called starch granules *[12]*. Starch granules contain growth rings composed of semi-crystalline and amorphous zones *[13]*. In semi-crystalline zones amylopectin forms lamellar structure consisting of crystalline, ordered double helical structures and rigid amorphous branching zones *[14]*. Some of the amylose may be a part of these amylopectin double helices *[15]*. Amorphous zones in starch granules are composed of random ordered amylose and amylopectin structures [13].

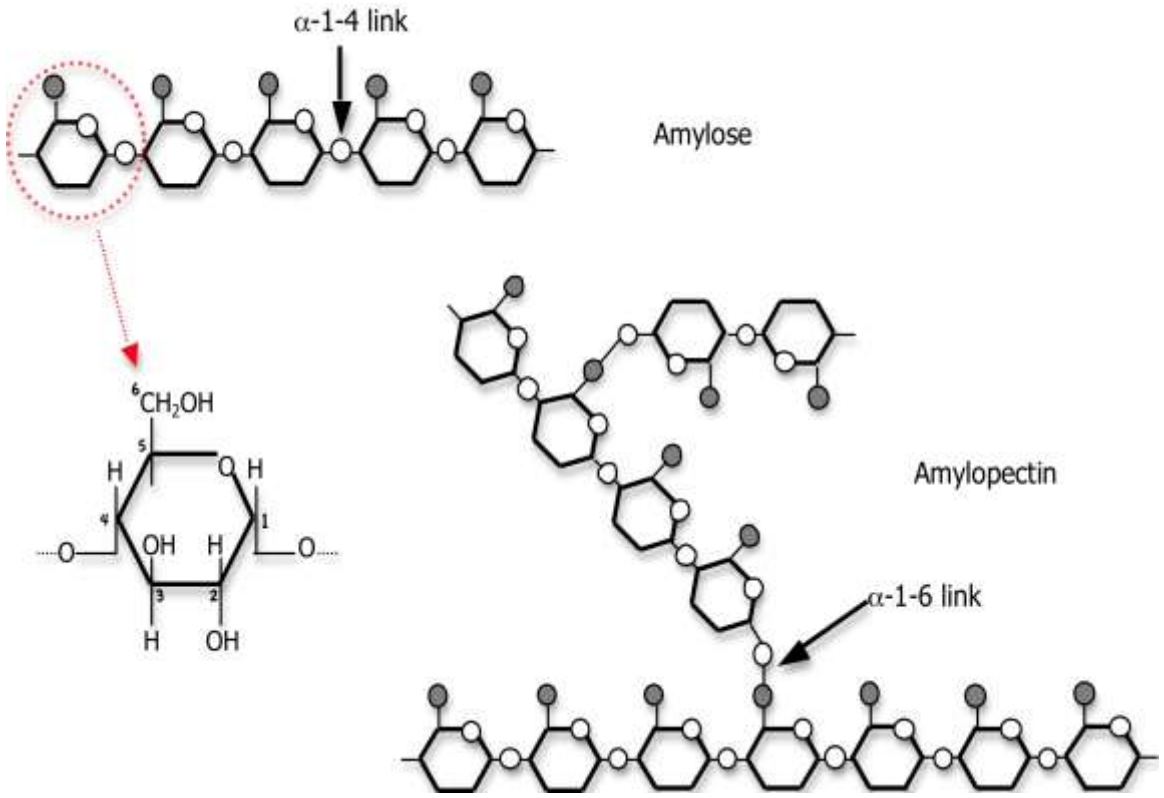


Figure 1.2 Chemical structure of amylose and amylopectin.

Gelatinization

Starch granules are insoluble in cold water. When this is heated in excess of water starch granules swell and the ordered structure is disrupted at gelatinization temperature resulting in an increase in viscosity *[16]*. This gelatinization temperature is more appropriately as a relatively narrow temperature range rather than one specific temperature *[12]*. In the gelatinization process agitation or mixing is needed to maximize amylose and

amylopectin leaching into water. From a mechanistic perspective, swelling of the granule results from water adsorption in the amorphous region of the starch granule where hydrogen bonds are less numerous and the polymer chains are more susceptible to dissolution *[17]*. When the swelling of the granule increases more amorphous regions come available for water adsorption followed by disruption of ordered structures. As heating continues the system increases the viscosity and the medium is completely pasted. Starch gelatinization is needed to obtain the starch gel, macromolecular network structure, which is formed during cooling of gelatinized starch.

Retrogradation

Starch retrogradation is a process, which occurs when starch chains begin to reassociate in an ordered structure *[12]*. In its initial phase, there is a formation of the double helical chain segments of amylose, which form helix-helix aggregates. This process can be seen upon cooling. In the other hand amylopectin molecules need more time to reassociate and form hydrogen bonds. With time, the starch paste becomes an opaque gel.

Cassava starch

Cassava (Manihot esculenta Crantz) is a perennial plant cultivated and growing for the populations in the humid tropics (Figure 1.3). To the people in these areas is a main staple food due to its high energy content and low cost.

According to the United Nations Food and Agriculture Organization *(FAO),* cassava ranks fourth as a food crop in the developing countries, after rice, maize and wheat.

Cassava is one of the most important tropical root crops. Recently Brazil , Paraguay and parts of Central America have been considered the countries of origin for cassava [18]. But according to other reports lowlands of Southern Mexico, Guatemala, Honduras, Venezuela and Colombia are also believed to be the place of the origin *[19]*. Cassava was a staple food to pre-Columbian indigenous in the Americas. In the 16^{th} century the conquistadores introduced this crop in Africa and in the 17^{th} century was introduced in India. In 2000, the production of cassava reaches 172 million tones produced worldwide. Africa accounted for 54%, Asia for 28% and Latin America for 19% of the total world production. The largest producer of cassava is Brazil and the main exporter is Thailand. *[20]*.

Cassava is mainly utilized as human food in the countries where it is cultivated and constitutes the major staple food of more than 300 million people. Cassava roots are incorporated into the human diet in several forms (fresh, fermented, flour and starch) Due to the diversity of countries where it is used cassava has received other names such as Mandioca and Aipim in Brazil; Yuca in Colombia and Tapioca as starch extracted from the root.



(A) (B) (C)

Figure 1.3 (A) Cassava tree, (B) Cassava root, (C) Cassava starch

1.4.4 Plasticizers

Polysaccharides films are often brittle and stiff due to extensive interactions between polymer chains through hydrogen bonding, electrostatic forces, and hydrophilic bonding. Plasticizers increase the free volume of polymer structures or the molecular mobility of polymer molecules. The result of plasticizer addition is a reduction in polymer chain-to-chain interactions, a lowering of the biopolymer glass transition temperature, and an improvement in film flexibility (lowering of film elastic modulus). Also, film elongation (stretchiness or ductility) increases, and film strength decreases *[5]*.

Mostly the addition of low molecular weight and non-volatile compounds is a common practice making edible films. Also, water is a very good plasticizer, but it can easily be lost by dehydration at a low relative humidity *[21]*. But addition of chemical plasticizers, such as monosaccharides, oligosaccharides, lipids, and polyols, to films can reduce water loss through dehydration, increase the amount of bound water and maintain a high water activity.

Glycerol

Glycerol (1,2,3-propanetriol, figure 1.4) is a colorless, odorless, viscous liquid with a sweet taste, low toxicity and is used in food and pharmaceuticals formulations. Glycerol is also called glycerine and glycerin referring to a commercial solution of glycerol in water. Glycerol is one of the most versatile and valuable chemicals substances known, with diverse uses and applications.

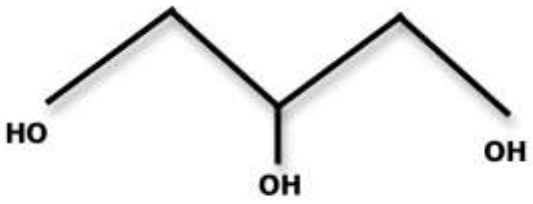


Figure 1.4 Structure of glycerol

Glycerol is one of the most popular plasticizers used in filmmaking techniques, due to stability and compatibility with hydrophilic biopolymeric packaging chain *[22].* Glycerol has three hydrophilic hydroxyl groups that are responsible for its solubility in water and its hygroscopic nature.

1.4.5 Additives

The new generation of edible films and coatings is being especially designed to increase theirs functionalities by incorporating natural or chemical antimicrobial agents, antioxidants, enzymes or functional ingredients such as probiotics, and nutraceuticals *[23]*. Edible films can enhance the nutritional value

of foods by carrying basic nutrients and / or nutraceuticals in its matrix. Antimicrobial and antioxidants compounds provide protection to food products prevent microbial spoilage, oxidation and improving food safety. Colors, flavors and aromas improve visual perception and taste of food products.

Nutraceuticals

Nutraceuticals are diet supplements that deliver a concentrated form of a presumed bioactive agent from a food, presented in a non-food matrix, and used with the purpose of enhancing health in dosages that exceed those that could be obtained from normal foods *[24]*. Nutraceuticals are sold in presentations similar to drugs: pills, extracts, tablets, etc. These can be grouped into the following three broad categories *[25]*:

- Substances with established nutritional functions, such as vitamins, minerals, amino acids and fatty acids - *Nutrients*
- Herbs or botanical products as concentrates and extracts - *Herbals*
- Reagents derived from other sources (*e.g.* pyruvate, chondroitin sulphate, steroid hormone precursors) serving specific functions, such as sports nutrition, weight-loss supplements and meal replacements – *Dietary supplements*.

Nutrients play significant roles in the human body to prevent certain diseases and these may be obtained from different food products. But with

the change of dietary habits, consumption of vegetables, fruits, whole grains, milk and milk products and seafood is lower than recommended. The most recent Dietary Reference Intake (DRI) of some nutrients is low enough to be of public health concern in the United States. These nutrients include: potassium, dietary fiber, calcium, and vitamin D. In addition, intake of iron, folate, and vitamin B12 is of concern for specific population groups (pregnant women and individuals ages 50 years and older) *[26].*

Iron

Iron is an essential component of virtually all-living cells, and it certainly is a necessity for all human cells [27].Iron is involved in energy metabolism as an oxygen carrier in hemoglobin, and structural component of a large number of enzymes covering wide array of diverse metabolic functions. The Daily Reference Intake (DRI) for iron is show in the Table 1.1.

For women, the average DRI for iron is 15 milligrams per day, 5 milligrams more than DRI for men. Women need more of this mineral because they lose an average of 15 to 20 mg of iron each month during menstruation. Animal products such as meat, fish and poultry are good sources of iron. An additionally, another sources of iron are: peas and beans, spinach and other green leafy vegetables and potatoes, those are called non-heme sources.

Table 1.1. Dietary Reference Intakes (DRIs) for Iron:

Life Stage Group	Iron (mg/day)
Children	
0-6 mo	0.27
6- 12 mo	11
1-3 y	7
4-8 y	10
Males	
9-13 y	8
14-18 y`	11
19-30 y	8
31-50 y	8
51-70 y	8
>70 y	8
Females	
9-13 y	8
14-18 y	15
19-30 y	18
31-50 y	18
51-70 y	8
>70 y	8
Pregnancy	
14-18 y	27
19-30 y	27
31-50 y	27

(Food and Nutrition Board, Institute of Medicine, National Academies)

Without enough iron, iron deficiency anemia can develop, and cause symptoms that include headaches, pallor and fatigue. Iron deficiency is a global problem affecting the health, quality of life, and productivity of millions of people worldwide. It is the most prevalent micronutrient deficiency impacting particularly on the health of infants, children and women childbearing age, especially during pregnancy. Despite the widespread impact of this condition,

little progress is being made towards effective prevention and control *[28]*. To surpass this problem existing many nutrient supplements and among the most common forms used are ferrous fumarate, ferrous gluconate, and ferrous sulphate.

Iron (II) gluconate is a fine yellowish-gray powder having a slight odor of burned sugar. One gram dissolves in about 10mL of water in slight heating. Iron gluconate has GRAS status and is used such as color additive and dietary supplement. Figure 1.5 shows the structure of Iron gluconate.

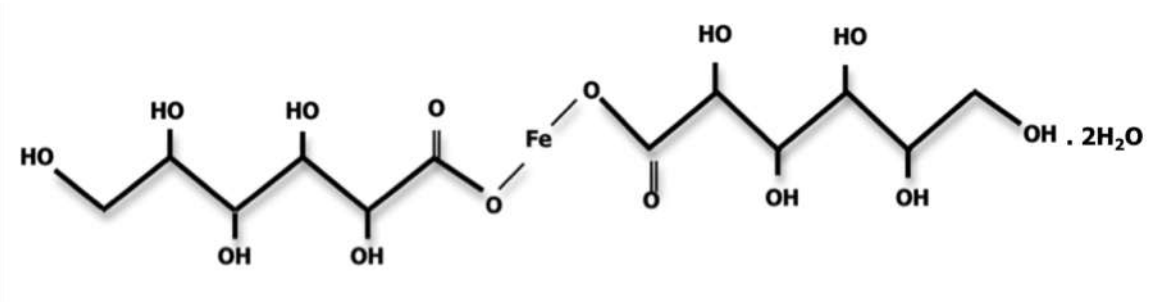


Figure 1.5 Structure of iron gluconate dehydrate.

1.5 Film formation and drying process

There are various film forming processes such as spraying, casting, thermo-molding and extrusion. The casting process is the most used techniques to form edible films. Usually, heating with solvent is needed to disrupt the native structure of biopolymers to obtain a film forming solution. The next step is the addition of Plasticizer to the film forming solution, at a convenient stage of the process, to obtain flexible and elastic films. A film forming solution is cast on a non-adhesive surface (plastic, metal, glass or Teflon). Water or solvent is

evaporated from the solution, generally in a ventilated oven during several hours to obtain a stand-alone film. Environmental properties, such as temperature and air relative humidity, during the evaporation stage could be used to control some of the film properties *[29]*.

1.6 Characterization of film forming solutions

1.6.1 Rheological measurements

Viscosity is the measure of fluids ability to resist flow. The more viscous a solution is the more force it will take to push the fluid and the more energy required to flow the material. Isaac Newton defined viscosity with the next equation

$$\frac{F}{A} = \eta \frac{dv}{dx} \qquad (1)$$

Where F/A indicates the force per unit area required to produce the shearing action, dv/dx indicates the velocity gradient at which the intermediate layers of fluid are moving with respect each other, and η is a constant for a given material called viscosity. Based on this principle there are two types of fluids, Newtonian and Non-Newtonian. Newtonian fluids show a constant viscosity over a whole range of shear rate (following Newton equation). Examples of Newtonian fluids are water, glycerol, alcohol, oil, etc. Non-Newtonian fluids are defined as flows that do not show a constant viscosity when the shear rate is variable. These fluids include solutions with high density like honey and solutions with polymers like starch solutions. Therefore viscosity is a

valuable tool for material characterization and processing. However, there are other important factors, which can affect the viscosity of a fluid. Those are:

Concentration

The rheological properties of dilute solutions are different from those of concentrated ones. For example, increasing the concentration of a polymer component in a solution will increase the viscosity. At low concentrations, molecules are sufficiently far apart in solution and viscosity is approximately linearly related to concentration. At a critical concentration, starch molecules entangled by overlapping and interpenetrating into each other and this behavior restricts the fluidity of starch and increases viscosity *[12]*.

Temperature

Temperature can have pronounced effects on the viscosity of a fluid. Often when materials are heated the result is a decrease in viscosity because of intermolecular Van deer Waals bonds being reduced and hence raising molecular mobility. In general, polymers exhibit temperature effects as elevated temperatures can break intermolecular bonds such as hydrogen bonds [30].

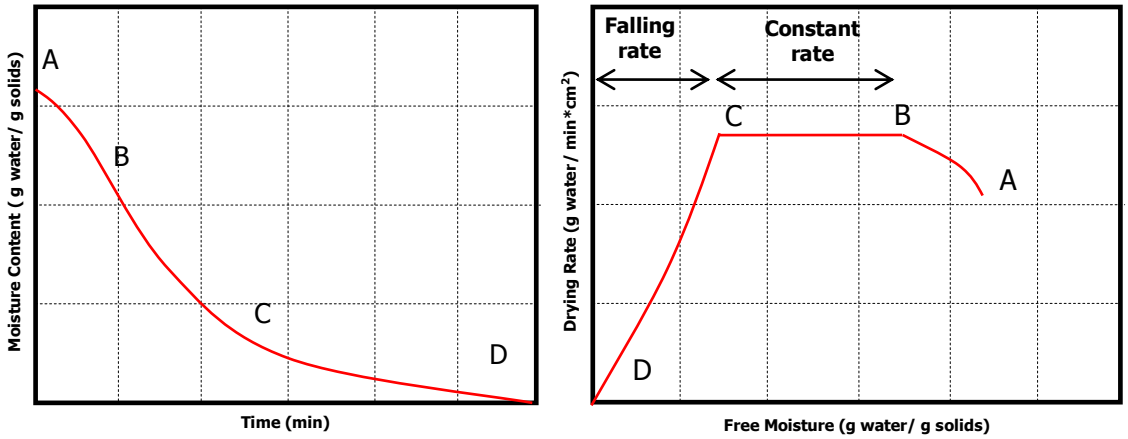
Shear Rate

When a material is to be subjected to a variety of shear rates in processing or use, it is essential to know its viscosity at the projected shear rates *[31]*. For instance, Pseudoplastic fluids such as starch show low viscosity at high shear

rates making pumping easier.

1.6.2 Drying Kinetics

Drying kinetics is the description of the changes of moisture content of material during drying. Drying is a complex process involving heat, mass and momentum transport. Drying kinetics of films can be expressed as a drying curve which is shown in Figure 1.6 (A). This curve is obtained experimentally by plotting the free moisture content Vs drying time. With this plot is possible to calculate a drying rate curve (1.6.B) by calculating the derivative of the curve over time.



(A) (B)

Figure 1.6 Typical drying curve and drying rate curve (Okos et al., 1992) (A) Drying curve, (B) Drying rate curve [32].

From these two types of curve it is seen that drying can be divided in different stages *[32].* The drying process begins with an initial short period that allows that material surface that is heated to reach similar conditions as the environment (line AB). The next one is the constant rate period, in which

unbound water is removed (line BC). Water evaporates and its rate of evaporation is not dependent on the material being dried. In this stage of drying the rate-controlling step is the diffusion of the water vapor across the air moisture interface. This period continues until water from the interior is no longer available at the surface of food material. The subsequent period is, the falling rate period (line CD), the wet areas on the surface of the drying material become completely dry. When the surface is dry, the evaporation continues moving toward the center of the material. The water that is being removed from the center of the material moves to the surfaces as a vapor. The drying rate in the falling rate period is controlled by diffusion of moisture from the inside to the surface and then mass transfer from the surface. During this stage some of the moisture bound by sorption is being removed. As the moisture concentration is lowered by drying, the rate of internal movement of moisture decreases. The rate of drying falls even more rapidly than before and continues to drop until the equilibrium value and therefore drying process stops.

1.6.3 Raman Spectroscopy

Nowadays the kinetics of starch retrogradation have been monitored by light scattering, thermal analysis, iodine binding, and X-ray diffraction *[33]*. However, these studies involve many hours and days, and none gave information on the processes involved at the molecular level. Raman spectra can usually acquired without touching or modifying the sample *[34].*

Basically, Raman spectroscopy is a technique based on the discrete vibrational transitions that occur in the ground electronic state of molecules, which correspond to various stretching and bending deformation modes of individual chemical bonds *[35].* A Raman spectrum is obtained by plotting the intensity of scattered light as a function of the Raman shift, and gives information based on stretching and bending vibrational modes. *Fechner [36]* has reported that native starch granules show a typical pattern of Raman bands. These skeletal vibrations appear below 800 cm^{-1} with a typical band at about 480 cm^{-1}, assigned to skeletal modes of pyranose ring. Therefore, it is possible to obtain the evolution of starch retrogradation recording the conformational changes on the molecular level Vs time.

1.7 Characterization of films

The main attributes involved in characterizing films are: optical properties, water sorption, thickness, microstructure, thermal behavior, barrier properties and mechanical behavior *[23]*.

1.7.1 Physical Appearance of films

1.7.1.1 Gloss

Reflective characteristics of film surfaces are important physical aspects of quality evaluation, because they are related to surface composition and morphology. These can determine the ability of a surface to reflect light into the specular direction due to interaction of light with the surface forming material.

Specular gloss is widely used in the industry for the characterization of appearance of a surface by specific reflectance measurements. The measurement geometry and conditions are well defined in international and national standards [37]. Three major factors affect gloss: the refractive index of the material, the angle of incident light and the surface topography. Surface gloss is considered the amount of incident light that is reflected at the specular reflectance angle of the mean of that surface.

The specular reflectance R_s, for a non-polarized light of intensity I_0, at angle of incidence θ, can be evaluated using Fresnel equation [38]:

$$R_s = \frac{I_r}{I_0} = \frac{1}{2}\left[\left(\frac{\cos\theta - \sqrt{n^2 - \sin^2\theta}}{\cos\theta + \sqrt{n^2 - \sin^2\theta}}\right)^2 + \left(\frac{n^2\cos\theta - \sqrt{n^2 - \sin^2\theta}}{n^2\cos\theta + \sqrt{n^2 - \sin^2\theta}}\right)^2\right] \quad (2)$$

Where I_r the intensity of specularly reflected beam and n is the refractive index of the surface film material. In this sense, very smooth surfaces are usually highly glossy and the rougher the surface, the lower the gloss [39]. Values at 60° angle are considered as medium gloss by ASTM D523 [40] indicating that a gloss value greater than 70 (gloss units) is considered high gloss, and a gloss values smaller than 10 is considered low gloss, using the same angle of incident.

1.7.1.2 Color

Color is one of the important parameters related to the visual appearance and wholesomeness of the food materials. It is often closely related to the

consumer acceptance and marketability of food products *[23].* Color may be considered an important parameter in the film characterization, because it is related to the raw material used in its production. The color measurement is normally done in an indirect way to estimate the color changes since it is simpler and faster than the chemical analysis *[41].* Hunter *Lab* system is one type of measuring color systems. The color parameters are expressed as *L* (whiteness or lightness) with 0 for black and 100 for white sample; a shows the magnitude of red color (+a*) to green color (-a*); and b represents the yellow direction (+b*) towards blue direction (-b*).

1.7.1.3 Morphology

Image analysis of films is an important parameter to evaluate film homogeneity, surface smoothness, and to detect pores and cracks. These properties are relevant to the film functionality because of their great impact on the appearance on the final product.

1.7.2 Water Sorption

Water sorption of any material can be studied using sorption isotherm, which shows the amount of adsorbed water as a function of Relative humidity at a constant temperature. Sorption of water at the surface the material may have physical or chemical origin and adsorbed water may occupy one or several layers. Therefore to determine the film stability under different conditions, the moisture absorption can be calculated from the difference in the weight at

equilibrium time and initial time (dry weight of the sample), according to the following equation:

$$\%M = \frac{Wi - Wo}{Wo} * 100\% \quad (3)$$

Where M is the moisture sorption (%), *Wi* is the weight of film at time t (g) and Wo is the initial weight of oven-dry film (g). For starchy products the isotherms showed a similar sigmoid shape Type II, according to Brunauer's classification [42]. Two bends are noted in this type of isotherm: one around at water activities of 0.2–0.4 and another one at 0.65–0.75*. DeMan [43]* has suggested a division of the dominating events in water sorption isotherm separated by the two bends observed: the first part, before the first bend, describes the adsorption of the monolayer of the water; the second part, before the second bend, corresponds to adsorption of additional layer of water, and in the third part, after the second bend, shows the condensation of water in capillaries and pores of the material dominates. (Figure 1.7)

Many mathematical models to represent sorption isotherms have proposed in the literature because are useful for predicting the interaction of water and film components. Therefore, knowledge of sorption isotherm is important for predicting stability and quality changes during packaging and storage for food product [44].

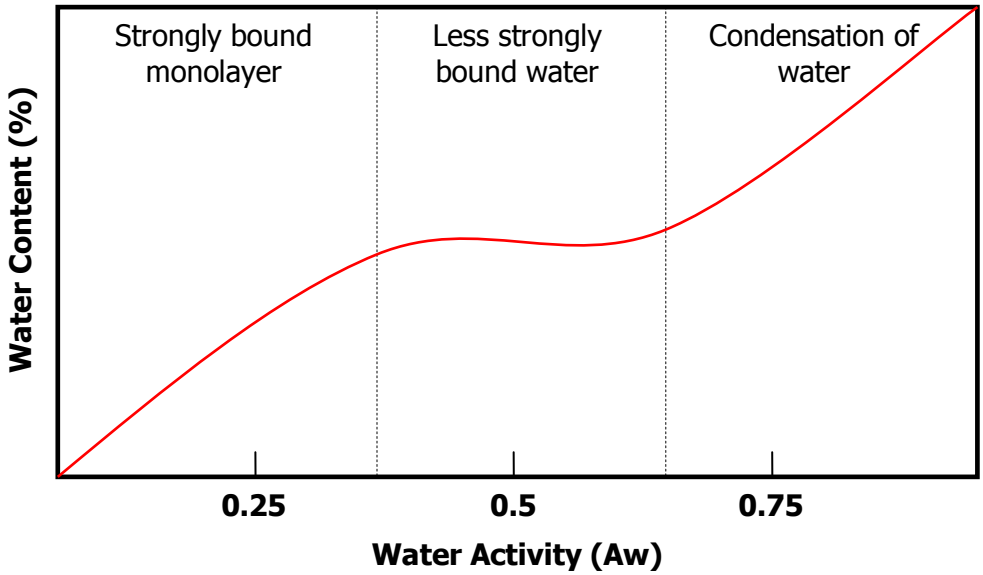


Figure 1.7 Water sorption isotherm

1.7.3 Thermal properties

Differential scanning calorimetry or DSC is the most common widely used analytical method to study thermal properties and phase transitions of starch, since Stevens and Elton first used DSC to measure gelatinization and retrogradation of starch in 1971 *[45].* The objective of DSC is to record the thermal differences between a sample and a reference material. The equipment is programmed to heat them at a constant rate and then difference between these two are function of: the enthalpy change, the heat capacity and total thermal resistance to heat flow. DSC studies can provide information about interactions with starch and other components such as water and plasticizers present in the sample. Thermal properties typically reported using DSC method

include gelatinization onset (T_o), peak (T_p) and conclusion (T_c) and enthalpy (ΔH) of material.

1.7.4 Mechanical Properties

Edible films should have adequate mechanical strength and extensibility to maintain integrity and withstand the external stress that occurs during processing, handling and storage *[46].* Typical methods used for evaluation of mechanical properties of synthetic materials can also be used for edible films. These measurements are important once the mechanical properties of films or coatings depend on the filmogenic nature of the material used, which is directly related to its structural cohesion *[23].* Multiple factors, such as film composition, temperature, relative humidity, and storage time, affect tensile properties.

The properties evaluated in the tensile tests are tensile strength, elongation at break and elastic modulus. Tensile strength is defined as the maximum tensile stress, which a material can sustain and is taken to be the maximum load exerted on the test specimen during the test. Elongation is the maximum change in the length of the test specimen before breaking and is expressed as the percent change of the original length of the material. Elastic modulus or Young's modulus is defined as the ratio of stress to strain in the initial linear part of the stress- strain curve. It is a fundamental measurement of inherent stiffness of a single film since it is nearly independent of dimensions and stress from small strains *[47].* In general, the addition of plasticizers leads to a decrease of Tensile strength and an increase of Elongation *[48]*.

1.8 Water – starch – plasticizer interactions using Flory-Huggins theory

Thermodynamics is an important tool to obtain valuable information about the interaction between components in a system. The Gibbs free energy (G) is a parameter that reflects the balance among the driving forces behind a particular reaction. The Gibbs free energy of a system at any moment in time is defined with the following equation:

$$G = H - T * S \tag{4}$$

The change in the free energy of the system that occurs during a reaction measures the balance between the two driving forces (enthalpy, H and entropy, S) that determine whether a reaction is spontaneous. A polymer system is not very different from that used for dilute ideal solutions of small molecules. In fact, it involves calculating entropic and then enthalpic effects and determining their contribution to Δ*Gmix*. Therefore, the miscibility of one component in another can be calculated the change in free energy of mixing following the next equation:

$$\Delta G_{mix} = \Delta H_{mix} - T * \Delta S_{mix} \tag{5}$$

When ΔGmix is the Gibbs' free energy of mixing; ΔHmix is the enthalpy of mixing; ΔSmix is the entropy of mixing, and T is the absolute temperature. A homogeneous polymeric solution satisfies of stability condition when ΔGmix is negative and ΔSmix is positive because of the entropy increases upon mixing.

Therefore, ΔGmix depends on ΔHmix, which describes the interactions between the components of a mixture. In 1953, [49] reported the simplest thermodynamic equation for mixing polymer systems as a lattice model where each lattice is occupied by either a polymer segment or a solvent molecule. Because of the large size molecule of starch is possible compare a glucose segment of it with a synthetic polymer segment. Then the general expression of Flory–Huggins theory for free energy of mixing for ternary systems is given as:

$$\Delta G_{mix} = RT\left[n_1 Ln\varphi_1 + n_2 Ln\varphi_2 + n_3 Ln\varphi_3 + n_1\varphi_2 X_{12} + n_2\varphi_3 X_{32} + n_3\varphi_1 X_{13}\right] \quad (6)$$

Defining the solvent (water) as component 1, the polymer (starch) as component 2, and the low-molecular-weight solute (glycerol) as component 3. Where n is the number of moles of each component, ϕ is the volume fraction of each component, X_{12} is the interaction parameter of component 1 and 2 , X_{13} is the interaction parameter of component 1 and 3, X_{32} is the interaction parameter of component 3 and 2, R is the gas constant and T is the temperature of mixing. Consequently, using the Flory-Huggins theory it is possible to account for equilibrium thermodynamic properties of polymer solutions.

1.9 In-vitro nutraceutical release kinetics

In-vitro dissolution test are used as a guide for formulation and optimization

of drug release rates. They compare the impact of different formulations on the vehicle and the methods used to produce them. Dissolution is defined as the rate of mass transfer from a solid surface into the dissolution medium or solvent under standardized conditions, temperature and solvent composition. There are several models to describe the drug dissolution profiles as a function of time and/or the amount of drug dissolved in the system [50]. The most common mathematical models that have been reported in the literature for the characterization of drug release are Zero order, First order, Korsmeyer Peppas and Higuchi.

1.10 Research problem statements

We propose three problems statements for our research:

1. What is the effect of glycerol on the physical properties of cassava-starch films?

2. What is the appropriate combination of cassava-starch, glycerol to prepare edible films with desirable matrix to carry nutraceuticals?

3. How the incorporation of Minerals (Iron) affect the physical properties of cassava-starch films.

1.11 Rationale

Cassava is an economically crucial crop for many developing countries in South America (Brazil), Asia (Thailand) and Africa (Nigeria). Cassava starch is used as a raw material for a wide range of food products and industrial goods, including paper and textile industries [20]. In recent studies especially conducted

in Brazil; cassava starch has been used to produce edible films *[22, 51-54]*. Principally, these studies seek the possible effect of some plasticizers (glycerol and sorbitol) in the glass transition temperatures and water sorption properties of films. Also, another authors [54] have been studying different gelatinization conditions that impact the physicochemical properties of films. To conclude, there is no a study that develops a cassava-starch film from formulation going through drying process and finally produces a film with required physicochemical properties.

In the other hand, incorporation of nutraceuticals into edible films is one the important emerging functions of edible films. However, few studies have actually reported integration of these components in coatings and edible films [55, 56]. Basically these studies have been evaluating feasibility of milk-protein and chitosan based films to incorporated calcium, and zinc. In fact, many other nutrients, which are low intake in American diet *[26],* have not been investigated. Therefore, there is a possibility of incorporation another minerals such as Iron to fortify cassava starch edible films, previously formulate with glycerol and capable to carry it.

1.12 Objectives of the study

The overall objective of the present research was develop a biomaterial film based on cassava starch and glycerol containing iron as nutraceutical and evaluate the properties and functionalities of films.

The specific objectives of the project were:

(1) Identify proper conditions to prepare cassava starch glycerol blends

(2) Determine rheological properties of film precursor and select the most suitable Rheology model.

(3) Monitor retrogradation and conformational changes of cassava starch films during drying process.

(4) Investigate the impact of cassava starch/glycerol ratio on optical and morphological properties of the films.

(5) Determine water sorption, thermal and mechanical properties of cassava starch glycerol.

(6) Find the equilibrium thermodynamic properties of water-starch-plasticizer.

(6) Formulate the best solution cassava starch/glycerol to incorporate iron into the matrix of the film

(7) Evaluate properties of film forming solutions (Rheology) and functionalities (mechanical properties and water sorption) of dried films containing iron.

2 Materials and methods

2.1 Materials

Cassava Starch, food grade, was provided by Penta, International, Inc (Livingston, New Jersey, USA). Glycerol, analytical grade, was supplied by Fisher Scientific (Pittsburg, Pa, USA). Ferrous Gluconate dyhydrate 94% food grade was obtainded by Alfa Aesar (Ward Hill, Ma, USA). Saturated salt solutions used in this study were prepared with salts (NaOH, CH_3CO_2K, $CaCl_2$, K_2CO_3 $NaNO_2$, NaCl, KCl,) supplied by VWR International (Pittsburg, Pa, USA).

2.2 Methods

2.2.1 Film forming process and film casting

Solutions without plasticizer were prepared (Figure 2.1) with four different concentrations of cassava starch in water to obtain 2%, 3 %, 4% and 5 % (w/w) suspensions. Solutions with plasticizer (Glycerol) were prepared in six different concentrations (0, 10, 20, 30, 40 and 50 g/100g of starch) and the concentration of starch was kept constant. Lastly, Iron gluconate was incorporated into the cassava starch-glycerol solutions in six different concentrations: 0,20,40,60,80, and 100% (based on the maximum Dietary Reference Intake for pregnant women, 27 mg/day accounted for 100% Iron). The forming solutions were heated in sealed conical flasks on a hotplate under continuous stirring to gelatinize starch completely. When the dispersions achieved a temperature of

85°C (20% above of the gelatinization temperature) were retired of heat *[54]*. Subsequently the solutions were cooled at room temperature for around 1 hour to permit that bubbles inside of solution were dissolved.

Cassava starch films were prepared by casting the starch solution in polystyrene Petri dishes. A certain amount of the paste was poured and spread onto the Petri dishes (60 x 15 millimeters) and dried in a convection oven at 28°C for 36 hr [54]. After film constitution was separated form the Petri dish to obtain translucent films.

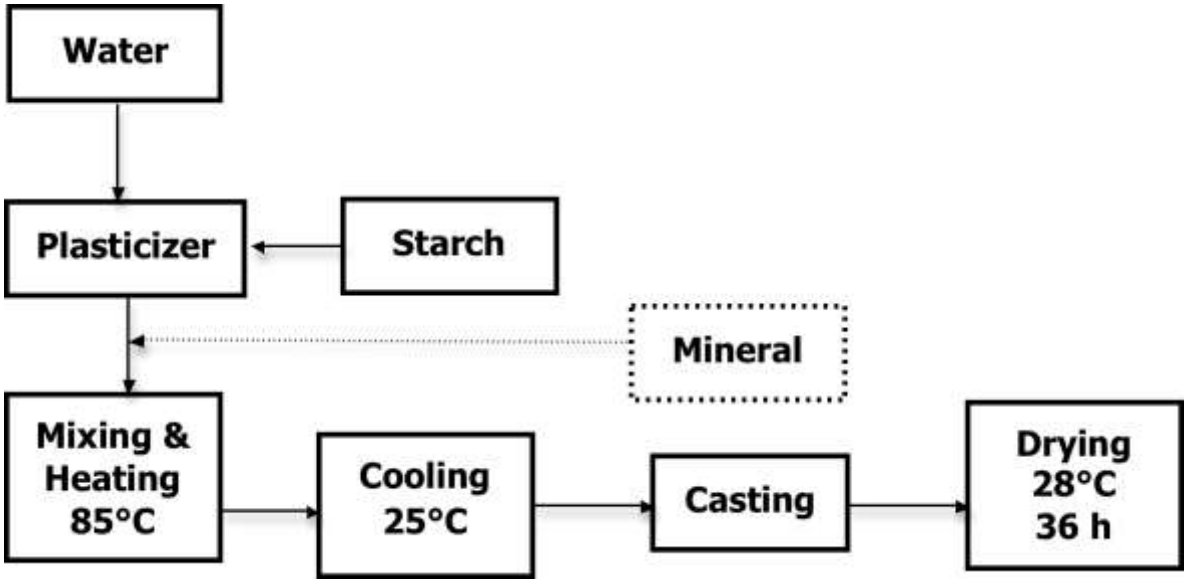


Figure 2.1 Film forming process and film casting.

2.2.2 Characterization of film forming solutions

Viscosity of starch, starch-glycerol and starch glycerol-iron solutions were evaluated to observe the effect of these on the rheological properties.

2.2.2.1 Rheological measurements

Starch exhibits unique viscosity behavior with change of concentration, temperature and shear rate. These characteristics can be measured by a Brookfield DV-III Ultra programmable Rheometer. Solutions were analyzed using a small sample adapter (13R/RP, 19.05 mm of diameter and depth of 64.77 mm), and a spindle SC4-31 (11.76 mm of diameter and 25.15 mm length), the volume of each sample was 9 mL (Brookfield Engineering Laboratories, MA, USA). A Thermo Scientific K10/ Haake DC-30 circulation bath (Thermo Scientific Fisher Corporation, Waltham, Ma USA) was used to adjust the temperature of the sample in the range of 35–85 °C. For measurements conducted above 35°C a plastic cover was fitted to the rheometer to prevent water evaporation (Figure 2.2) Continuous shear rate measurements were performed to establish the effects of increasing shear on viscosity. Shear rates in the range of 0.01-100 s^{-1} were studied with an equilibrium period at each given shear rate of 60 s. All measurements were done in duplicate and Rheocalc software was used to program directly the rheometer under PC control. Also flow curves and models were evaluated with it (version V3.2, Brookfield Engineering Laboratories, MA, USA).



Figure 2.2 Brookfield DV-III Ultra Rheometer with small adapter

To understand the flow curves (rheograms) of compounds, different models have been proposed. Five different models were selected for fitting the experimental data .The simplest model is the Power law model described by Ostwald and de Waele [57] and is shown in the next equation, where is κ consistency index and n the flow index.

$$\tau = k\gamma^{n} \tag{7}$$

The power law states that for n < 1 the mixture is a shear thinning fluid, for values of n > 1 the mixture is a shear thickening fluid, and when n = 1 the fluid is Newtonian.

Also, some of the most widely models used to evaluate rheological properties of fluids are: Casson, Herschel- Bulkley, Bingham and IPC Paste model.

Casson:

$$\sqrt{\tau} = \sqrt{\tau_0} + \sqrt{\eta\dot{\gamma}} \quad (8)$$

Herschel-Bulkley:

$$\sqrt{\tau} = \sqrt{\tau_0} + \sqrt{\eta\dot{\gamma}} \quad (9)$$

Bingham:

$$\tau = \tau_0 + \eta D \quad (10)$$

IPC Paste:

$$\eta = kR^N \quad (11)$$

2.2.2.2 Drying Kinetics

The determination of the kinetics of drying was performed in duplicate at film-forming solutions. Petri dishes with 9 ml of Cassava starch pastes (3% w/w) with different amounts of Glycerol (0. 20, 30 g/100g of starch) were mounted on a Mettler Toledo Scale (Hightstown, NJ) and kept to constant drying at 25C, determining the weight loss of the film every 10 min until constant weight. The scale was isolated to prevent the convection effect from the environment. The next step was to build drying curves of weight loss of water Vs time and rate of drying Vs time. Table 2.1 shows the parameters obtained to film drying process.

Table 2.1 Description of the parameters of drying kinetics of film forming solutions.

Parameter	Description	Units
Rc	Rate of drying	g H_20 / min cm^2
Ws	Mass of dry solids	g
A	Exposed area	cm^2
X	Free moisture content	g H_20 / dry solids
t	Drying time	min

2.2.2.3 Raman Spectroscopy

Raman Spectra were measured in the spectral range from 100 to 4000 cm^{-1} at 4 cm^{-1} of resolution, with a Raman spectrometer system from Kaiser Optical Systems Inc. 9 ml of Cassava starch pastes (3% w/w) with different amounts of Glycerol (0. 20, 30 g/100g of starch) were put on Petri dishes and analyzed during 24 Hr, taking measurements of spectra every 10 min to detect the differences of molecular composition during dying process.

2.2.3 Characterization of films

2.2.3.1 Physical appearance

The gloss of the films was measured at 60° angle from the film surface, using a portable surface gloss meter (BYK-Gardner). Measurements were taken in duplicate of each sample. All results are expressed as gloss units and highly polished surface of black glass standard was used to calibrate the machine with a value of 94. The film morphology was studied using images taken from a Nikon

SMZ 10A stereomicroscope. The images were taken at ambient temperature without any conditioning or treatment of the films. Film color was measured with a spectrophotometer Konica Minolta CM-2500d. Measurements were taken in triplicate for each sample.

2.2.3.2 Water sorption

Cassava starch films of size 1 x 1 cm^2 were cut. The initial moisture content of the films of different compositions was measured on a dry-weight basis by drying them in an oven at 85C during 48 hr. The films were cooled down in a dessicator for 30 min until these reached room temperature. A set of seven plastic hermetic containers with different salt solutions *[58]* was used to create different relative humidity levels (Table 2.2) Inside of each container was placed a beaker with saturated solution and a mesh to support the samples and permit the air circulated below them. The containers were maintained at 25C during the experiment. Samples were withdrawn for weighing intervals until they had reached constant mass when two consecutive weightings were equal. Samples came to equilibrium after approximately 48 Hours. Also, Water activity measurements were performed with a humidity temperature indicator (HygroLab, Rotronic, Switzerland part of the HW4 humidity measurement system to record automatically in the PC) apparatus. Each sample was introduced inside of the sample holder until the equipment automatic recorded the measure in the

PC. The samples were evaluated at the same times that were weighted during water sorption test.

Table 2.2. Relative humidity of saturated salt solutions at room temperature

Name	Formula	Relative Humidity
NaOH	Sodium hydroxide	7%
CH_3CO_2K	Potassium acetate	23%
$CaCl_2$	Calcium chloride	30%
K_2CO_3	Potassium carbonate	43%
$NaNO_2$	Sodium nitrate	65%
NaCl	Sodium chloride	75 %
KCl	Potassium chloride	85 %

Isotherm models from the literature were selected for fitting the experimental data of films commonly applied to starchy products *[59].* The quality of the fitting was evaluated through the R^2.The models are expressed and rearranged as given below.

Halsey model:

$$m = \left(-\frac{A}{Lna_w} \right)^{\frac{1}{B}} \quad (12)$$

Where m is the equilibrium moisture content on a dry basis and aw is water activity. A, and B are constants.

Oswin model:

$$m = A\left(\frac{a_w}{1 - a_w} \right)^{B} \quad (13)$$

Where A and B = constants.

Smith model:

$$m = A + B\ln(1 - a_w) \quad (14)$$

Where A, and B are constants

BET model:

$$m = m_0 \frac{ca_w}{(1 - a_w) - (1 - a_w + ca_w)} \quad (15)$$

Where mo is BET monolayer moisture content and C is a constant.

GAB (Guggenheim-Anderson-de Boer) model:

$$m = m_0 \frac{kca_w}{(1 - a_w) - (1 - a_w + kca_w)} \quad (16)$$

Where m_o is GAB monolayer moisture content, k is the factor correcting properties of the multiplayer molecules corresponding to the bulk liquid.

2.2.3.3 Differential scanning calorimetry

The gelatinization temperatures and enthalpy of the films were determined by DSC. Samples of 2 to 5 mg were weighed in aluminum pans and

were sealed; an empty pan was used as reference The DSC measurements were carried out in a Perkin-Elmer DSC-7 with Thermal Analysis Controller TAC-7/DX (Figure 2.3). Each sample was heated from -30 to 120 C and kept at this temperature for 1 min. The heating rate for the experiment was 10C/min. The program Pyris Series Thermal Analysis (Version 7.0, Perkin Elmer, Waltham, MA) was used to analyze thermograms obtained during the experiment.



Figure 2.3. DSC-7 Perkin-Elmer

2.2.3.4 Mechanical properties

The films formed were examined by a Texture Analyzer (Model TA.XT2), supplied by Stable Microsystems (England) (Figure 2.4). Standard penetration tests were carried out using a 0.5-inch spherical probe. In the penetration study, individual films were fixed on a hollow plate by a frame. The film was held rigidly

in a stationary position by tightening the screws on the frame. Samples were exposed at room temperature before testing so that the films reach equilibrium moisture content. The probe was lowered from a height of 25mm at a rate of 10 mm per second with a 50 N load cell. The results are the average of three samples. Also, Tensile strength and percentage elongation were measured according to ASTM D412-98a [60] using small tensile grips with a 50 N load cell and at a velocity of 0.2 mm/s. The results are the average of three samples.



Figure 2.4 Texture Analyzer (TA-XT2) with tensile grips.

2.2.3.5 Dissolution studies of Iron gluconate

The drug release studies were carried out using dissolution vessels, which were filled with 900 ml of simulated saliva [61]. To obtain a homogenous

concentration was in the solution was utilized a paddle and the rotation was 100 rpm. The samples were withdrawn at predetermined time intervals each time fresh medium was replaced in same amount. Samples absorbance was measured spectrophotometrically at a wavelength of 259 nm. The content drug in each sample was calculated using a standard calibration curve. The in-vitro drug release was carried out in triplicate for each film.

To analyze the in-vitro release data were used various kinetic models [62]. The Zero kinetics (the compound release is independent of its concentration), First order kinetics (release rate is concentration dependent), Higuchi model (It is a square root of time dependent process based on Fickian diffusion) and Korsmeyer-Peppas model (it is applied when more than one type of release phenomena could be involved or is not well known).

3 Results and Discussion

3.1 Characterization and formulation of cassava starch films with glycerol.

It is common the study of interactions between films components such as liquid state (film forming solutions) as solid state (stand alone films) to provide enough information to determine their possible applications. In this section we will be discussing our results regarding the properties of the film forming solutions and stand-alone films. Also, based on the results obtained, we will be choosing the best film formulation to incorporate nutraceuticals.

3.1.1 Rheology of film forming solutions

During processing, starch dispersions suffer changes such as high heating and shear rates that modify their theological behavior of the flow and affect the characteristics of the final product. So, in order to understand those changes we will be discussed how concentration (starch), temperature, shear rate and plasticizer (glycerol) may change the flow regime of solutions.

3.1.1.1 Flow behavior of cassava starch solutions at different concentrations and temperature.

Flow behavior studies were carried out after starch gelatinization. Granular starch is insoluble in cold water but when heat is applied the granules undergo changes that are irreversible and dependent on the amount of heat, concentration of starch and water available on system *[12]*. Since viscosity is affected for the concentration of starch, the flow behavior of solutions with different amount of cassava starch (1, 2, 3 and 4 %w/w) has been investigated. Figure 3.1 shows the efecct of cassava concentration on viscosity. Cassava starch solution with 1 and 2% maintained a viscosity constant indicating a newtonian behavior, when the concentration increased above 3% of cassava, the solutions show shear-thinning behavior and the deviation from Newtonian behavior increases with the increasing cassava concentration. Starch molecules entangled by overlapping and interpenetrating into each other at higher concentrations and this behavior restricts the fluidity of starch *[12]*. Also as shear rate increases, the starch molecules alignment in the direction of the shear resulting in decrease of apparent viscosity.

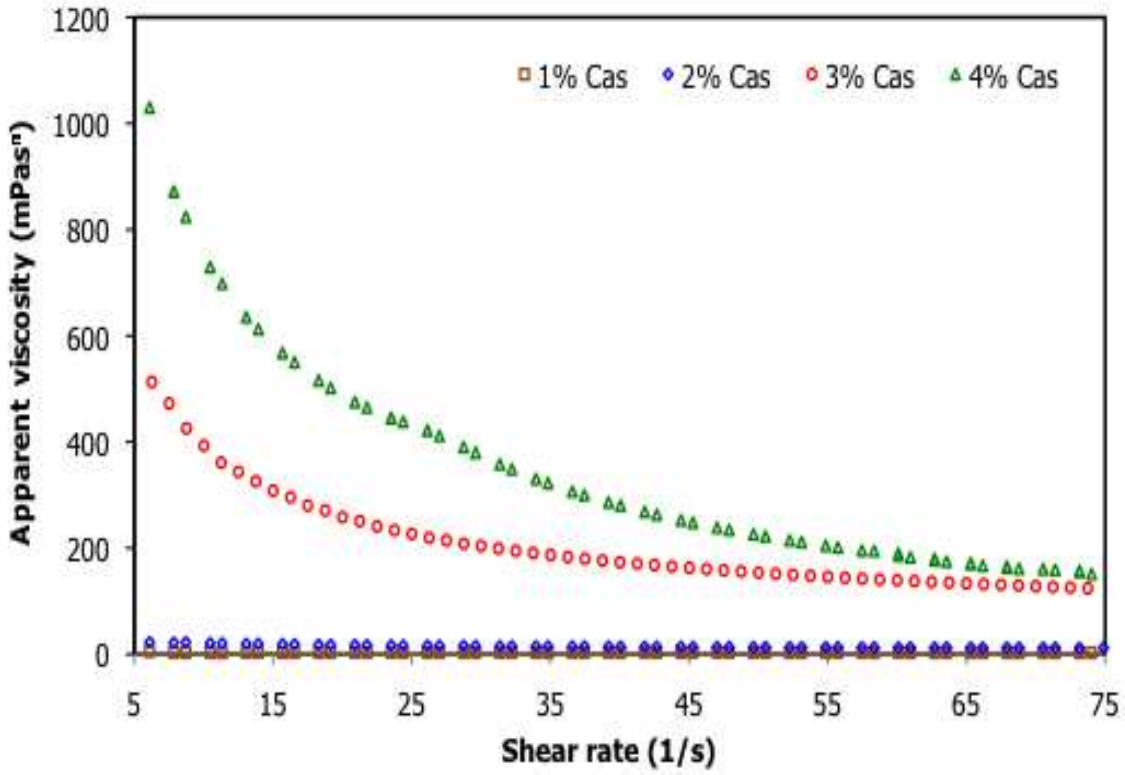


Figure 3.1 Apparent viscosity of 1, 2, 3 and 4% of cassava starch solutions at 35°C.

In the other hand Figure 3.2 shows the effect of temperature on rheological behavior of cassava starch solutions. The data obtained for 1, 2, 3 and 4% depicted the same behavior. As temperature increases, starch molecules vibrate more dynamically, thus breaking the intermolecular hydrogen bond and allowing penetration of water. As a result, there is more free water available to facilitate the movement of particles in suspension. Apparent viscosity values

were examined as a function of temperature and it was observed that apparent viscosity decrease with increasing temperature.

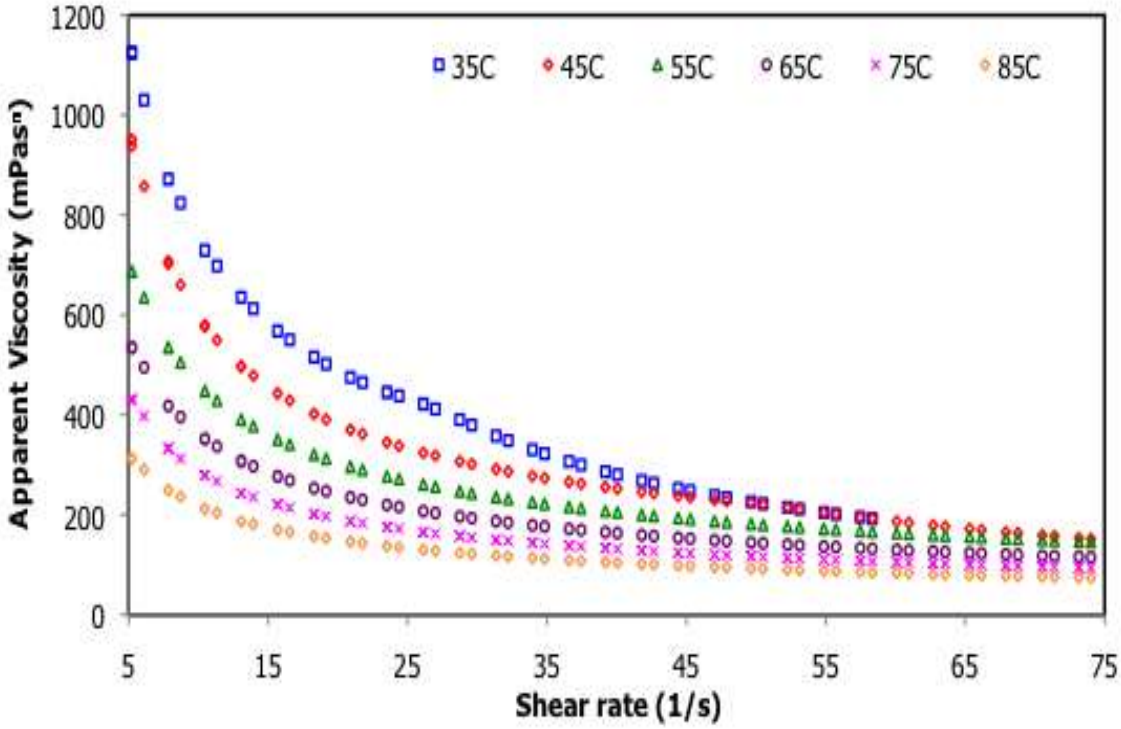


Figure 3.2 Apparent viscosities of 4% of cassava starch solutions at different temperatures (35, 45, 55, 65, 75, 85°C).

The rheological data for the cassava starch solutions could be adequately described using three of the models before reported (equations 3, 4, 5, 6 and 7) and the parameters of the models obtained are summarized in Table 3.1. The IPC Paste (Institute for Interconnecting and Packaging Electronic Circuits) analysis is based on the Power Law equation and intended to calculate the shear sensitivity factor (pseudoplasticity) of pastes. The Power law model generally has been reported to describe the behavior of gelatinized starch because of high R^2

[63, 64], and the Casson model has been applied to a range of food products (gums, fruit purees and tomato products). [65].

Table 3.1 Comparison of different models for the flow behavior of cassava starch solutions with different concentrations and temperature.

Starch (w/w)	Models	35 (°C)			85 (°C)		
		R^2	n	Vis (mPas)	R^2	n	Vis (mPas)
1	Power L.	0.987	0.87	15.2	0.987	0.95	7.2
	IPC Paste	0.97	0.14	10.5	0.943	0.19	8.4
	Casson	0.965	0.01	6.84	0.962	0.01	5.35
2	Power L.	0.967	0.77	33.2	0.965	0.84	18.9
	IPC Paste	0.97	0.23	18.5	0.965	0.18	14.2
	Casson	0.965	0.04	8.84	0.952	0.01	6.73
3	Power L.	0.989	0.43	1456	0.986	0.54	379.7
	IPC Paste	0.989	0.58	737	0.986	0.47	219.6
	Casson	0.986	1.83	39.3	0.986	0.44	24
4	Power L.	0.941	0.39	1683	0.965	0.69	521.8
	IPC Paste	0.941	0.61	1119	0.957	0.52	498.0
	Casson	0.940	4.73	73.2	0.943	1.63	58.1

Since R^2 values for all the models were very close to unity indicating a good fit, it is possible to say that the power law model properly explained the flow behavior of cassava starch film forming solutions. In all cases R^2 values were higher than 0.94. Flow index for all analyzed samples were ranged between 0.39 (4% starch w/w)) and 0.95 (1% starch (w/w)) in a temperature range 35-85°C. The solutions exhibited a shear thinning (pseudoplastic) behavior because the values of flow index were less than 1 for all temperatures.

A decrease in flow index with starch concentration was observed. As starch concentration is lowered, the solutions exhibit almost a Newtonian

behavior. Also, observing the flow index changes with the increasing of temperature, it is possible to say that the solutions almost reached the Newtonian behavior, especially the concentration of 1% of cassava (n=0.95 at 85°C). The pseudoplastic property of gelatinized starch is important in films since pseudoplastic solutions have diffetent properties, at low shear rates (casting film) its viscosity is high and it is sufficiently low when the solution is processed at higher shear rates (film preparation).

3.1.1.2 Effects of Glycerol in flow behavior of cassava starch solutions at different concentrations and temperature.

In Figure 3.3 the rheological behavior of cassava starch film forming solutions (3% of cassava and different glycerol content) is shown at 35°C. The marked points represent the average values of the experimental data of the rheograms and the continuous lines are the fit results calculated from the Power Law model. The decrease of apparent viscosity with glycerol concentration reflects the effects of the plasticizer on the behavior of solutions. As glycerol concentration increases, interactions between glycerol and water become dominant and a greater number of water molecules are trapped. Also, It was found that the concentration of 20g Gly/100g starch had the lower apparent viscosity. At this point when the increase of glycerol concentration (30,40 and 50g gly/100 g of starch), the apparent viscosity increase obtaining the same viscosity of solution without glycerol. As previously stated, at high shear rate

values, apparent viscosity reaches a constant value related to completion of structure reorganization.

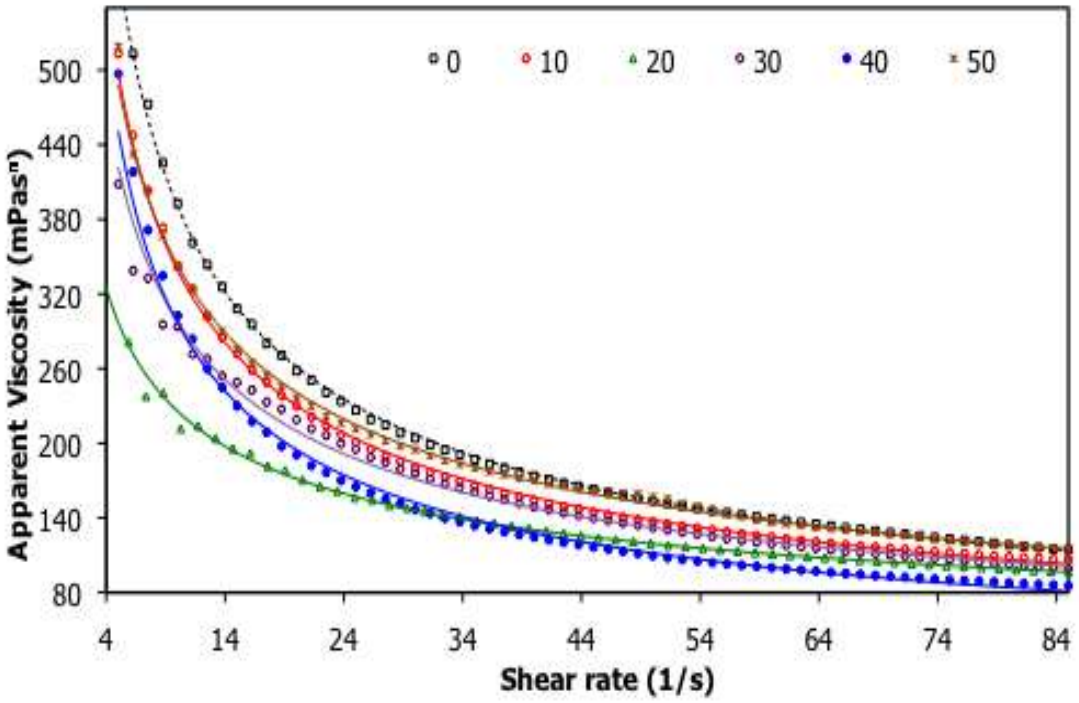


Figure 3.3. Apparent viscosity of 3% of cassava starch solutions with different glycerol content (0, 10, 20, 30, 40, 50 g/100 g of starch) at 35°C.

All experimental data fitted the Power Law model with correlation coefficients greater than 0.95. The parameters obtained from the models are shown in Tables 3.2. Flow index for all analyzed samples were ranged between 0.43 and 0.63 in a temperature range 35-85°C.

Table 3.2 Comparison of different models for the Rheology of cassava starch film forming solutions at different temperatures (35°C and 85°C), and glycerol content (0,10,20,30,40,50 g/100g of starch).

Glycerol (g/100g starch)	Models	35 (°C)			85 (°C)		
		R^2	n	Vis (mPas)	R^2	n	Vis (mPas)
0	Power L.	0.989	0.43	1356	0.986	0.54	379.7
	IPC Paste	0.989	0.58	737	0.986	0.47	219.6
	Casson	0.986	1.83	39.3	0.986	0.44	24
10	Power L.	0.986	0.45	1205	0.983	0.53	388.4
	IPC Paste	0.987	0.56	623.9	0.984	0.48	222.1
	Casson	0.987	1.49	38.5	0.986	0.45	22.5
20	Power L.	0.981	0.61	544	0.984	0.63	186.4
	IPC Paste	0.982	0.39	339.3	0.988	0.38	119.9
	Casson	0.886	0.38	65.6	0.979	0.2	20.2
30	Power L.	0.971	0.52	874.8	0.988	0.6	250.7
	IPC Paste	0.975	0.49	495.6	0.990	0.4	155.4
	Casson	0.97	1.15	43.3	0.981	0.28	22.9
40	Power L.	0.971	0.41	1237	0.985	0.54	278.9
	IPC Paste	0.969	0.62	594.7	0.986	0.46	161.9
	Casson	0.995	1.49	25.5	0.984	0.32	18
50	Power L.	0.985	0.48	1119	0.956	0.46	550.4
	IPC Paste	0.986	0.62	606.5	0.957	0.50	284.6
	Casson	0.982	1.36	48.5	0.968	0.42	27.4

Apparent viscosity values flow index were examined as a function of temperature and glycerol content. Figure 3.4 illustrates the apparent viscosity of solutions. The viscosity of solutions decreased with the increase of temperature and glycerol content but at 35°C and 20% Glycerol is behavior was marked, showed an erratic pattern in this plot. (Viscosity changed from 544 to 599.1 mPas).

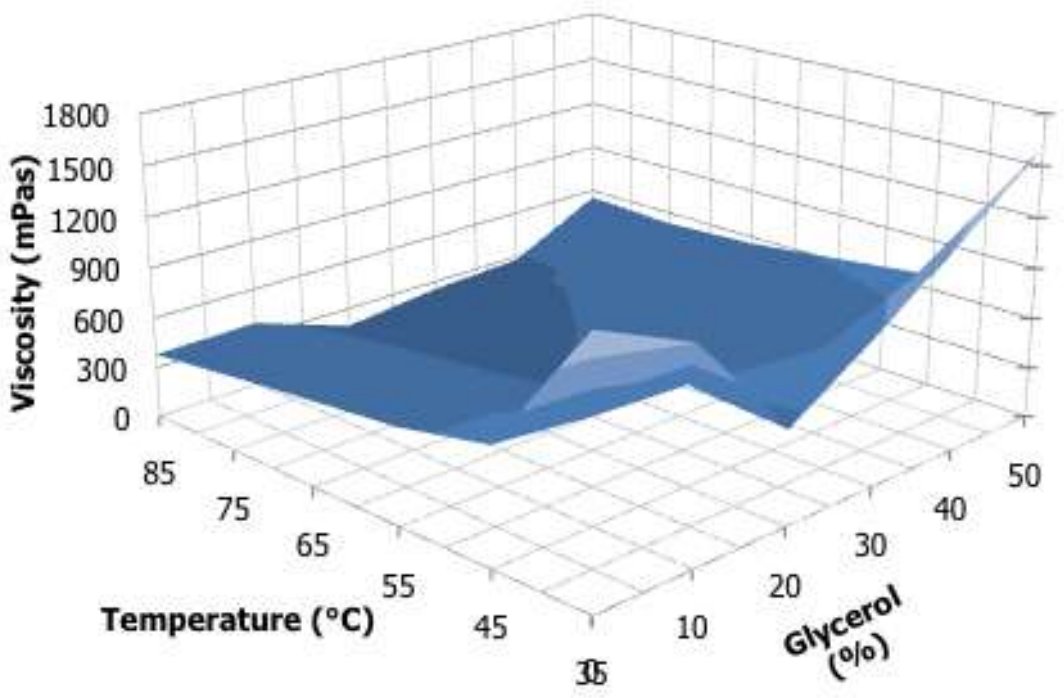


Figure 3.4 Effects of concentration and temperature on viscosity of cassava starch solutions with glycerol.

Figure 3.5 shows the flow index obtained form Power Law. The behavior of these solutions was relatively diverse. The values of flow index above 45°C do not represent significant differences to all solution with different glycerol concentrations. Although at 20% of glycerol content and 45°C the flow index decrease notably from 0.61 to 0.54. In plasticized films interaction between hydroxyl groups of starch, glycerol and water is complicated due to the abundantly existing hydrogen bonds in their structures *[5].* For instance, hydroxyl groups of glycerol and starch can form many hydrogen bonds between each other, leaving less sorption sites available for water in starch. In the other hand, Glycerol is very hydrophilic and hygroscopic and the hydroxyl groups of the backbone of it can attract water molecules and form a large plasticizer complex. These could be explaining the rheological behavior of the plasticized

film forming solutions. Exist a threshold at 20% glycerol concentration (dry basis) when the viscosity was decreased and flow index was increased significantly due to glycerol interacts more with starch than with water.

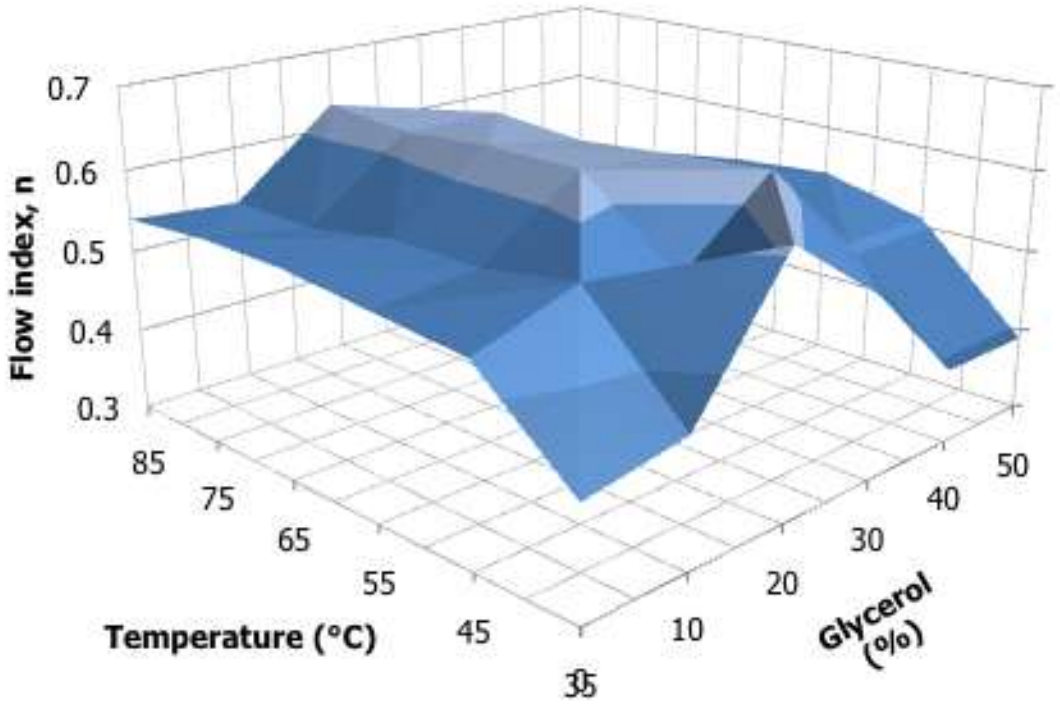


Figure 3.5 Effects of concentration and temperature on flow index of cassava starch solutions with glycerol

In plasticized films interaction between hydroxyl groups of starch, glycerol and water is complicated due to the abundantly existing hydrogen bonds in their structures*[5].* For instance, hydroxyl groups of glycerol and starch can form many hydrogen bonds between each other, leaving less sorption sites available for water in starch. In the other hand, Glycerol is very hydrophilic and hygroscopic and the hydroxyl groups of the backbone of it can attract water molecules and form a large plasticizer complex. These could be explaining the rheological behavior of the plasticized film forming solutions. Exist a threshold at

20% glycerol concentration (dry basis) when the viscosity decreases significantly due to glycerol interacts more with starch than with water.

3.1.2 Comparison of time evolution of water loss of cassava starch solutions with different concentrations of glycerol

The removal of solvent (water) from polymer solutions is important to understand the film formation process. The components into solution could alter the drying time and the final structure of the film. Therefore, in this section we will be studying the drying time curves of cassava starch films without and with glycerol (20 and 30%) at room temperature. Figure 3.6 shows these three film-forming solutions, the water loss, as a function of the drying time was linear in the initial part of the curve; then after this constant rate region, the drying rate slowly decreased until reach a constant weight at the end of the drying process. This drying profile is typical of the two-stage mechanism observed in the drying process of films *[66].* Due to the high initial water content, the water can move relatively freely from the medium in this linear part. As the polymer concentration increases during the drying time, the polymer structure (entanglement) and the drop of molecular mobility affect the drying rate explaining the decrease of the drying rate in the non-linear region*[67].* Regarding glycerol concentration, it can be seen that the plasticized films required 3600 and 3420 min, for 30 and 20% glycerol, respectively. In the other hand, the unplasticized films needed 2960 min to be completely dried. This could be attributed to glycerol because it is a hydrophilic plasticizer; films with a higher

glycerol concentration could adsorb more water in their matrix and this led to increased drying time to reduce the film moisture.

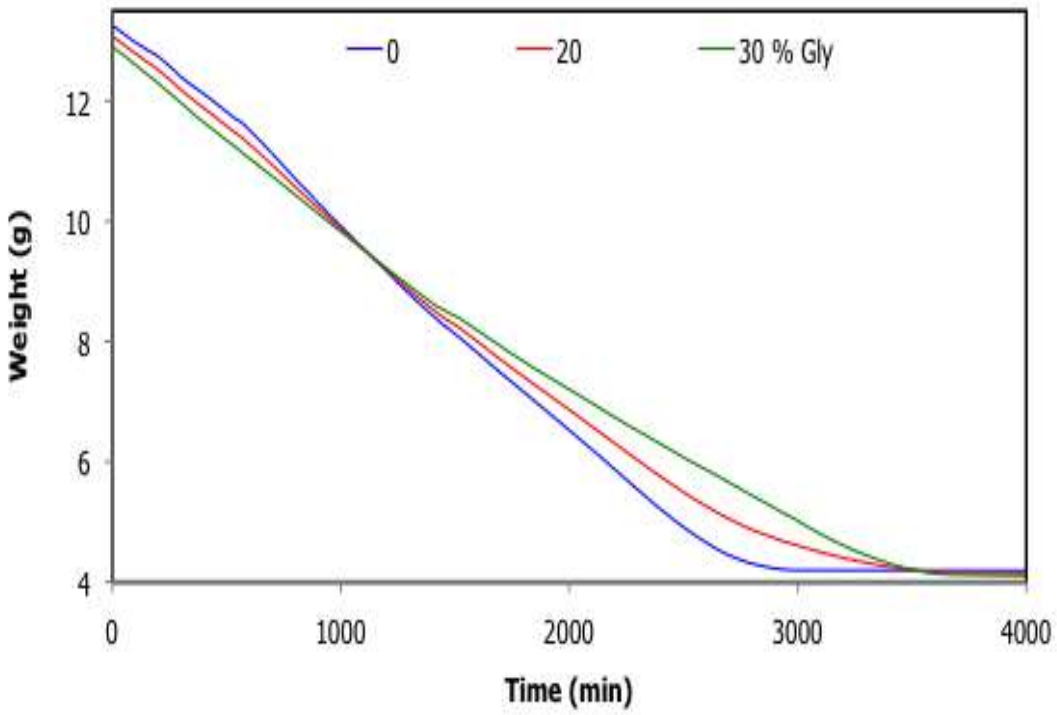


Figure 3.6 Drying time curve of cassava starch films with different concentrations of glycerol at 25°C. The dashed lines represent the constant drying rate trendline

In Figure 3.7 are shown the mass flux of water loss for different samples in function of free moisture (g water/g solids). The drying process begins with an initial short period that allows for the film surface that is heated to reach similar conditions as the air (A to B). This first was marked to films without glycerol while the plasticized films showed this phase less marked. This period is normally considered insignificant compared with the other two periods of drying process. The next phase is constant rate period (B to C) where the solution surface was

saturated of liquid water due to movement of water from the interior to surface and from the surface to the environment, showing significant reductions in moisture content. This phase occurred between 500 and 3000 min of drying and observed that the plasticized films increased the mass flux of water compared with unplasticized films. At a certain point in drying process where the gel surface began to dry due to decrease of the water movement from interior to surface, this phase is called the falling rate period (C to D). This behavior was observed at 2250 min, 2500 min and 3150 min to the films with 0, 20 and 30% glycerol respectively.

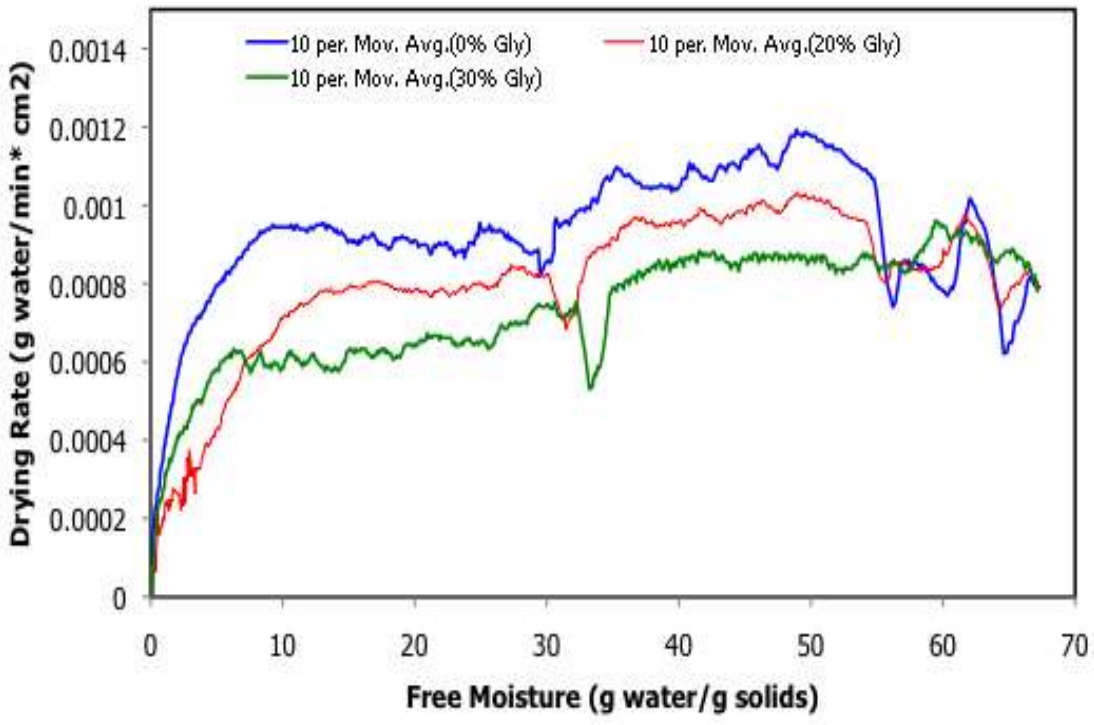


Figure 3.7 Mass flux of water in cassava starch films with different amounts of glycerol during drying at room temperature

Using the drying curve rates is possible to estimate the drying time of films during constant rate period. Figure 3.6 was used to calculate the slopes (constant drying rates) of three drying curves with different glycerol contents and with Figure 3.7 was obtained the free moisture values during this phase. The determination of the length of the constant rate period, can be expressed by:

$$R = -\frac{Ws}{A} * \frac{dX}{dt} \tag{17}$$

Where R= rate of drying, Ws (mass of dry solids in grams), A (the exposed surface area in cm^{-2}), X (free moisture content in grams water/g of dry solids) and t (drying time in seconds). By integration of this equation between $X=X_1$ for t=0 and $X=X_2$ for t2=t the drying time in minutes is:

$$t_c = \frac{Ws}{A * R_c}\left(X_1 - X_2\right) \tag{18}$$

Where Rc is the constant drying rate (grams water/min cm^2). Table 3.3 shows time during constant rate period obtained to films without plasticizer and plasticized films. It can be seen that unplasticized films obtained short times, around 2280 minutes, than plasticized films that have 2311 and 2786 minutes for 20 and 30% glycerol content (100 g starch) respectively. This could be attributed

to the hygroscopic nature of glycerol that bind more water to films during drying process *[68]*.

Table 3.3. Parameters obtained during constant drying rate for three different concentrations of glycerol in cassava starch films.

% Glycerol Content	**Rc** (g H_2O/min * cm^2)	**R^2**	**X_1** (g H_2O/dry solids)	**X_2** (g H_2O/dry solids)	**Ws** (g)	**tc** (min)
0	-0.0245	0.998	48	8	4.190	2280
20	-0.0216	0.995	53	12	4.143	2311
30	-0.0188	0.992	57	7	4.097	2786

3.1.3 Conformational changes during drying of cassava starch solutions

Upon complete gelatinization and solubilitization of starch, retrogradation takes places in the system. To study this reorganization of starch molecules after heat treatment, on-line Raman spectroscopy scanning allows a measurement of this process during drying time of films. In the beginning of drying, freshly prepared starch films are basically amorphous [5] and with time amylose and amylopectin are able to reorganize into a organized structure. In Figure 3.8 is possible to observe a typical series of Raman spectra taken immediately after casting the film at the beginning of drying of films. Three different films were compared based on glycerol content (0, 20, and 30%).

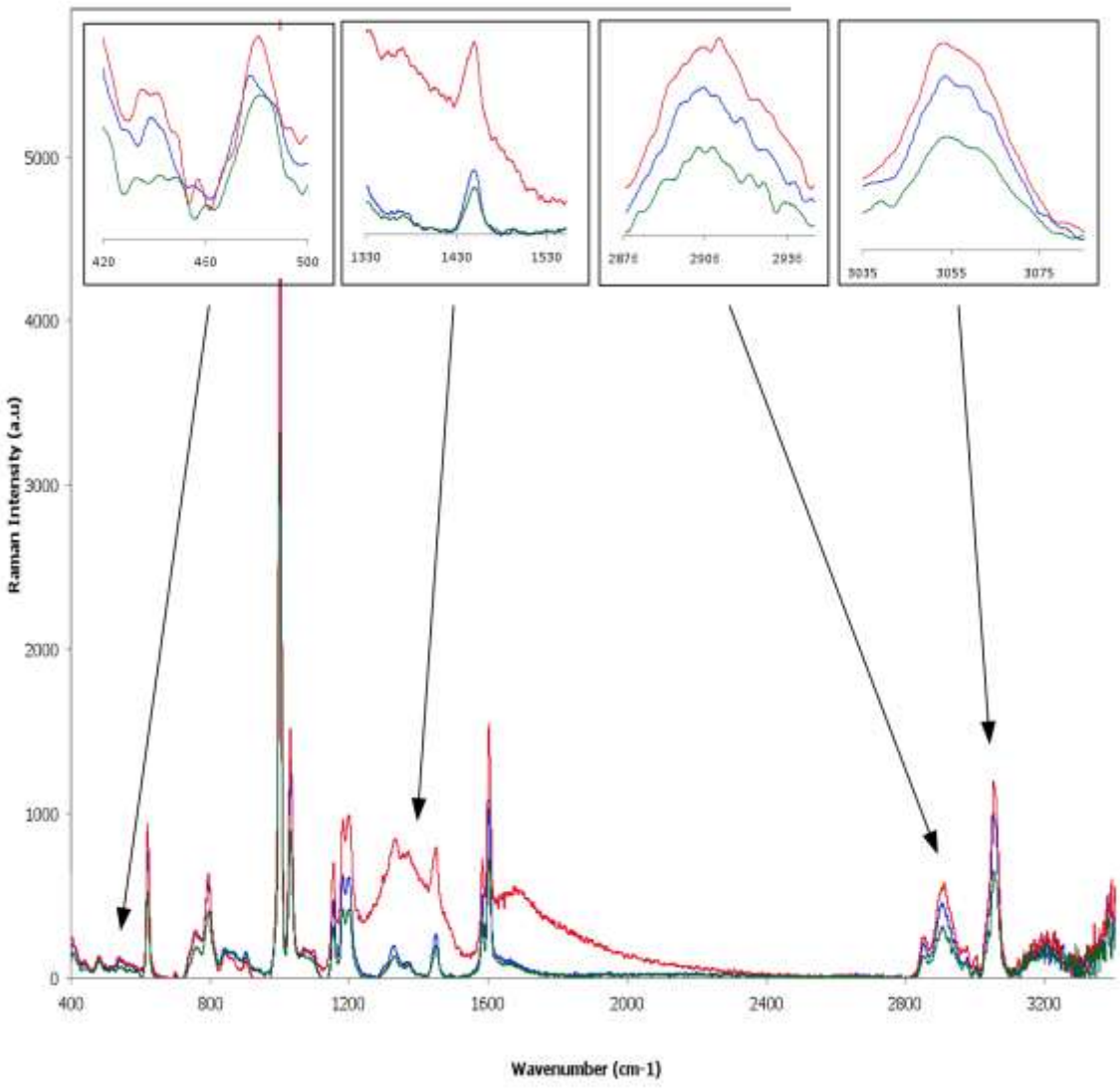


Figure 3.8 Series of Raman spectra taken after casting the cassava starch films with different glycerol contents.

Some differences in terms of band shape and intensity can be observed in the cassava starch films because of adding glycerol. Skeletal modes of pyranose ring show vibrations below 800 cm^{-1} with a typical band at 478 cm^{-1} *[36].* In films without glycerol this peak was observed at 477.6 cm^{-1}, became more prominent and presented a displacement to 481.2 cm^{-1} for 20% glycerol concentration, in

the other hand films with concentration of 30% presented a decrease in intensity but a displacement to 481.5 cm^{-1}. Also was observed that peak at 1449 cm^{-1} assigned to CH_2 deformation was modified to 1449.6 cm^{-1} for films with glycerol. Another interesting peaks affected by glycerol content are those between 2800 and 3050 cm^{-1}. These peaks, initially observed at 2910.60 cm^{-1}(CH stretching modes) in films without plasticizer, were shifted to 2909.70 cm^{-1} and 2908.50 $cm^{-1}$for films with 20% and 30% glycerol (100 g starch). Also the peak to CH deformation at 3053.7 cm^{-1} for 0% glycerol content was displaced to 3053.4 cm^{-1} and 3052 for 20 and 30% of glycerol (100 g starch) respectively.

To observe this evolution of firm forming solutions into a gel were observed the shifts in Raman bands in a continuous measurement (10 minutes) of spectra. In Figure 3.9 can be seen the time evolution (24 hours) of Raman band at 480 cm^{-1} (skeletal modes of pyranose ring) for films without and with glycerol (20 and 30). Vans Soest *[69]* has proposes that retrogradation as a multi-stage process. The fist stage was ascribed to conformational ordering of amylose and short-range ordering of amylopectin chains. The second stage was described as an induction time for the onset of amylopectin helix aggregation. In stage three, amylopectin aggregation and crystallization proceeds and finally the last stage involve separation of water. Based on our results, it is possible consider the retrogradation mechanism in films as a process of two stages. In the initial phase film with 0, 20 and 30% of glycerol started the retrogradation process at 360, 720 and 825 min, respectively. It is clear that films with glycerol need around

the double of time to start this process. During this stage Raman shift might be considerer as constant when two or more starch chains may form a simple juncture point which then may develop into more extensively ordered regions [12]. The second phase the Raman shift has a tendency to decrease the wavenumber of spectra showing the evolution of the solution into an ordered structure, and it could be refer to amylopectin aggregation. Therefore, films with glycerol trap more water into the solution and the tendency to reassociate and form hydrogen bonds is bigger in plasticized films.

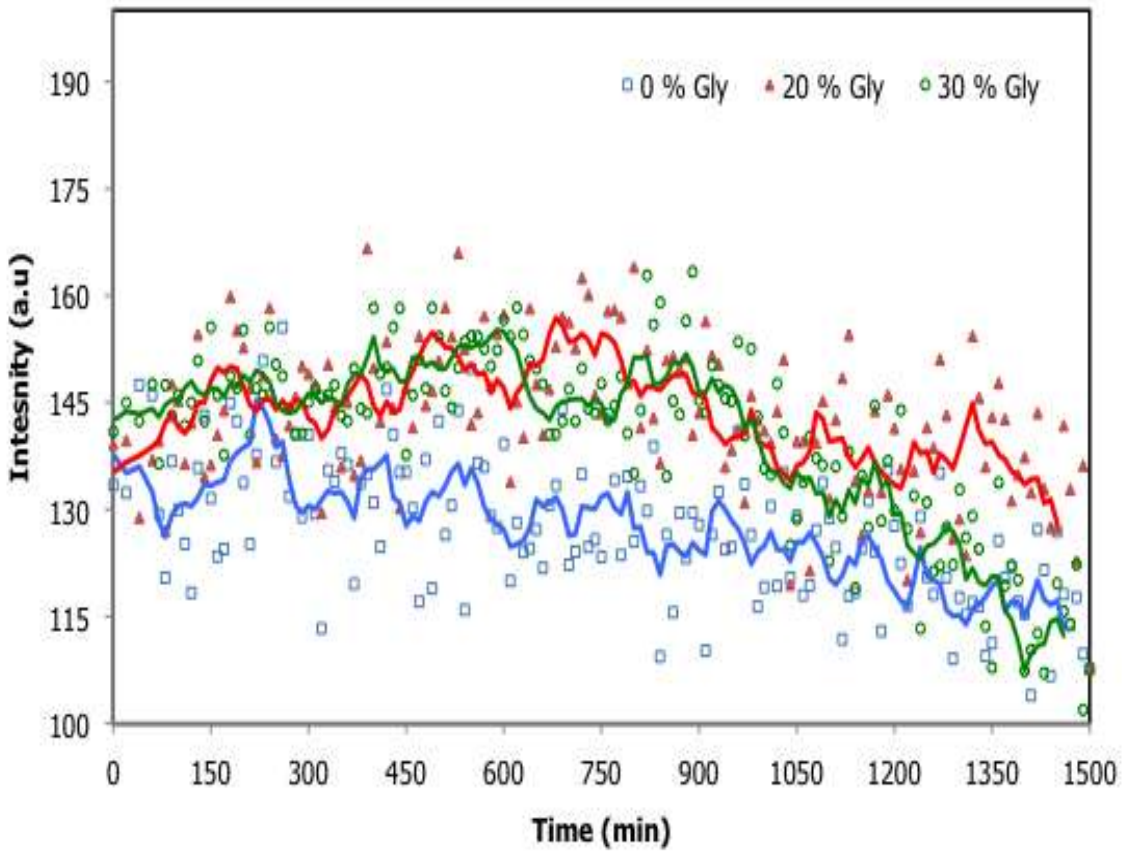


Figure 3.9 Raman band at 480 cm^{-1} for 0, 20 and 30% glycerol with time (24 hours).

3.1.4 Basic physical properties of stand alone films

Polymeric films should be uniform and free of defects for their applications. Uniformity of the films is critical for functionality. During the drying process, films could present cracks and shrinkage, due to polymer concentration and temperature and/or speed of drying. Consequently, this section shows how the concentration of polymer and plasticizer affect the visual appearance of the films.

Films obtained from starch solutions were translucent and they showed a homogeneous and transparent appearance, smooth surfaces without pores and cracks. It was possible to obtain stand-alone films without plasticizer, which indicated that starch is a good matrix-forming material. However films without plasticizer remained brittle for 1 and 2% of cassava (w/w). The addition of glycerol, increased starch films flexibility, making them easier to handle. The maximum compatible concentration of glycerol in the formulations was 40% (dry basis). When this limit was exceeded, phase separation occurred, leading to a physical exclusion of the plasticizer from the film, which corresponded to an extra adhesiveness of the films and an undesirable sticky aspect. Figure 3.10 shows how the concentration of cassava, water and plasticizer affect the appearance and characteristics of the films. This schematic illustration showed the approximate amounts of 3 components in the system, appropriate to obtain films with good appearance. Inside of yellow spot can be categorized transparent, flexible, elastic and easy to handle films. To study how the amount of plasticizer affected the characteristics of the films was chosen the

concentration of 3% cassava because it covers films with better characteristics between 0 to 50% glycerol (100g starch) compared with the others cassava concentrations.

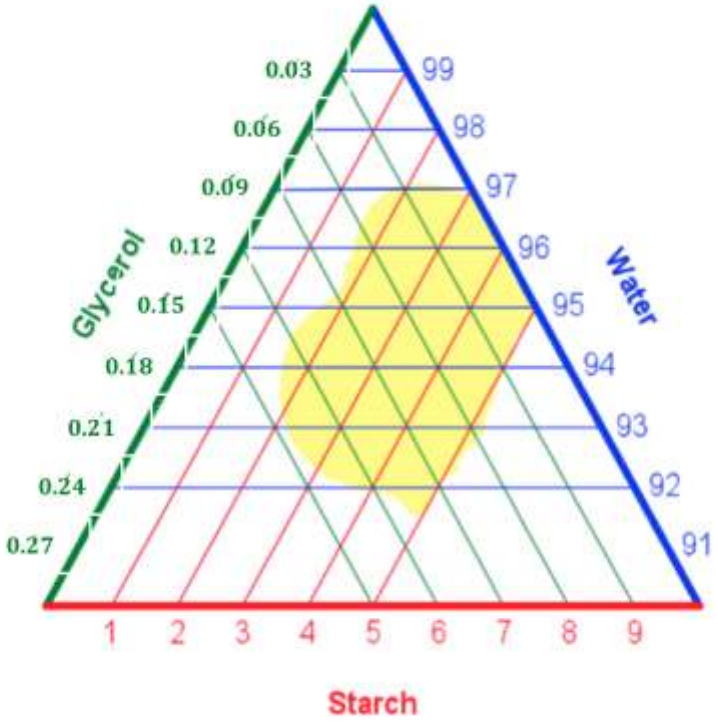


Figure 3.10 Ternary Diagram of the Appearance of cassava starch films.

3.1.5 Optical properties and morphology of films.

In general the unplasticized films showed an increase in gloss as the starch concentration increased (Figure 3.11). It could be attributed to surface roughness, at low starch concentration; the uneven surface film cannot form a continuous film and the gloss measurement in different points of it showed dissimilar values. In the case of plasticized films the general pattern showed a decrease in gloss as the glycerol content increased. It effect could be explained

by the interaction of glycerol in films (Figure 3.11). At high glycerol concentration (> 40%), physical exclusion of plasticizer can be seen in the surface, showed a heterogeneous film.

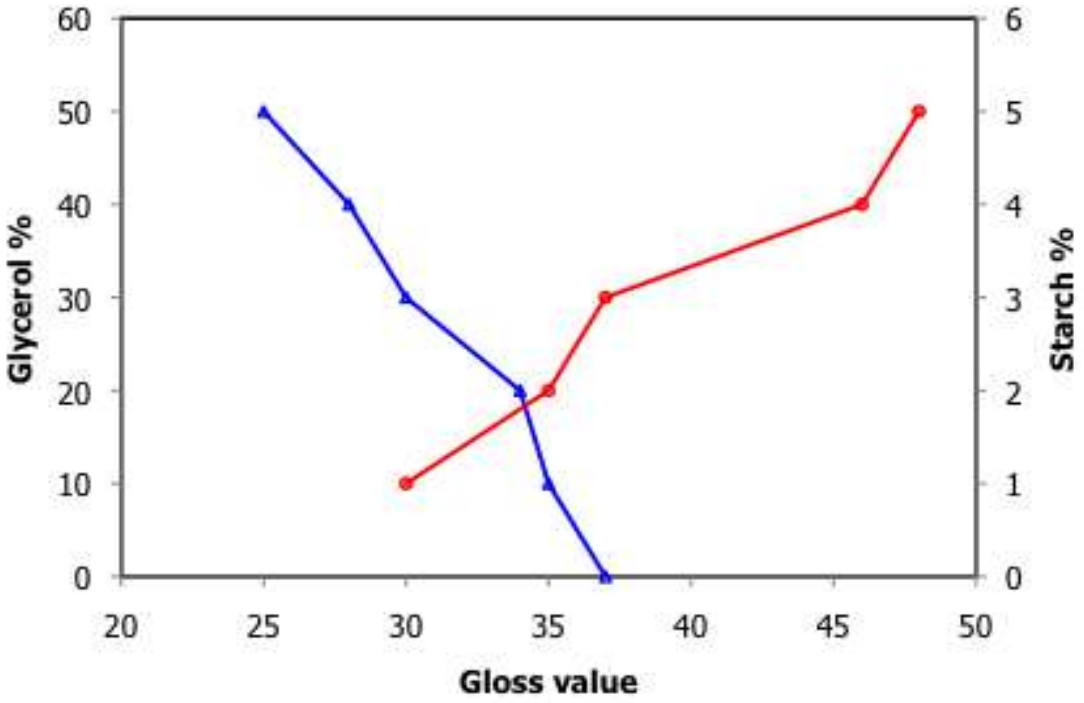
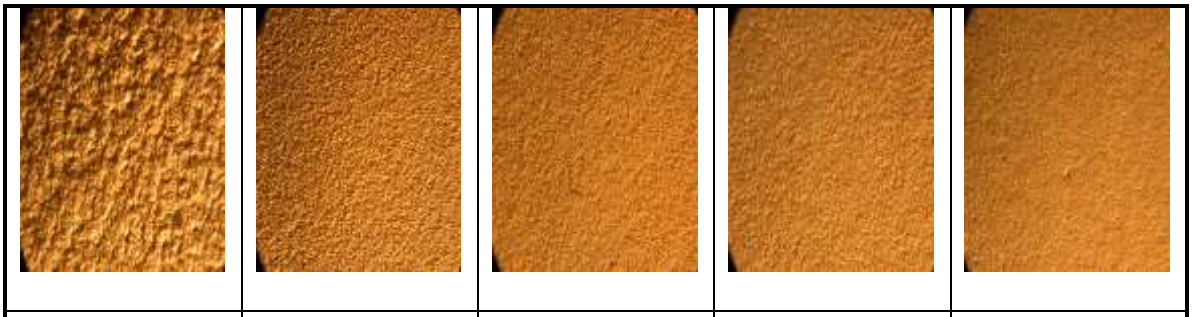


Figure 3.11 Gloss values at 60° angle for films with different content of starch and glycerol

Film microstructure was analyzed with stereomicroscopic images of the surfaces of the pure starch films with five different concentrations (1,2,3,4,and 5% w/w). In Figure 3.12 from left to the right can be seen differences in the structure of the films. Films with a concentration of 1% of cassava showed an irregular matrix with some pores. With increase of cassava concentration, the

obtained films had a continuous structure of sufficient thickness and homogenous appearance.



1% Cas	2% Cas	3% Cas	4% Cas	5% Cas

Figure 3.12 Stereomicroscopic images of unplasticized films with different cassava starch concentration (Zoom 4.9X)

Also, in Figure 3.13 can be observed the structure of plasticized films. The glycerol content of plasticized films has a positive effect in smoothness surface; these films were homogeneous with good structural integrity, they exhibited flat and compact surface with some small particles distributed into the film.



0 g Gly	10 g Gly	20 g Gly	30 g Gly	40 g Gly

Figure 3.13 Stereomicroscopic images (Zoom 4.9X) of plasticized films (3% Cassava w/w) with different glycerol concentration (0,10,20,30,40 g/100 g starch).

3.1.6 Sorption isotherms studies

Water sorption isotherms are useful to determine the stability of the films under different conditions, as many film constituents, especially polysaccharides that are sensitive to relative humidity and temperature *[23].* In this section we will be describe how the concentration of starch and plasticizer affect the water sorption of the films.

3.1.6.1 Water sorption studies for cassava starch films

The sorption isotherms at 25°C of cassava starch films (3, 4, 5 % w/w) were compared in the Figure 3.14. The films needed around 48 Hrs to encounter equilibrium. All sorption isotherms demonstrate and increase in equilibrium moisture content with increasing relative humidity (RH). These isotherms showed a similar sigmoid shape Type II, according to Brunauer's classification *[42]*. It was similarly observed by other authors, who found this behavior in cassava starch *[59, 70].* Moisture content of films was influenced by storage relative humidity (RH). At RH less than 20% all films absorbed almost the same amount of water. When the surrounding relative humidity rose all films took up more water especially films with 5% of cassava. Films with 3 and 4% of cassava had the same moisture content between 20 to 60% RH. When the RH increased between 60 to 85% films with 3% of cassava had the lower moisture content of water followed by films with 4 and 5% of cassava respectively.

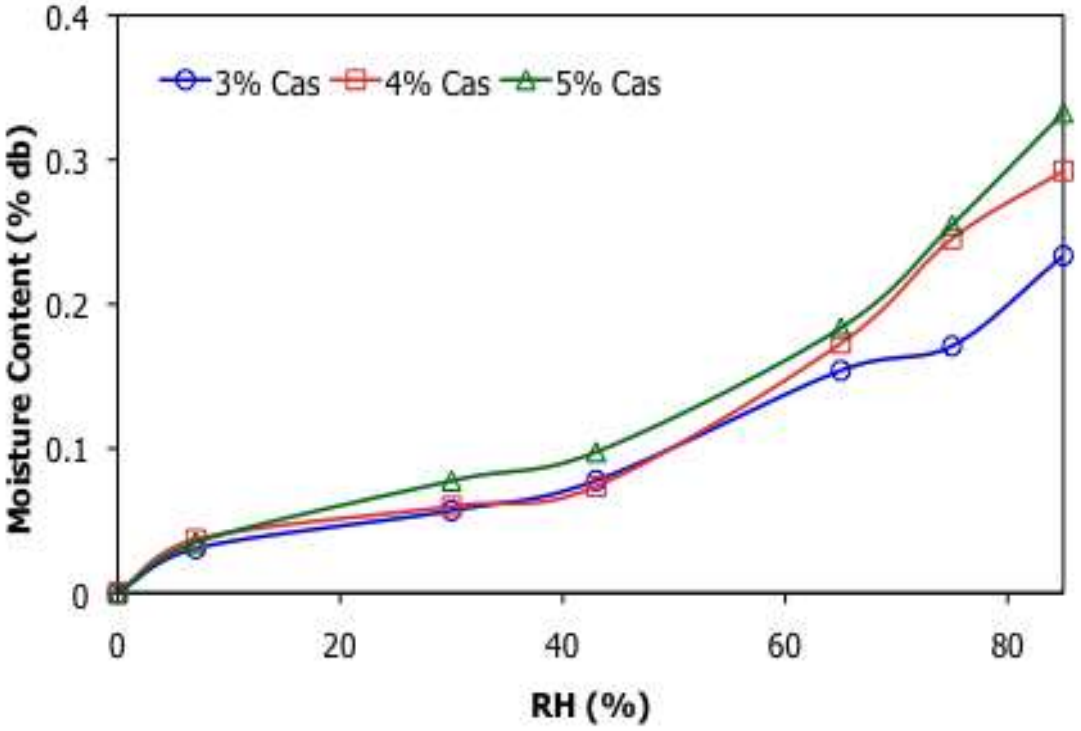


Figure 3.14 Sorption Isotherms of cassava starch films without plasticizer as a function of relative humidity (RH)

3.1.6.2 Water sorption studies for cassava starch films with glycerol

The effect of glycerol concentration on moisture content, at different relative humidity values, can be seen in Figure 3.15. At lower glycerol content (0 -10%), the amount of water absorbed increased very slight for all relative humidity values. When glycerol content reaches more than 20% of starch, film moisture content increased notoriously. These results could be related to structural modifications of starch network produced by the plasticizer. The addition of plasticizer provides more active sites by exposing its hydrophilic

hydroxyl groups in which the water molecules could be adsorbed *[51].* Even though other authors have reported antiplasticizing effect of glycerol in starch films. *Lourdin [71]* and *Chang [72]* reported the minimum film hydration between 10% and 15% of plasticizer content for cassava starch based films.

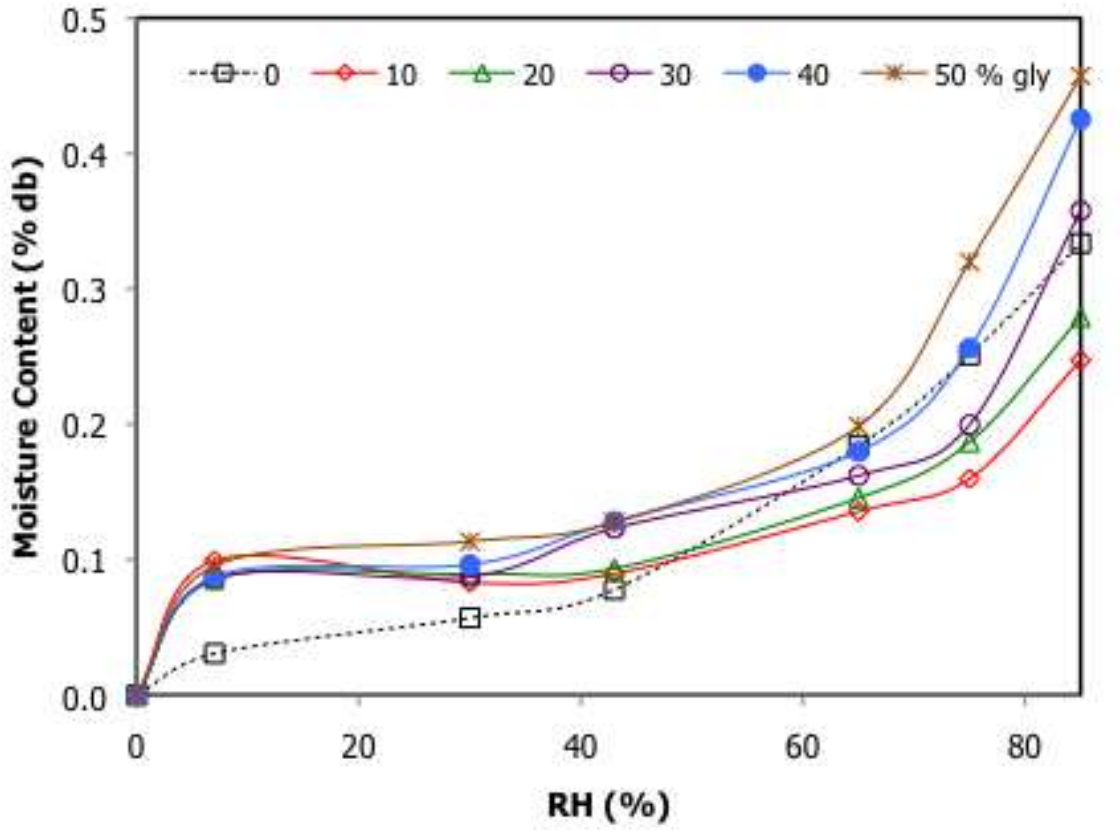


Figure 3.15 Moisture content of 3% cassava starch films as a function of glycerol content and relative humidity.

The data obtained were adjusted to five different sorption models commonly applied to starchy products *[59].* Linear and non-linear regression statistical analyses were performed and the quality of the fitting was evaluated through the R^2 (Table 3.4).

Table 3.4 Sorption isotherm model constants and confidence fit (R2) of cassava starch films (3%Cassava) with different glycerol contents.

Model	Constants	Glycerol content (%)					
		0	**10**	**20**	**30**	**40**	**50**
BET	m_o	0.0409	0.0561	0.0489	0.0648	0.0702	0.0849
	C	24.813	19.102	20.789	16.042	14.802	12.095
	R^2	0.904	0.9647	0.9252	0.9765	0.9679	0.9745
GAB	*mo*	0.0534	0.0854	0.0512	0.0812	0.084	0.0966
	C	13.638	32.693	-71.574	44.672	104.8	97.331
	k	0.9344	0.8632	0.9793	0.9355	0.949	0.9652
	R^2	0.8548	0.8897	0.9025	0.9131	0.872	0.8569
Halsey	*A*	-2.6944	-2.1895	-2.3817	-2.1044	-1.9825	-1.8349
	B	-0.7486	-0.6187	-0.6234	-0.6384	-0.6003	-0.6264
	R^2	0.9811	0.9683	0.9194	0.9817	0.9342	0.95
Oswin	*A*	0.0992	0.1538	0.1272	0.1691	0.1873	0.2201
	B	0.4896	0.4055	0.3898	0.4094	0.38	0.3963
	R^2	0.9803	0.9716	0.8394	0.943	0.8742	0.882
Smith	*A*	0.0203	0.0427	0.0131	0.037	0.0453	0.0414
	B	-0.1131	-0.1517	-0.1574	-0.1811	-0.1937	-0.02
	R^2	0.9896	0.9312	0.8237	0.9521	0.9297	0.9388

The Smith model fits well for water activities in the range 0.4-0.9. The Smith constants A and B lie in the ranges -0.1937 to -0.02 and 0.0131 to 0.0453 respectively and the confidence fit was between 0.82-0.98. The Oswin model is applicable for water activities between 0.5-0.9.The Oswin constants A and B fall within the ranges 0.0902 to 0.2201 and 0.38 to 0.4896. The confidence fit was in the ranges 0.83 to 0.98. The Halsey and BET models depicted better the moistures sorption of cassava films, which had a confidence fit range more than 0.90. The Halsey model has a range of applicability for water activity between 0.1 - 0.8. The Halsey constants A and B varied from -2.69 to -1.83 and -0.74 to -0.62 respectively. On the other hand BET model provide other parameters such

as monolayer value, important to obtain the amount of water that is being trapping on the surface of the film. However The BET equation is generally applicable up to water activities (a_w) values of 0.5, because capillary condensation becomes important and the model is not applicable above this water activity. Having is in consideration the minimum monolayer value found was to unplasticized films (0.0409 g H_20/g solids) and the maximum was to plasticized films with 50g/ 100g of starch. The monolayer water content increased as the glycerol content increased to all films, except to the film with 20g/100g of starch. The GAB isotherm equation is an extension of the BET model, taking into account the modified properties in the multilayer region with the introduction of a constant (K). In literature GAB model has been recognized for modeling the moisture sorption isotherms *[58],* and other studies with cassava starch have demonstrated the applicability of the model *[51, 59, 73].* The GAB parameters for unplasticized films and plasticized films (20g/100g of starch) presented the lowest monolayer value (0.0534 and 0.0512 g H_20/g solids, respectively) and the highest monolayer value (0.0966 g H_20/g solids) was observed to higher plasticized films (50g/100g of starch) and the values of R^2 for GAB model were between 0.85-0.90. In accordance with these two models (BET and GAB) the glycerol concentration affects in notable form how the films interact with water. Also, if we compared the results of GAB and BET monolayer values (m_o), the data reported higher m_o for GAB than BET.

Also, in Figure 3.16 can be observed the relationship between water activity for films with different glycerol content and relative humidity of the environment. At relative humidity less than 40% all films showed a significantly increase of water activity, except the films with 20 g glycerol (dry basis) that showed an increase less than the other films. To relative humidity between 40 and 65% the increase of water activity was lineal to all films. And the last region between 65%-85% RH, the films increased their water activity as glycerol content increased. A possible effect that depresses water activity in films with 20 g glycerol (dry basis) could be attributed to the capillary effect. The presence of capillaries (pores) in these films can trap more water molecules that interact with each other decreased the available water on the film surface.

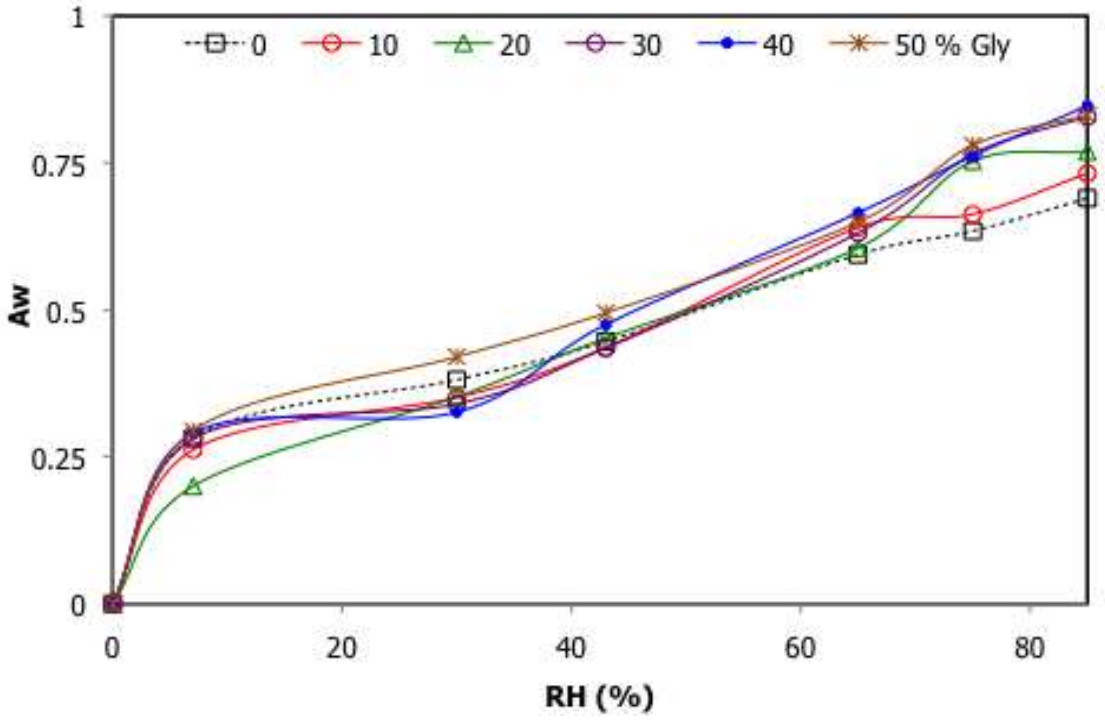


Figure 3.16 Water activity as a function of Relative Humidity of the environment (different glycerol content)

From the point of view of water adsorption mechanism the isotherm showed two different regions: below 0.5 Aw all plasticized films binding more water than unplasticized films and above this water activity the effect was opposite, then unplasticized films had more water content than plasticized films. In films with glycerol, there are interactions between water molecules and hydroxyl groups of glycerol. As hydroxyl groups located at both ends of glycerol backbone there are more accessible to water molecules than the glucose molecules of starch *[74].* Probably these end hydroxyl groups of plasticizer are also more available to form hydrogen bonding with water during film formation resulting in increase amount of hydroxyl groups that could be accessible to bind water molecules at low water activities. Furthermore, at constant Aw of 0.5 the films with less water content were which containing 10% of glycerol. This minimum could correspond to the saturation of starch-binding sites, that it depends on the availability of these sites *[75].* The combination of H-bonding of starch with water and glycerol is stronger when the amount of glycerol added is low and the water activity is around of 0.5, at this point all the starch sites available were occupied by water or glycerol and these films could not bind more water in their network.

3.1.7 Changes of thermal properties of cassava starch films with the addition of glycerol

Differential scanning calorimetry (DSC) is a powerful tool used to investigate thermal properties and phase transitions of starch. Film preparation

affects the thermal properties of the films. Accordingly Endothermal and exothermal changes in a DSC curve indicate transitions or reactions such as glass transition, gelatinization and melting, occurring during DSC testing *[76].* DSC has been often used to investigate the influence of plasticizers on glass transition (Tg) of polymers. For instance, homogeneous mixtures have only one Tg, whereas heterogeneous (immiscible blends) show the separate glass transitions of the components *[77].* In this study all the thermograms (Figure 3.17) showed only one transition could be observed for the samples analyzed, then the glycerol, cassava starch and water created a homogeneous mixture.

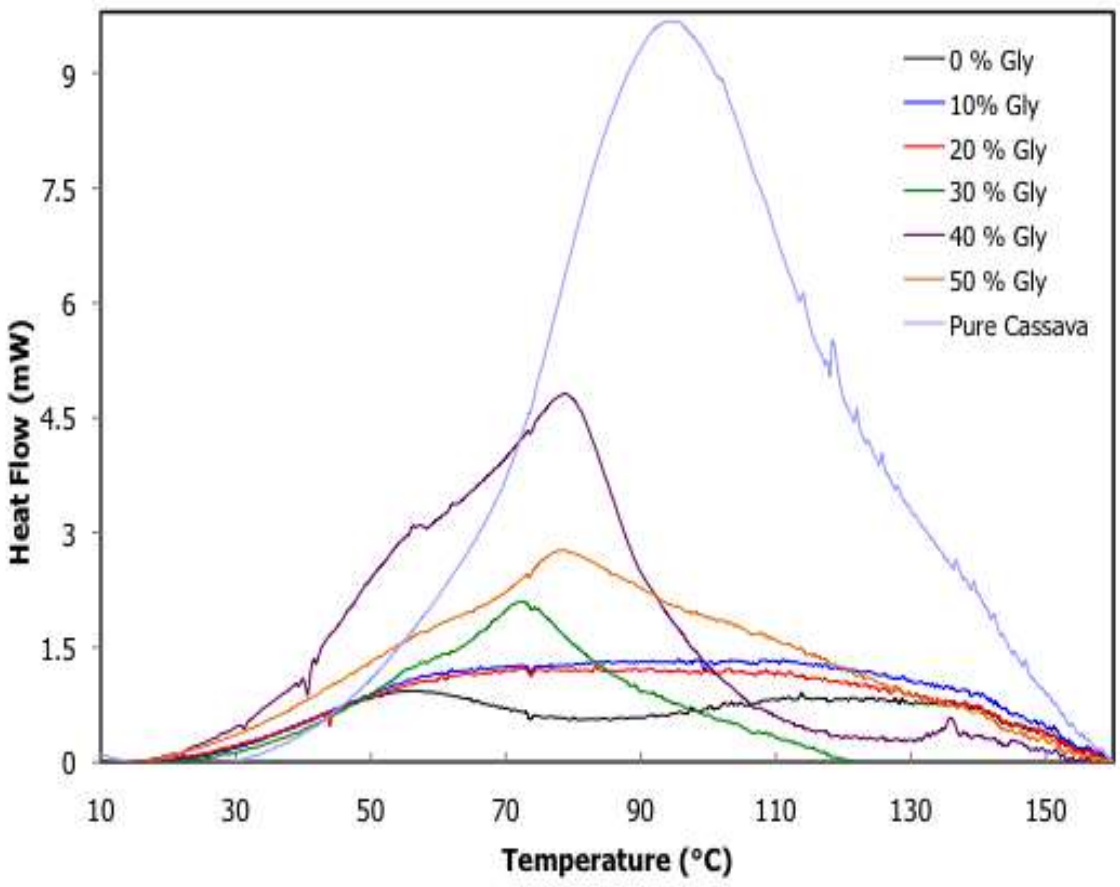


Figure 3.17 DSC thermogram for cassava starch films with different contents of glycerol

Once defined that the mixture is homogeneous is suitable establish the temperature (Tsg) and enthalpy of gelatinization (∆Hsg). Figure 3.17 shows a typical DSC curve to determinate gelatinization parameters of starch. This figure showed transitions to different samples with peak temperatures between 50°C and 80°C. This peak is related to the starch gelatinization and apparently both the temperature and the area correspond with the starch variety *[78]*. The area between the base line and the thermogram represents the gelatinization enthalpy, which is the energy necessary to complete the process of gelatinization and this depends on a number of factors like crystallinity, intermolecular bonding, rate of heating of the starch suspension and the presence of other chemicals.

Figure 3.18 showed the relationship between glycerol concentration in films with gelatinization temperature and enthalpy. For cassava starch, the values reported in the literature for gelatinization temperature range between 64 - 74°C and for gelatinization enthalpy range between 4.8 - 16 kJ/kg *[19].* Therefore, the values found during this experiment are among the ranges reported in the literature. Also, it is clear from the Figure 3.17 that gelatinization temperatures and enthalpies increased when the quantity of glycerol is enhanced and it indicated that more energy is required to initiate starch gelatinization. It has recently been reported that the addition of high molecular weight plasticizers

such as polyols in mixture of water and starch increase the gelatinization temperature of starch and that the gelatinization temperature of starch is related to the plasticizer concentration *[78]* Also, Habitante *[76]* has studied that increasing the glycerol content, increases the gelatinization onset and peak temperatures of starch dispersions with glycerol solutions. Consequently, to relate the glycerol concentration with the other two variables, the data were fitted to a polynomial regression, with R^2=0.981 for equation 19 and 0.954 for equation 20.

$$T_{sg} = 53.748 + 1.0625X - 0.115X^2 \quad (19)$$

$$\Delta H_{sg} = 6.52 + 0.659X - 0.0046X^2 \quad (20)$$

These results suggest a strong interaction between water-starch-glycerol than water-starch. Probably, because glycerol has larger molecular size and the capacity to form hydrogen bonding either with water or starch.

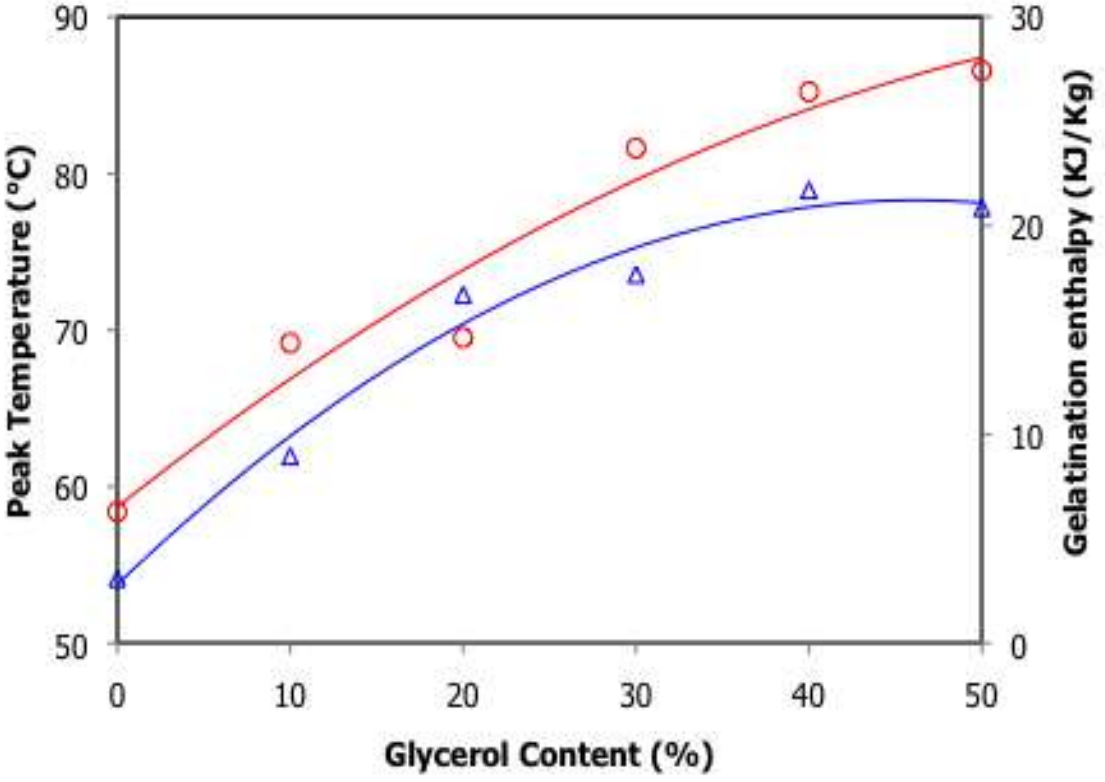


Figure 3.18 Starch gelatinization temperature and enthalpy for films with different glycerol concentrations (0-50%) Blue line (peak temperature) and Red line (Enthalpy)

3.1.8 Mechanical properties of cassava starch films

The mechanical properties of films depend on the type of film forming material and its structure. Also, it depends on the film forming conditions such as evaporation rate and production (casting, knife coating, etc). In this section will be discussed the deformation at break and tensile strength according to polymer and plasticizer composition.

3.1.8.1 Effects of starch content

The relationship between cassava starch, tensile strength and elongation at breaks is represented in the Figure 3.19. The tensile strength values of starch films containing 2, 3, 4, and 5 % cassava were 27.72, 33.42. 43.75, and 44.33 MPa, respectively. These changes in tensile strength of films are giving by the strengthening the intermolecular forces between starch molecules. Moreover, the elongation at break values of films with 2, 3, 4, and 5 % cassava were 0.015, 3.60, 4.94, and 5.094 %.

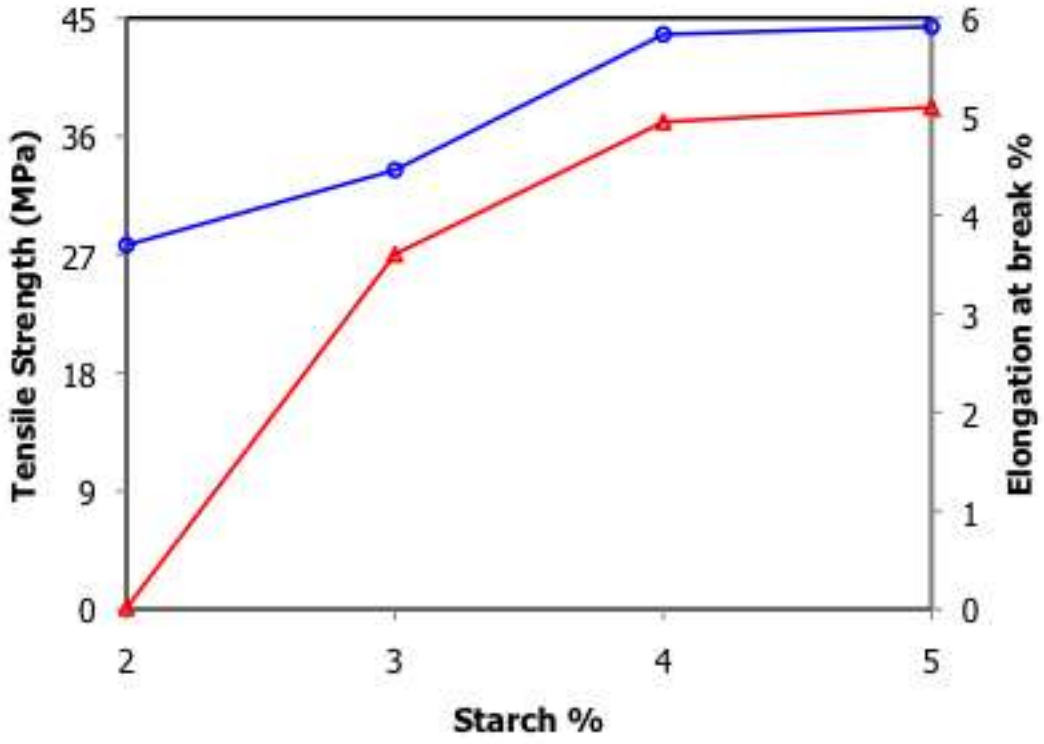


Figure 3.19 Effect of starch concentration on tensile strength and elongation at break of films.

3.1.8.2 Effects of glycerol content

In general, all starch films plasticized with polyols behaved like viscoelastic materials. In the Figure 3.20 obtained in the mechanical experiment there was first a linear part that shows elasticity of material and obeys Hook's law. This linear region is used to calculate Young's modulus, which is a measure of material stiffness. The second part is followed by a curve that in the end is reaching a maximum force before at break.

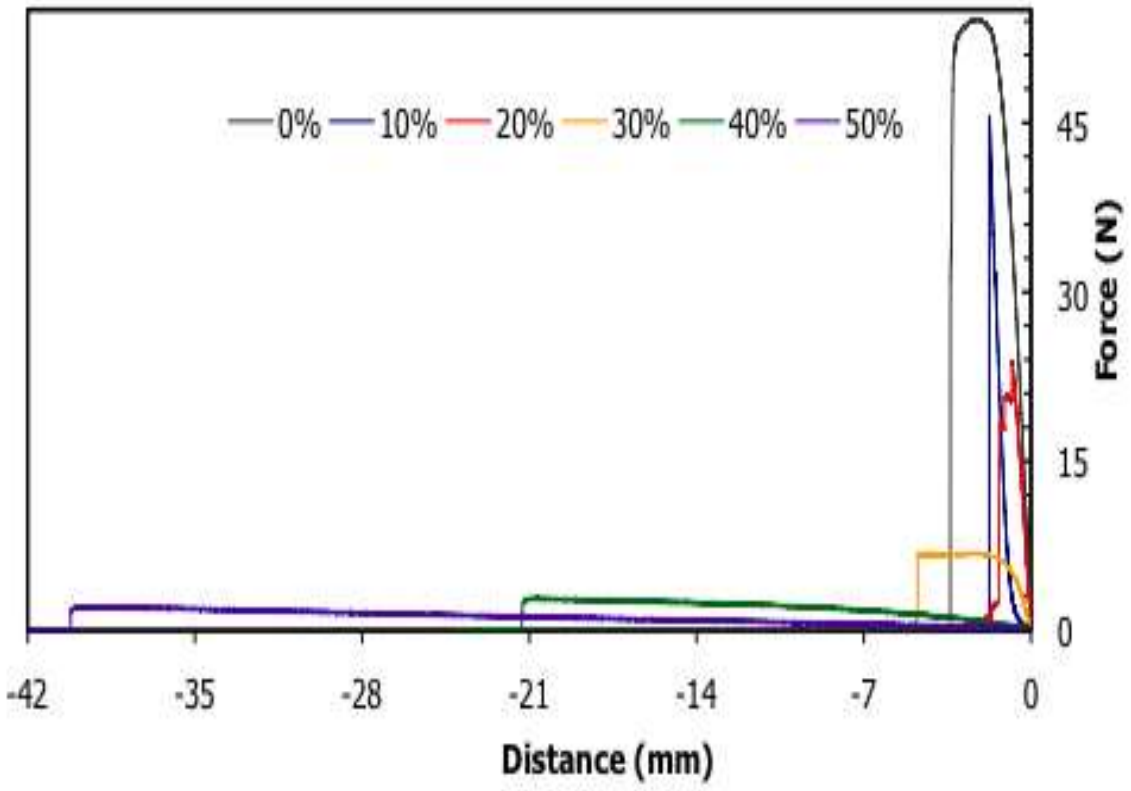


Figure 3.20 Force Vs Distance curves of cassava starch films with different amount of glycerol.

Based on this curves is possible to calculate the other parameters. In Figure 3.21 is showed the effect of glycerol content on tensile properties of

plasticized films. The tensile strength values of 3% of starch films containing 0, 10, 20, 30, 40, and 50 % glycerol were 33.42, 31.14. 14.74, 1.79, 1.29, and 0.88 MPa, respectively. It is clear that as increasing the amount of glycerol, especially around 10% glycerol decreases substantially the tensile strength. This trend probably is due to the reduction in interactions between the polymer chains and is well know and discussed in the literature *[29, 51]*. The elongation at break values of films with 0, 10, 20, 30, 40, and 50% glycerol were 3.55, 1.44, 1.74, 4.57, 21.96, and 41.98 %. Accordingly with the elongation at break values, it is found that the addition of 10 and 20 % glycerol decrease the elongation values. However, as increasing glycerol content above 30% the elongation values increase notably. Thus, it appears that glycerol can exert an antiplasticizing effect because glycerol did not affect the extensibility of plasticized films when it is introduced at low levels. Some authors *[71, 72]* have been reported the antiplasticizing effects on starch films. They reported that the inclusion of plasticizer could produce an antiplasticizer effect when present in low concentrations (15%), by inducing rigidity in the glassy material due to a decrease in flexibility and an increase in the elastic modulus. Also, *Gaudin [79]*, the cause of this behavior has not been clearly elucidated, but it would appear that local molecular nobilities play an important role in this mechanism.

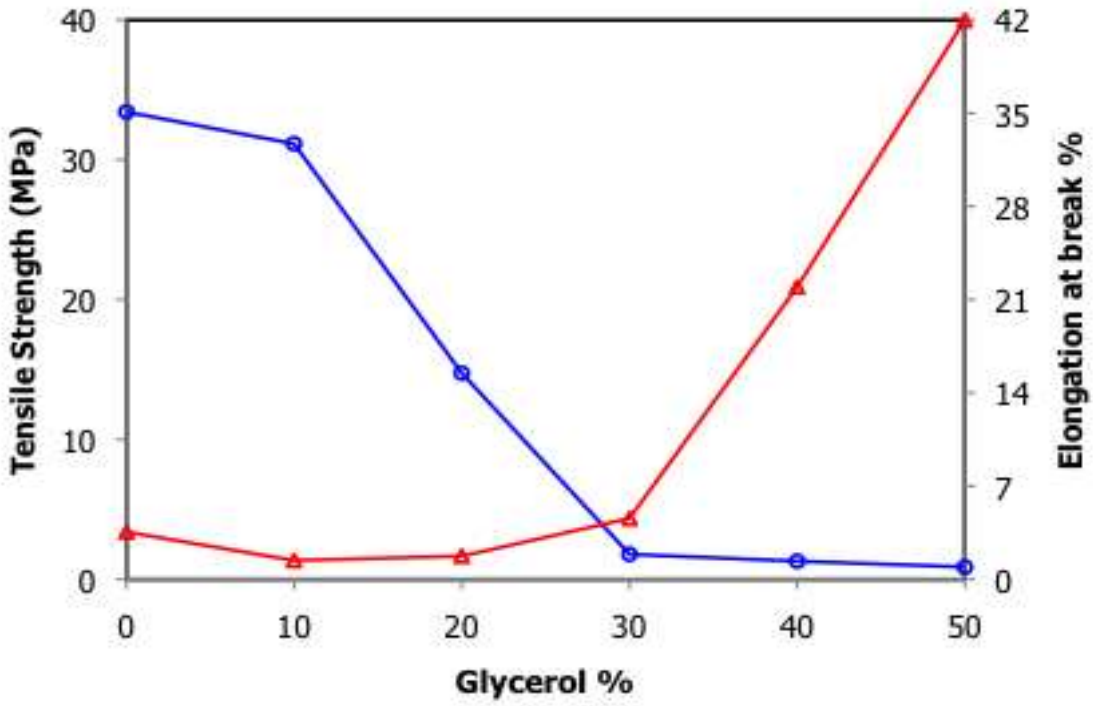


Figure 3.21 Effect of glycerol concentration on tensile strength and elongation at break of 3% cassava starch films.

3.1.9 Interaction between water-starch-glycerol

To calculate the free energy of mixing of our solutions were used data reported earlier of starch-water-solute systems by Habeych et al. *[80].* Table 3.5 presents these predicted Flory-Huggins parameters. Where water is represented as component 1, starch as component 2, and glycerol a component 3. Also to calculate the volume fraction of each component the next equation was used:

$$\varphi_1 = \frac{\varphi_1}{\varphi_1 + \varphi_2 + \varphi_3} \qquad (21)$$

Table 3.5 Flory-Huggins parameter to water-starch-glycerol.

Partial molar volumes (cm^3/mol)			**Interaction parameters**		
Water	Starch	Glycerol	χ_{12}	χ_{13}	χ_{32}
18.1	97.5	73	-0.4	0.21	1.64

With all parameters was possible to obtain the Gibbs free energy of mixing (equation 6) for solutions with and without plasticizer. Figure 3.22 shows the Gibbs free energy of mixing Vs cassava composition. The dashed line represents a hypothetically mixture of starch and water with concentrations between 1 to 99% of starch. In addition, it is possible to study our real values of cassava mass fraction during drying process of films and calculate the Gibbs free energy of mixing for films. Based on Figure 3.7 we calculated the mass fraction of cassava at the beginning of drying process, constant rate period, falling rate period, and when the film was completely dried (Table 3.6). For all concentrations of starch, the curves are located in the region of negative values, which is indicative of the spontaneous formation of starch-water-glycerol and thermodynamic stability of all systems.

Table 3.6 Mass fraction of water, cassava starch and glycerol during drying process.

Drying process	Components %	Films with different glycerol content (%)		
		0	**10**	**20**
Initial	H_2O	97.0	96.94	96.91
	Cassava	3.0	3.0	3.0
	Glycerol	0.0	0.06	0.09
Constant	H_2O	96.30	96.25	96.16
	Cassava	3.67	3.67	3.72
	Glycerol	0.0	0.08	0.12
Falling	H_2O	85.60	85.41	81.00
	Cassava	14.40	14.30	18.44
	Glycerol	0.0	0.29	0.56
Final	H_2O	57.60	54.53	51.76
	Cassava	42.50	44.57	46.83
	Glycerol	0.0	0.9	1.41

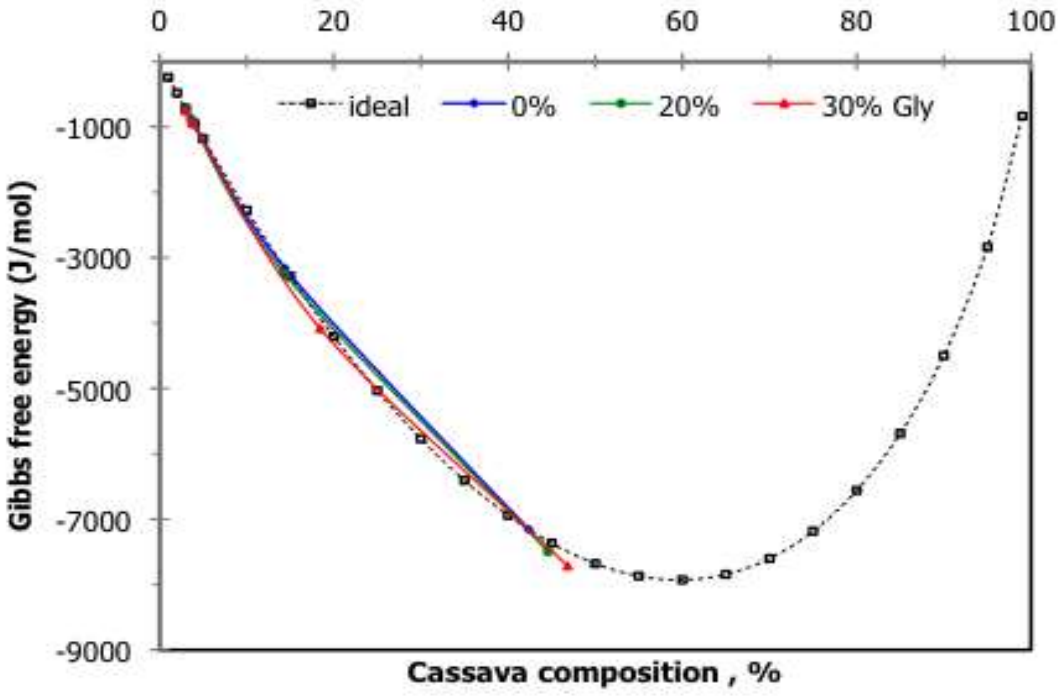


Figure 3.22. Plot of Gibbs free energy as a function of cassava composition.

3.1.10 Conclusion

The effects of concentration of starch and glycerol are concludes as follow:

- Cassava starch solutions with and without plasticizer exhibited a shear-thinning behavior at temperatures between 35°C and 85°C. The increase of starch in solutions yielded paste more viscous deviating even more from Newtonian behavior. Also, the temperature affected the solutions decreased their viscosity with the increase of it. Regarding on the better model that depicted the flow behavior of cassava starch solutions, was found that Power Law model showed R^2 >0.94. In relation to how the glycerol changed the viscosity of solutions could conclude that at concentrations less than 30% glycerol the viscosity decrease around 60% compared with unplasticized solutions. Also, concentrations above 40% glycerol, exhibited viscosities similar to unplasticized films at temperatures between 35°C and 85°C. Another important parameter found was the flow index (pseudoplasticity of solution) was influenced by temperature and glycerol content. The flow index increased with increasing temperature and glycerol content but is behavior was marked in films with 20% glycerol when the solutions exhibited a behavior closer to Newtonian behavior (n=0.61) compared with unplasticized films and films with 50% glycerol (n=0.43 and 04.9, respectively).
- The drying of cassava starch films was investigated at various glycerol contents from 0 to 30% Glycerol. It experiment concluded that films

presented two important periods of drying: the constant drying rate and falling drying rate. Unplasticized films showed an initial short period at the beginning of drying, when the film found equilibrium with environment, it could be attributed to the difference in temperature between the film forming solution and the air, probably a suddenly change in room temperature led this phenomenon. Regarding on how glycerol affected the drying process can be observed that unplasticized films had a constant rate bigger tan plasticized films (0.0027, 0.0026 and 0.0019 g/min cm^2). As well this behavior can be appreciated observing the times during const drying rate for unplasticized films the time was around of 2280 minutes and increased to 2311 and 2786 minutes for films with 20 and 30% Glycerol (dry starch), respectively.

- Raman spectroscopy was used as a non-invasive and on-line technique to monitor the retrogradation of films during drying and allowed observing conformational changes at molecular level. The incorporation of glycerol into films shifted to higher wavenumber Raman bands associated to skeletal modes of pyranose ring at 480, 1450, 2800 and 3050 cm^{-1}. When the drying process was followed by Raman Spectroscopy at 480 cm^{-1} during the first 24 hours, the results showed that this process occurred in two phases. First stage showed a constant wavenumber around 6 to 12 hours while the solutions obtained equilibrium with the environment and started the drying process. In this first phase the unplasticized films

required half of the time than plasticized films to reach start retrogradation process. Second stage showed a change in intensity and is characterized by a change from liquid to gel form that also was observed during the drying kinetics. This could be associated to the addition of glycerol that changes the conformational order involving the formation of hydrogen bonds with starch and water

- The results obtained from the physical properties of the films showed the great impact of starch and glycerol in the film structure. The gloss of the films was related with the surface morphology. The higher the surface roughness, the lower the films gloss. The structure of films with higher starch concentration showed a smoother surface and the values of gloss increased form 30 to 48 to starch concentrations from 1 and 5% and these data were confirmed by stereomicroscopic images of the films. On the other hand when the glycerol concentration was increased from 0 to 50% the gloss values decreased from 37 to 25, in this case the decreasing of gloss values is due to physical exclusion of glycerol, above 40% the films showed a heterogeneous structure.
- Sorption studies on cassava starch films unplasticized and plasticized with glycerol exhibited a sigmoid shape Type II isotherm. Increasing the concentration of starch gave a result films with a greater level of hydration, especially at RH above 70%. Moreover, the successful modeling by BET and GAB (R^2=0.85 and 0.9, respectively) showed that the

presence of glycerol into the films changed the sorption profile and it is dependent on the relative humidity. These models were useful to calculate the monolayer values at different concentrations of cassava and glycerol. The most important relation found was that the monolayer valued increased with glycerol content, but at 20% glycerol content the monolayer value decreased notably. This behavior suggests the presence of minimum water content in these films.

- DSC measurements confirmed the effect of glycerol on starch gelatinization. As the concentration of glycerol increased, the gelatinization peak temperature increased, as well gelatinization enthalpy. Additionally, two equations were obtained by non-linear regression with R^2=0.98 that related the glycerol concentration with gelatinization temperature and enthalpy.
- Film formulation, mainly glycerol concentration, had a marked influence on mechanical properties. Glycerol behaved as a typical plasticizer in starchy films. In general, as the film structure softens, tensile strength decreases and elongation at break increases. A higher elongation indicates that the films are more flexible when subjected to mechanical stress. However, some antiplasticization was found in films with 10 and 20% glycerol indicating lower performing films.
- Based on these results obtained during this study, it is possible suggest how starch, water and glycerol interact when there is an increase in

glycerol ratio. We found a minimum film water sorption at around 20% glycerol, which indicates that, a mechanism when glycerol and water competes by binding sites (Carbon 1 and Carbon 6) of starch molecule. Also, observing the results from Rheology of solutions at 20% glycerol, the viscosity of these decreased considerably, showed that in the system there is more water available than in systems without glycerol. Moreover, the inclusion of glycerol modified the mechanical properties of films, decreasing the elongation at break at 20% glycerol, giving films more brittle than films without plasticizer. Therefore, the interaction of starch and glycerol at 20% plasticizer is greater than any other concentration, affecting the basic properties of films. In this sense, glycerol concentration less than 20% does not enhance the properties of the films and above 40% of glycerol we found physical exclusion of plasticizer. We expect that the concentration range of 30% glycerol allowed the incorporation of active compounds into the films, improving their physical properties.

3.2 Characterization of cassava starch films with glycerol enriched with Iron gluconate.

In this section, we will evaluate the possibility of using cassava starch films plasticized with glycerol as a film forming material to carry minerals such as iron gluconate (IG) and evaluate the basic properties of solutions and functionalities of films.

Recommendations for Iron are provided in the Dietary Reference Intakes (DRIs), developed by the Institute of Medicine of the National Academy of Sciences. They suggest the average daily intake of Iron is between 8 to 27 mg/day depending on the age and genre. Based on these numbers, our goal is to incorporate the maximum daily intake value, 27 mg/day that will be equivalent to 100% Iron fortification. Therefore, to observe how Iron changes the properties of films, it was incorporated in 5 different concentrations (20,40,60,80,100 % IG)

3.2.1 Effects of Iron gluconate in flow behavior of cassava starch films plasticized with glycerol

To compare the rheological behavior of cassava starch films with iron, the viscosity was measured under the same conditions of our previous studies with glycerol. The flow behavior, at 35°C of films at various concentrations of IG is shown in Figure 3.23. The marked points represented the average values of the experimental data of the rheograms. As reported previously, cassava starch based films with glycerol showed shear-thinning behavior, and the inclusion of iron did not change this behavior. The apparent viscosity of solutions increased as IG concentration increased. This indicates more intensive intermolecular association between water-starch-glycerol-iron. Also, it is possible observe at low shear rates (10 s^{-1}) the increase of the apparent viscosity is more marked with

values from 423.98 to 658.82 mPas for 0 and 100% IG concentration, respectively.

The comparative analysis realized concerning the rheological models showed before, indicate that Power Law model was the best in the studied models (R^2 between 0.97 to 0.99). And to evaluate how the Power Law parameters were affected with the incorporation of IG was plotted the consistency index and flow index Vs Iron concentration as shown in Figure 3.24. The apparent viscosity of films increased with the addition of IG from 875 to 1306 mPas for films with 0 to 100% IG, respectively. Also, the flow index of films decreased with the increasing of IG from 0.52 to 0.43 for films with 0 and 100% IG. Bircan and Barringer [81] correlated the increase in viscosity of maize starch on addition of sodium chloride to the strong starch-salt interaction, and suggested that this interaction leads to reduced mobility for the gelatinized starch leading to higher viscosity. Also, Jyothi [82] studied addition of ferrous sulphate. It enhanced the viscosity at lower concentrations and with increase in concentration of the salt, the viscosity values showed a gradual decrease. In this sense, our solutions are in these lower viscosities (0.025% w/w) and showed the same behavior.

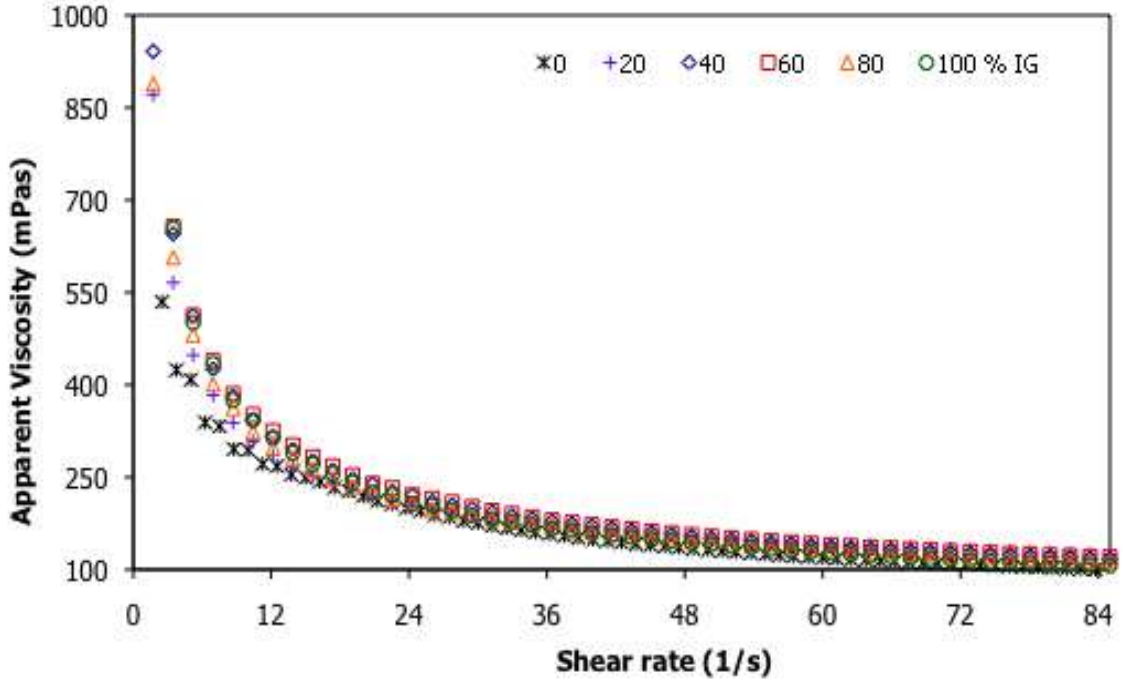


Figure 3.23 Apparent viscosity of cassava starch solutions with different IG content (0, 20, 40, 60, 80, 100%) at 35°C.

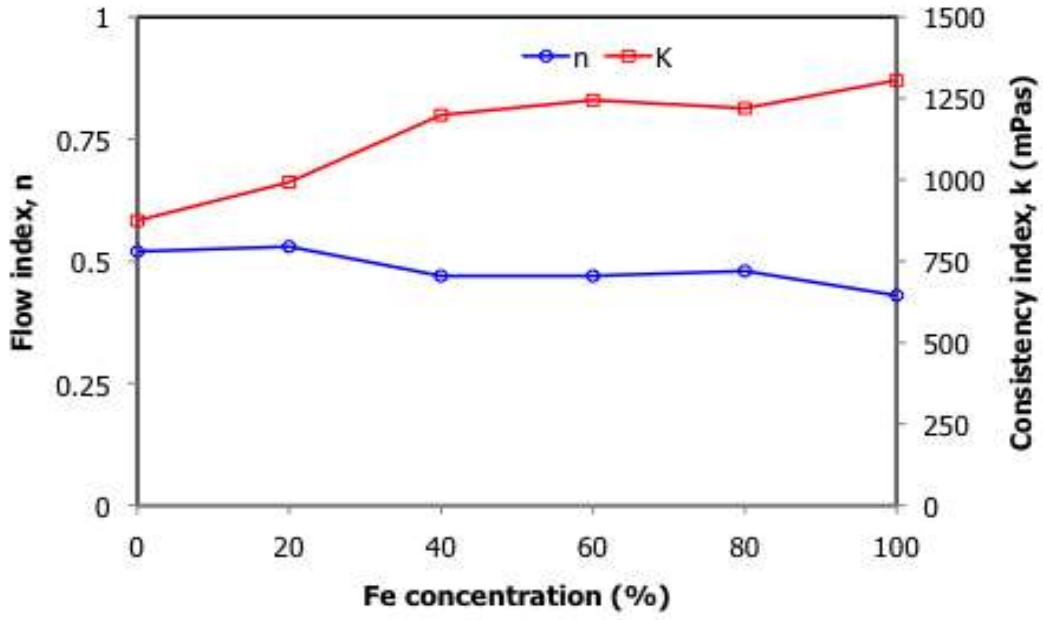


Figure 3.24 Evolution of apparent viscosity and flow index with Iron concentration. Blue line is the flow index and red line is the consistency index.

The effect of temperature on rheological behavior of solutions with iron is shown in Figure 3.25. As expected, the apparent viscosities of films decreased as temperature was increased. Although from the point of view of IG concentration, samples increased the apparent viscosity when IG was incorporated into the films. For instance, films at 85°C had apparent viscosities of 250.7 to 433.3 mPas with 0 to 100% IG.

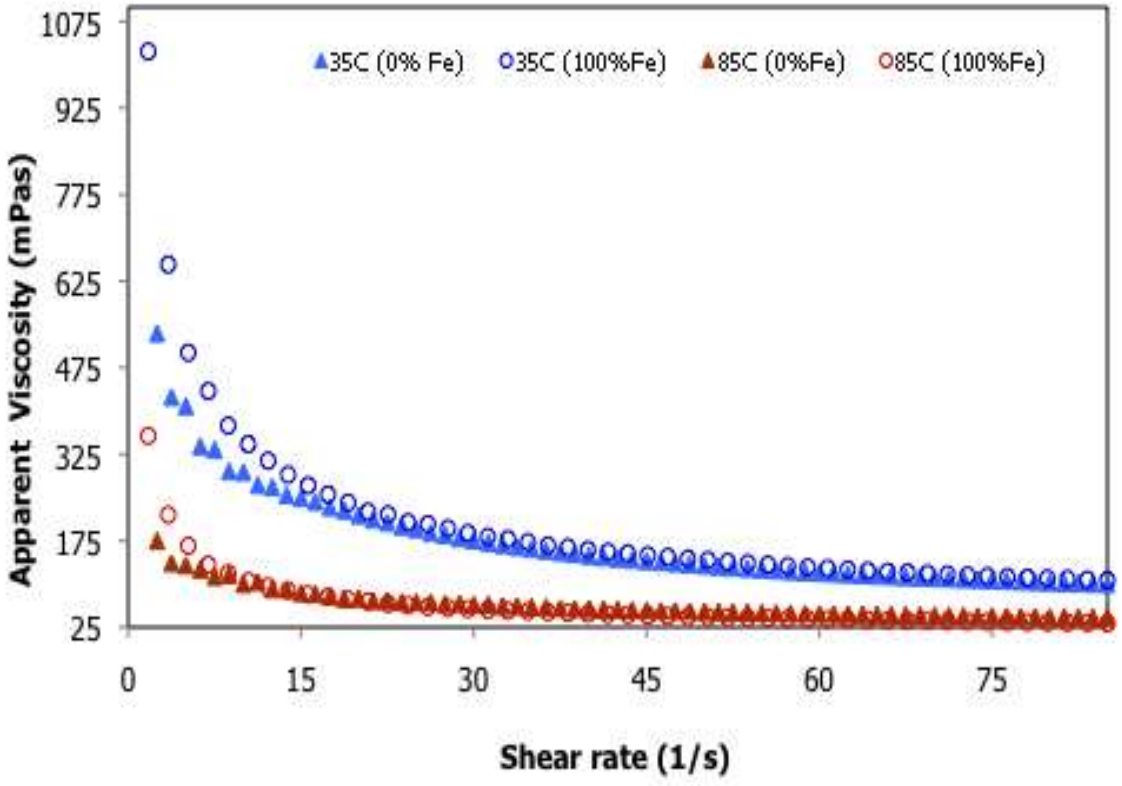


Figure 3.25 Effects of temperature on viscosity of cassava starch solutions with iron (0 and 100%)

3.2.2 Film color and appearance

Films obtained from all concentrations (20,40,60,80, and 100% IG) showed a homogeneous appearance, smooth surfaces without pores. Phase separation and insoluble particle were not detected in any of the films. However, the inclusion of IG affected color of films and the differences are shown in Figure 3.26. Color of films with different concentration of iron is expressed as L* (lightness), a* (redness/greenness) and b* (yellowness/blueness). Results demonstrated that b* value is probably the most important parameter describing the film color with IG due to the natural brownish color of ferrous gluconate. Therefore, b* values increased as the content of iron incorporated increased. L* and a* values were less influenced with the incorporation of IG into edible films. The a* values (3 to -1 for films with 0 and 100% Fe, respectively) obtained for all films were very low and close to 0 indicating neutrality in terms of red or green chromaticity. Difference in color lightness was no visually evident among the films, although some significant difference in L* values were measured (92 to 82 for films with 0 and 100% Fe, respectively).

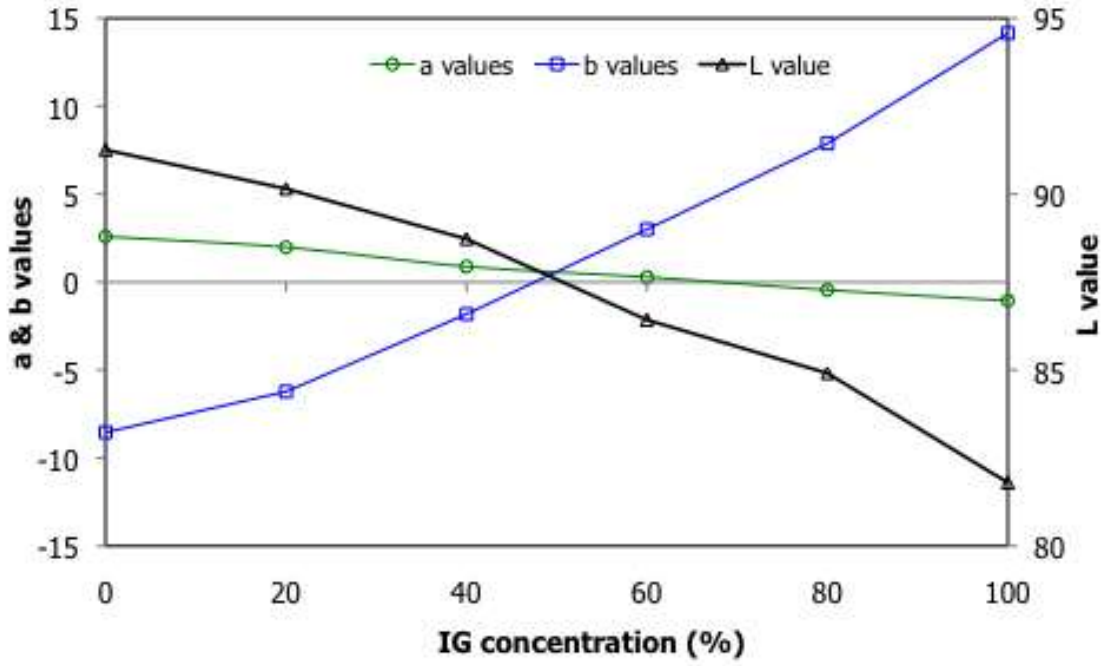


Figure 3.26 L, a* and b* values of cassava films incorporated with IG.*

3.2.3 Water sorption

Figure 3.26 shows the water sorption isotherms of cassava starch films with and without IG. These films needed around 52 Hrs to reach equilibrium. The concentration of IG was varied between 0 and 100%. The sorption isotherms gave the characteristic sigmoid shape type II isotherm curve similar to those found before for cassava starch films. As already mentioned, changes in water adsorption is influenced by storage relative humidity. Below 40% RH, the increase of IG concentration increases the water content of films. Above 40% RH, the level of hydration is opposite and the films with IG containing less water

than films without it. Therefore, the addition of iron compound decreased hydrophilicity of films, possibly because of hydroxyl groups of water and glycerol were saturated with IG and less water could be adsorbed in these sites. Moreover, at 40% IG concentration was found the presence of minimum water content, when the RH is around 65%.

The isotherms model used in this study and the calculated constant values are summarized in Table 3.7. Among other models tested, Hasley, Oswin and Smith models cannot be used to predict sorption behavior of iron films because R^2 values are below 0.9. Accordingly to this, BET and GAB model were found to be the best fit for predicting the equilibrium moisture content of films, because R^2 for these models are closer to 1. The results showed that the monolayer values for BET and GAB models were in the range of 0.0648-0.0437 and 0.0813-0.0520 g water/ g solids, respectively. As previously stated, the monolayer value is a good indicator or the maximum amount of water that could be adsorbed in a single layer per gram of dry film. These results showed that both, BET and GAB monolayer water contents (m_o), reported higher m_o for films with 0% IG than films with 20,40,60,80, and 100% Iron. Therefore, the incorporation of IG may cause a decreasing of water trapped into the films during this experiment, the hydrophilic sites of cassava starch films could interact more with IG and increase the interactions of film matrix, giving as result a film more compact.

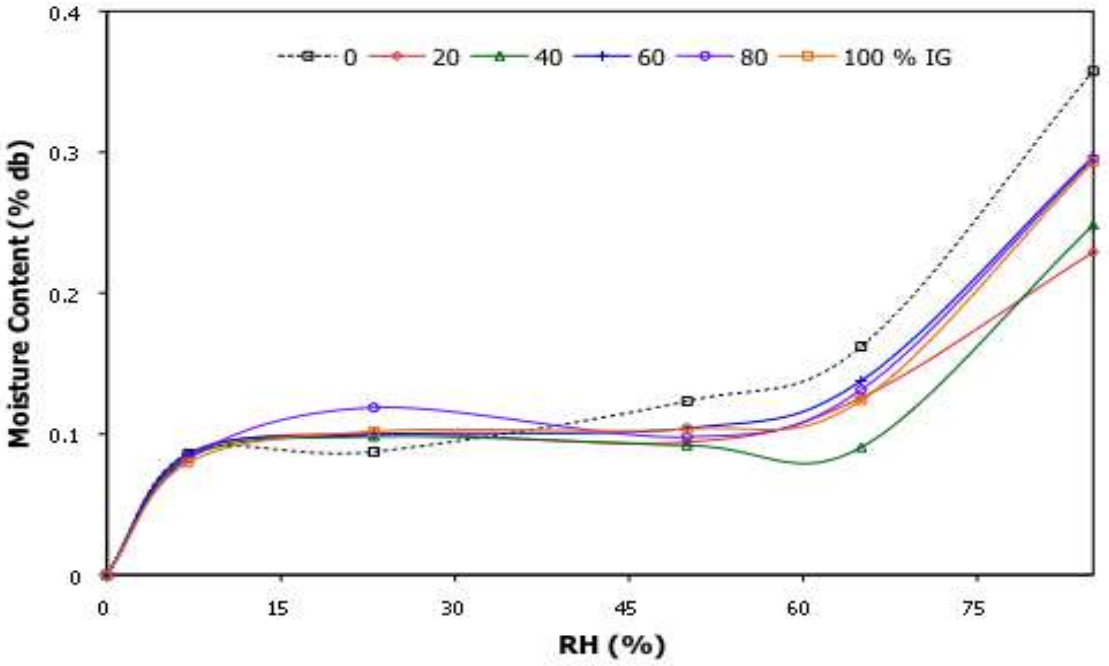


Figure 3.27 Sorption isotherm of cassava starch films with different IG concentration. (0 to 100%)

Table 3.7 Sorption isotherm model constants and confidence fit (R2) of cassava starch films (3%Cassava) with different iron contents.

Model	Constants	Iron gluconate content (%)					
		0	20	40	60	80	100
BET	m_o	0.0648	0.0370	0.0353	0.0453	0.0442	0.0437
	C	16.042	30.016	30.853	23.710	24.423	24.639
	R^2	0.9765	0.9622	0.9550	0.9904	0.9883	0.9866
GAB	m_o	0.0813	0.0527	0.0343	0.0542	0.0526	0.0520
	C	44.672	-24.919	22.607	-25.065	-18.104	-23.350
	k	0.9355	0.8914	0.8461	0.9473	0.9529	0.9448
	R^2	0.9361	0.9557	0.8461	0.9588	0.9063	0.9259
Halsey	A	-0.6384	-0.3316	-0.4216	-0.4216	-0.3990	-0.4214
	B	-2.1044	-2.2451	-2.1843	-2.1853	-2.1724	-2.2200
	R^2	0.9811	0.8199	0.6218	0.8549	0.7719	0.8384
Oswin	A	0.4094	0.2012	0.1945	0.2564	0.2594	0.2440
	B	0.1691	-2.0770	-2.1419	-1.9702	-2.0049	-1.9694
	R^2	0.9430	0.7162	0.5114	0.7491	0.7428	0.6837
Smith	A	0.0370	0.0662	0.0561	0.0552	0.0594	0.0523
	B	-0.1811	-0.0763	-0.0835	-0.1128	-0.1079	-0.0110
	R^2	0.9521	0.8749	0.7330	0.8796	0.8241	0.8542

3.2.4 Changes of thermal properties

DSC thermograms of cassava films with IG are shown in Figure 3.28. The thermograms of pure IG powder showed a peak at around 140°C that corresponds to melting point of component (data nor shown), however the films with IG did not show any changes at this temperature. Moreover, observing the peak around 75°C, that it is associated with gelatinization temperature of starch, had an impact with increasing of IG concentration.

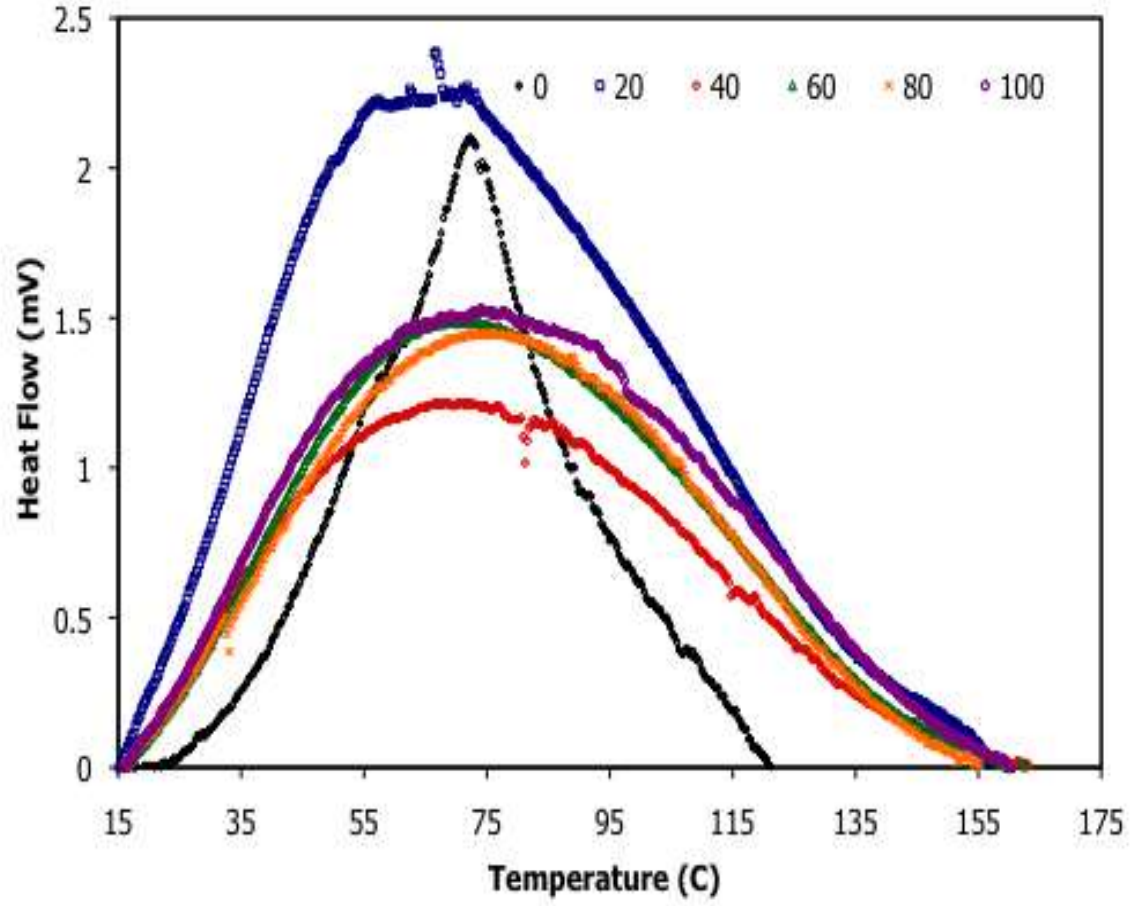


Figure 3.28 DSC thermograms of cassava-based films incorporated with Iron gluconate.

Films with IG showed the highest peak temperature at 100% Iron (Figure 3.29). At concentration of 0% IG the peak temperature was 73.55°C and when IG was increased around 20% the peak temperature decreased to 66.78°C. The peak temperature were raised from 66.78 to 76.06°C as the iron concentration was increased from 20 to 100% IG and the peak temperatures of 80 and 100% IG were still higher than those without added Iron. In the case of gelatinization enthalpy (∆Hg), when IG was added, ∆Hg increased from 23.72 to 33.294 KJ/Kg for films without IG and films with 20% IG, but the enthalpy associated with 40% IG decreased until 20.816 KJ/Kg and from this point the addition of IG increased the ∆Hg from 27.5 to 29.57 KJ/Kg for 60,80, and 100% IG, respectively. These resulted suggest that concentrations above 60% IG need greater energy to reach gelatinization of starch. Salts such as NaCl and CaCl2 have reported to cause and elevation or depression of gelatinization temperature and gelatinization enthalpy, depending on the types of salt and their concentration used (Ahmad & Williams, 1999, Jyothi et al., 2005). Jane, 1993 proposed that starch gelatinization in different salts seem to be controlled by two effects: water structure and electrostatic interaction between starch and ions.

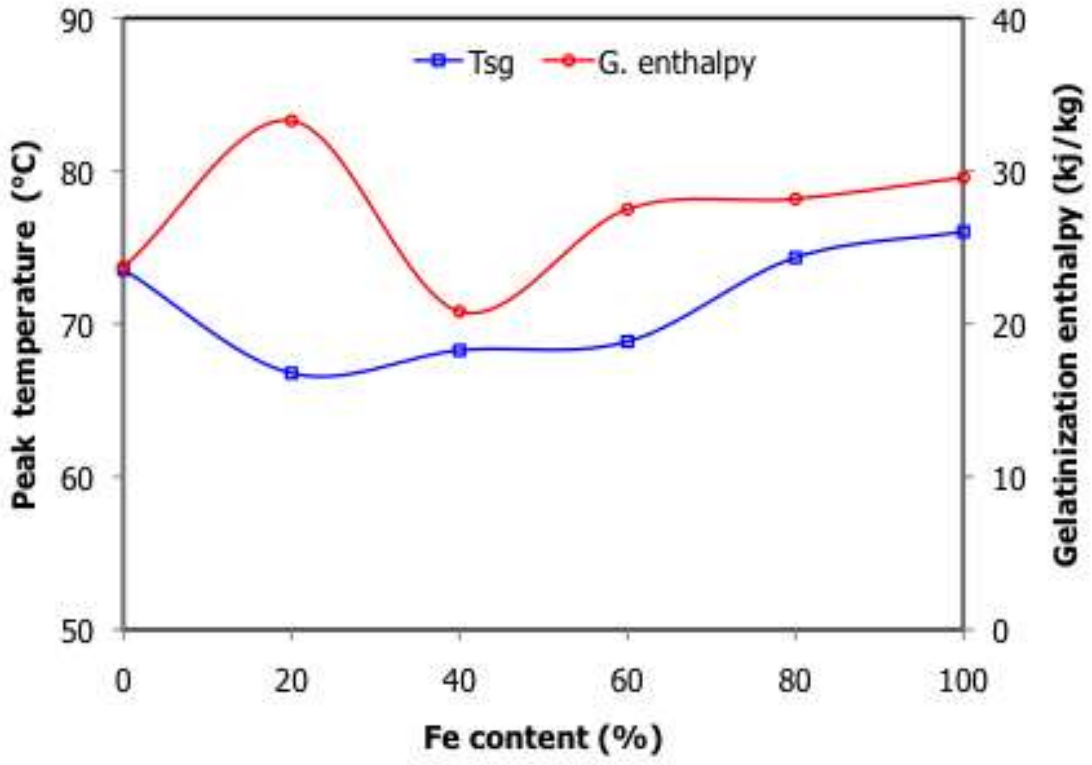


Figure 3.29 Starch gelatinization temperature and enthalpy for films with different Iron gluconate (0-100%) Blue line (Peak temperature), Red line (Enthalpy)

3.2.5 Mechanical properties

The tensile strength and elongation at break of films enriched with IG are shown in Table 3.8. The addition of IG to films increased the tensile strength form 1.79 to 2.61 MPa. For Elongation at break, the incorporation of IG significantly increased the stretchability of the films, improving the flexibility of films when these are subjected to mechanical stress (from 6.46 to 15.79%). The small increasing of tensile strength of the films with increasing concentration of IG could be attributed to the formation of intermolecular interaction between the

hydroxyl groups of starch, glycerol and IG. Intermolecular interaction between those resulted in a compact molecule structure. In the other hand, the values of elongation at break were increased especially when the concentration of IG were 20, 40 and 80%. This behavior may be explained by the plasticization effects of small molecules acting as fillers to reduce molecular reactions. This result are similar to that found by Park and Zhao [55] when the incorporation of Zinc in chitosan films strengthened the film matrix.

Table 3.8 Mechanical properties of cassava-starch film incorporated with Iron gluconate

% IG	Thickness (μm)	Tensile strength (MPa)	Elongation at break (%)
0	81.37	1.79	6.46
20	81.37	2.04	15.78
40	87.00	2.26	15.79
60	86.00	2.47	11.58
80	89.87	2.41	15.79
100	87.88	2.61	12.63

3.2.6 IG release kinetics

Release rate for all concentration was studied (in triplicate) during 6 hours. The plot of cumulative percentage released Vs time is shown in Fig 3.29. From the graph, it could be concluded that the maximum release of IG was around 15% during 6 hours of experiment (100%IG).

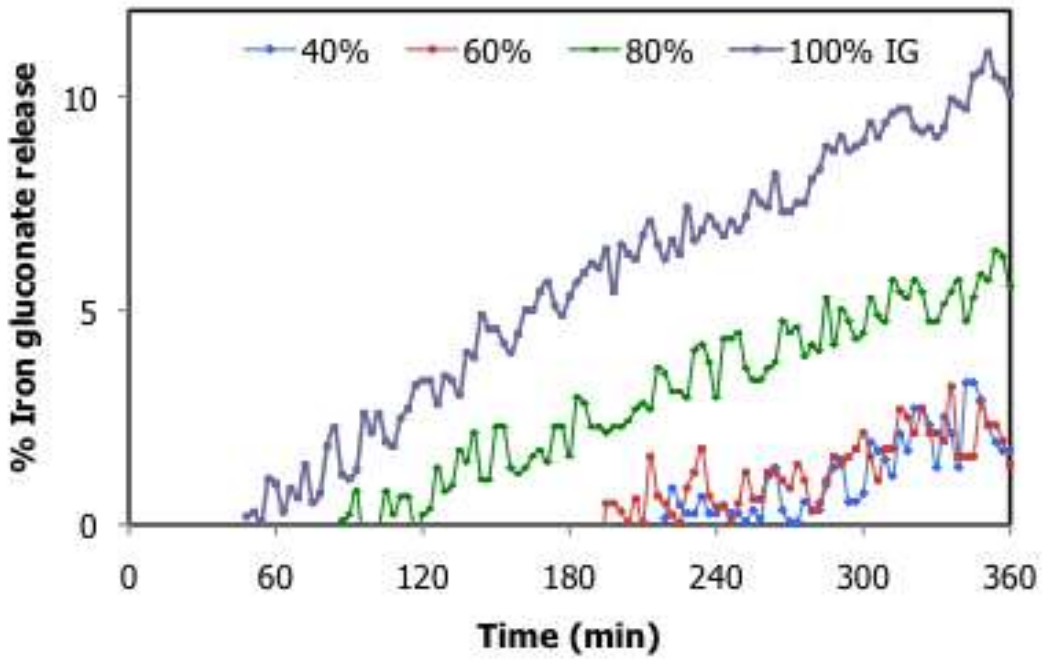


Figure 3.30 Iron gluconate release profile from cassava-glycerol films.

Further, to understand the drug release mechanism, the data were fitted to zero, first, Higuchi and Korsmayer-Peppas equations as reported above (Table 3.9). Considering R^2, the calculated Zero order and First order models obtained values between 0.901 and 0.979. Also, from the table, it is concluded that all the IG concentration followed the Higuchi model because R^2 are 0.931 and 0.978, indicating the release of drug from matrix as a square root of time dependent process based on Fickian diffusion [50]. In the other hand, when the data of 80 and 100% IG were fitted to Korsmayer-Pepas where n is the diffusional exponent, which characterizes the drug transport mechanism, therefore it is

possible to characterize different release mechanisms such as: Fickian diffusion (n< 0.5); Anomalous transport (0.5 < n < 1.0), Case-II transport (n=1) and Super Case-II transport (n > 1.0) [83]. In this case, n is 1.247 and 1.856 for 80 and 100% IG, suggesting that more that one mechanism may be involve in the release kinetics. Nevertheless, looking at R^2 values for 80 and 100% IG are between 0.81 and 0.92, and no definitive conclusion can be drawn concerning the dominating release mechanism.

Table 3.9 Dissolution parameters for IG concentration between 40 and 100%

Model	Constants	Iron gluconate content (%)			
		40	**60**	**80**	**100**
Zero order $Q_t = Q_0 + K_0 t$	K_o	0.0207	0.0205	0.0252	0.0351
	R^2	0.903	0.903	0.956	0.975
First order $LnQ_t = LnQ_0 + K_0 t$	K_o	0.0002	0.0002	0.0003	0.0004
	R^2	0.0905	0.901	0.979	0.959
Higuchi $Q_t = K_H \sqrt{t}$	K_H	0.500	0.4938	0.599	0.830
	R^2	0.935	0.931	0.971	0.978
Korsmeyer-Peppas $Q_t / Q_0 = K_k t^n$	K_k			1.247	1.856
	R^2			0.817	0.926

Where *Q* is the drug release in time *t*, *Qo* is the initial amount of drug in solution, *K* is the release constant, and n is the release exponent.

3.2.7 Conclusion

The effects of incorporation of Iron gluconate are concludes as follow:

- In general, the changes showed by rheology, moisture sorption, and thermal studies suggested an interaction between starch granules and iron ions present in IG. Cassava starch does not contain any lipids, proteins or fibers, which can interact with other component and change the physical properties of solutions and films.
- Cassava-glycerol solutions with and without IG exhibited a shear-thinning behavior within the temperatures studied (35 to 85°C). The best model that described the flow behavior of solutions with IG was Power Law model (R^2=0.97 and 0.99). In relation on how IG changed the viscosity of solution we concluded that the addition of IG enhance viscosity for all concentrations, suggesting that the interaction between IG and the other components reduced mobility of starch.
- Results demonstrated that b* value is probably the most important parameter describing the film color with IG due to the natural brownish color of ferrous gluconate.
- In the other hand, the sorption water properties of the films were significantly diminished by the incorporation of IG. The effect of IG addition could be explained by the increasing interactions between Iron and another components. IG ions interact with adjacent molecules and produce a stronger matrix, thus resulting in a decrease the hydrophilic tendency of starch films. Also, when is observed the m_o (monolayer value) for BET and GAB models, it is clear that less water is adsorbed on the film

when IG was incorporated into the film matrix, and this m_o was kept relatively constant between 0.04 for BET model and 0.05. *Park and Zhao [55]* confirmed that the incorporation of minerals such as Zinc and Calcium into Chitosan films decreased the hydrophilic tendency of it, and concluded that these minerals could act as fillers into the matrix.

- IG behaved as a typical plasticizer in starchy films. In general, as the film structure softens, tensile strength increases and elongation at break increases. A higher elongation indicates that the films are more flexible when subjected to mechanical stress.
- IG release kinetics of the films correspond best to Higuchi model (R^2 are between 0.931 and 0.978) suggesting that the mechanism present is Fickian diffusion. However IG release mechanism using Korsmeyer-Peppas model to predict n value cannot be verified clearly because the values of R^2 were not close to 1. Consequently, the release mechanism can involve more than one (swelling, diffusion and erosion).

4 General conclusion

The main objective of the present work was to investigate the preparation of edible films from biomaterials. The first stage was to evaluate the individual and interactive effects of glycerol and cassava starch concentration to obtain a film with good properties to carry active compounds in on it. The second stage was the incorporation of Iron gluconate into these films and quantifies the effects of it.

In summary, the cassava starch films using different glycerol concentration showed interesting characteristics. In general, Homogeneous, smooth and translucent films were obtained by casting method. Glycerol was found to be a suitable plasticizer to incorporate into starch films. And based in the results obtained, we found that a good formulation to incorporate nutraceutical into starch films is 3% cassava, 30% glycerol and 97% water.

The incorporation of Iron gluconate into the cassava-glycerol matrix affected some properties of films. Appearance was highly influenced because of changing of film color from transparent to yellowish films. In general, films with IG increased the elongation at break and viscosity, demonstrated that IG formed interactions with starch, water and glycerol. The release kinetics was conduced

by dissolution method, however the mechanism of release cannot be concluded at all.

5 Future work

It is recommended that the starch-glycerol-iron films will be further investigated. Some other possibilities for improvement may be considered, such as: the study of their barrier properties to compare the development of the iron films with the packaging films used currently in the industry. Also, investigate the possibility of incorporation of another micronutrients with low DRI value to be carried with iron and that enhance the physical properties of it. Additionally, conduct the sensory analysis of these films and evaluate the consumer perception and liking. Lastly, in terms of the film production technique, more research is needed for a future scale-up to a pilot plant to determine the production and drying process.

6 References

1. Tonukari, N.J. *Cassava and the future of starch*. 2004.
2. Lee, D.S., K.L. Yam, and L. Piergiovanni, *Food packaging science and technology*. 2008, Boca Raton: CRC Press.
3. Weber, C.J., et al., *Production and applications of biobased packaging materials for the food industry.* Food Additives and Contaminants, 2002. **19**: p. 172-177.
4. Gennadios, A., *Protein-based films and coatings*. 2002, Boca Raton: CRC Press.
5. Han, J.H., *Innovations in food packaging*. 2005, San Diego, Calif.; Oxford: Elsevier Academic ; Elsevier Science [distributor].
6. Robertson, G.L., *Food packaging : principles and practice*. 2006, Boca Raton, FL: Taylor & Francis/CRC Press.
7. Weber, C.J., *Biobased packaging materials for the food industry : status and perspectives : a european concerted action*. 2000, Frederiksberg: KVL Department of Dairy and Food Science.
8. Bourtoom, T., *Edible films and coatings: Characteristics and properties.* Int. Food Res. J. International Food Research Journal, 2008. **15**(3): p. 237-248.

9. Krochta, J.M. and C. DeMulderJohnston, *Edible and biodegradable polymer films: Challenges and opportunities.* Food Technology, 1997. **51**(2): p. 61-74.

10. Galliard, T. and I. Society of Chemical, *Starch--properties and potential*. 1987, Chichester [England]; New York: Published for the Society of Chemical Industry by Wiley.

11. Wang, T.L., T.Y. Bogracheva, and C.L. Hedley, *Starch: as simple as A, B, C?* Journal of Experimental Botany, 1998. **49**(320): p. 481-502.

12. Thomas, D.J., W.A. Atwell, and C. American Association of Cereal, *Starches*. 1999: Eagan Press.

13. Jobling, S., *Improving starch for food and industrial applications.* Current opinion in plant biology, 2004. **7**(2): p. 210-8.

14. Gallant, D.J., B. Bouchet, and P.M. Baldwin, *Microscopy of starch: Evidence of a new level of granule organization.* Carbohydrate Polymers, 1997. **32**(3-4): p. 177-191.

15. Jenkins, P.J. and A.M. Donald, *The influence of amylose on starch granule structure.* International journal of biological macromolecules, 1995. **17**(6): p. 315-21.

16. Biliaderis, C.G., T.J. Maurice, and J.R. Vose, *STARCH GELATINIZATION PHENOMENA STUDIED BY DIFFERENTIAL SCANNING CALORIMETRY.* J Food Science Journal of Food Science, 1980. **45**(6): p. 1669-1674.

17. Bogracheva, T.Y., et al., *Structural studies of starches with different water contents.* Biopolymers, 2002. **64**(5): p. 268-81.

18. Purdue University. Center for New, C. and P. Plant. *NewCROP the New Crop resource online program*. 1995; Available from: http://www.hort.purdue.edu/newcrop/.

19. Balagopalan, C., *Cassava in food, feed, and industry*. 1988, Florida: CRC Press, Inc.

20. Validation Forum On The Global Cassava Development, S., *The global cassava development strategy and implementation plan*. 2000, Food and agriculture organization of the United nations international funds for agricultural development, v.1.

21. Ackermann, P., et al. *Foods and packaging materials : chemical interactions*. 1995. Cambridge: Royal Society of Chemistry.

22. Chillo, S., et al., *Influence of glycerol and chitosan on tapioca starch-based edible film properties.* J Food Eng Journal of Food Engineering, 2008. **88**(2): p. 159-168.

23. Embuscado, M.E. and K.C. Huber. *Edible films and coatings for food applications*. 2009; Available from: http://public.eblib.com/EBLPublic/PublicView.do?ptiID=603144.

24. Zeisel, S.H., *Regualtion of "Nutraceuticals".* Journal Association of food and drug officals, 1999. **63**: p. 26-31.

25. Dureja, H., D. Kaushik, and V. Kumar, *Developments in nutraceuticals.* INDIAN JOURNAL OF PHARMACOLOGY, 2003. **35**: p. 363-372.

26. United States. Dept. of, A. *2010 dietary guidelines for Americans backgrounder, history and process*. 2010; Available from: http://purl.fdlp.gov/GPO/gpo4085.

27. Yehuda, S. and D.I. Mostofsky. *Iron deficiency and overload from basic biology to clinical medicine*. 2010.

28. Reilly, C., *The nutritional trace metals*. 2004, Oxford, OX, UK; Ames, IA, USA: Blackwell Pub.

29. Rindlavwestling, A., et al., *Structure, mechanical and barrier properties of amylose and amylopectin films.* Carbohydrate Polymers Carbohydrate Polymers, 1998. **36**(2-3): p. 217-224.

30. Abdelrahim, K.A., H.S. Ramaswamy, and F.R. van de Voort, *Rheological properties of starch solutions under aseptic processing temperatures.* Food Research International, 1995. **28**(5): p. 473-480.

31. Brookfield Engineering, L., *More solutions to sticky problems : a guide to getting more from your Brookfield Viscometer*. 1995, Stoughton, Mass: The Laboratory.

32. Singh, R.P., & Heldman, Dennis R, *Introduction to Food Engineering*. 2009: Academic Pr.

33. Karim, A.A., M.H. Norziah, and C.C. Seow, *Methods for the study of starch retrogradation.* Food chemistry., 2000. **71**(1): p. 9-36.

34. Pelletier, M.J., *Analytical applications of Raman spectroscopy*. 1999, Osney Mead, Oxford; Malden, MA: Blackwell Science.

35. Li-Chan, E.C.Y., *The applications of Raman spectroscopy in food science.* Trends in food science & technology., 1996. **7**(11): p. 361.

36. Fechner, P.M., et al., *Influence of Water on Molecular and Morphological Structure of Various Starches and Starch Derivatives.* STARCH - STUTTGART-, 2005. **57**(12): p. 605-615.

37. 08e1, A.S.D.-. *Standard test method for specular gloss of plastic films and solid plastics.* ASTM International, West Conshohocken, PA, 2008.

38. Elias, H.-G., *An introduction to plastics*. 1993, Weinheim; New York: VCH.

39. Ward, G. and A. Nussinovitch, *Gloss properties and surface morphology relationships of fruits.* Journal of Food Science, 1996. **61**(5): p. 973-977.

40. D523, A.S., *Garder Gloss.* ASTM International, West Conshohocken, PA, 1999.

41. Tosun, I. *Color changes and 5-hydroxymethyl furfural formation in zile pekmezi during storage*. 2004; Available from: http://grasasyaceites.revistas.csic.es/index.php/grasasyaceites/article/view/174/174.

42. Brunauer, S., et al., *On a Theory of the van der Waals Adsorption of Gases.* Journal of the American Chemical Society, 1940. **62**(7): p. 1723-1732.

43. DeMan, J.M. *Principles of food chemistry*. 1999.

44. Srinivasa, P.C., et al., *Storage studies of mango packed using biodegradable chitosan film.* European Food Research and Technology, 2002. **215**(6): p. 504-508.

45. Singh, J. and N. Singh, *Studies on the morphological, thermal and rheological properties of starch separated from some Indian potato cultivars.* Food chemistry., 2001. **75**(1): p. 67-77.

46. Yang, L. and A.T. Paulson, *Effects of lipids on mechanical and moisture barrier properties of edible gellan film.* Food Research International, 2000. **33**(7): p. 571-578.

47. McHugh, T.H. and J.M. Krochta, *Sorbitol- vs Glycerol-Plasticized Whey Protein Edible Films: Integrated Oxygen Permeability and Tensile Property Evaluation.* J. Agric. Food Chem. Journal of Agricultural and Food Chemistry, 1994. **42**(4): p. 841-845.

48. Wypych, G. *Handbook of plasticizers*. 2004; Available from: http://www.knovel.com/knovel2/Toc.jsp?BookID=1010.

49. Flory, P.J., *Principles of polymer chemistry*. 1953, Ithaca: Cornell University Press.

50. Costa, F.O., et al., *Comparison of dissolution profiles of Ibuprofen pellets.* Journal of Controlled Release, 2003. **89**(2): p. 199-212.

51. Mali, S., et al., *Water sorption and mechanical properties of cassava starch films and their relation to plasticizing effect.* Carbohydrate Polymers, 2005. **60**(3): p. 283-289.

52. Flores, S., et al., *Physical properties of tapioca-starch edible films: Influence of filmmaking and potassium sorbate.* Food Research International, 2007. **40**(2): p. 257-265.

53. Fama, L., et al., *Mechanical properties of tapioca-starch edible films containing sorbates.* Lwt-Food Science and Technology, 2005. **38**(6): p. 631-639.

54. Paes, S.S., I. Yakimets, and J.R. Mitchell, *Influence of gelatinization process on functional properties of cassava starch films.* Food Hydrocolloids, 2008. **22**(5): p. 788-797.

55. Park, S.I. and Y. Zhao, *Incorporation of a high concentration of mineral or vitamin into chitosan-based films.* Journal of agricultural and food chemistry, 2004. **52**(7): p. 1933-9.

56. Mei, Y. and Y. Zhao, *Barrier and mechanical properties of milk protein-based edible films containing nutraceuticals.* Journal of agricultural and food chemistry, 2003. **51**(7): p. 1914-8.

57. Chhabra, R.P. and J.F. Richardson. *Non-Newtonian flow and applied rheology engineering applications*. 2008; Available from: http://www.knovel.com/knovel2/Toc.jsp?BookID=2756.

58. Rockland, L.B., *MOISTURE SORPTION - PRACTICAL ASPECTS OF ISOTHERM MEASUREMENT AND USE - LABUZA,TP.* Food Technology, 1984. **38**(7): p. 112-112.

59. Perdomo, J., et al., *Glass transition temperatures and water sorption isotherms of cassava starch.* Carbohydrate Polymers, 2009. **76**(2): p. 305-313.

60. D412-98a, A.S., *Standard test methods for thermplastic rubbers and thermoplastic elastomers-tension.* ASTM International, West Conshohocken, PA, 1998.

61. Repka, M.A., et al., *Characterization of cellulosic hot-melt extruded films containing lidocaine.* European Journal of Pharmaceutics and Biopharmaceutics, 2005. **59**(1): p. 189-196.

62. Shoaib, H.M., *Evaluation of drug release kinetics from ibuprofen matrix tablets using HPMC.* J. Pharm. Sci., 2006. **19**(2): p. 119-124.

63. Nurul I, M., B.M.N. Mohd. Azemi, and D.M.A. Manan, *Rheological behaviour of sago (Metroxylon sagu) starch paste.* Food Chemistry, 1999. **64**(4): p. 501-505.

64. Lagarrigue, S. and G. Alvarez, *The rheology of starch dispersions at high temperatures and high shear rates: a review.* Journal of Food Engineering, 2001. **50**(4): p. 189-202.

65. Sopade, P.A. and K. Kiaka, *Rheology and microstructure of sago starch from Papua New Guinea.* Journal of Food Engineering, 2001. **50**(1): p. 47-57.

66. Steward, P.A., J. Hearn, and M.C. Wilkinson, *An overview of polymer latex film formation and properties.* Advances in Colloid and Interface Science, 2000. **86**(3): p. 195-267.

67. Gu, Z.Y. and P. Alexandridis, *Drying of films formed by ordered poly(ethylene oxide)-poly(propylene oxide) block copolymer gels.* Langmuir, 2005. **21**(5): p. 1806-1817.

68. Thakhiew, W., S. Devahastin, and S. Soponronnarit, *Effects of drying methods and plasticizer concentration on some physical and mechanical properties of edible chitosan films.* Journal of Food Engineering, 2010. **99**(2): p. 216-224.

69. Van Soest, J.J.G., et al., *Retrogradation of Potato Starch as Studied by Fourier Transform Infrared Spectroscopy.* Die St‰orke = Starch., 1994. **46**(12): p. 453.

70. Chang, Y.P., P.B. Cheah, and C.C. Seow, *Plasticizing-antiplasticizing effects of water on physical properties of tapioca starch films in the glassy state.* Journal of Food Science, 2000. **65**(3): p. 445-451.

71. Lourdin, D., et al., *Influence of equilibrium relative humidity and plasticizer concentration on the water content and glass transition of starch materials.* Polymer, 1997. **38**(21): p. 5401-5406.

72. Chang, Y.P., A.A. Karim, and C.C. Seow, *Interactive plasticizing-antiplasticizing effects of water and glycerol on the tensile properties of tapioca starch films.* Food Hydrocolloids, 2006. **20**(1): p. 1-8.

73. The, D.P., et al., *Influence of hydrocolloid nature on the structure and functional properties of emulsified edible films.* Food Hydrocolloids, 2009. **23**(3): p. 691-699.

74. Mathew, A.P. and A. Dufresne, *Plasticized waxy maize starch: Effect of polyols and relative humidity on material properties.* Biomacromolecules, 2002. **3**(5): p. 1101-1108.

75. Godbillot, L., et al., *Analysis of water binding in starch plasticized films.* Food Chemistry, 2006. **96**(3): p. 380-386.

76. Habitante, A., et al., *Phase transitions of cassava starch dispersions prepared with glycerol solutions.* Journal of Thermal Analysis and Calorimetry, 2008. **93**(2): p. 599-604.

77. Hˆhne, G.W.H., W.F. Hemminger, and H.J. Flammersheim, *Differential Scanning Calorimetry*. 2003, Berlin [etc.]: Springer.

78. Wasserman, L.A., et al., *Preparation of wheat resistant starch - Treatment of gels and DSC characterization.* Journal of Thermal Analysis and Calorimetry, 2007. **87**(1): p. 153-157.

79. Gaudin, S., et al., *Antiplasticisation and oxygen permeability of starch,Äìsorbitol films.* Carbohydrate Polymers, 2000. **43**(1): p. 33-37.

80. Habeych, E., et al., *On the applicability of FloryHuggins theory to ternary starchwatersolute systems.* Carbohydrate Polymers Carbohydrate Polymers, 2009. **77**(4): p. 703-712.

81. Bircan, C. and S.A. Barringer, *Salt-Starch Interactions as Evidenced by Viscosity and Dielectric Property Measurements.* Journal of Food Science, 1998. **63**(6): p. 983-986.

82. Jyothi, A.N., et al., *Gelatinisation Properties of Cassava Starch in the Presence of Salts, Acids and Oxidising Agents.* Die St‰orke = Starch., 2005. **57**(11): p. 547.

83. Goyal, A., *Factors influencing drug release characteristics from hydrophillic polymer.* Asian Journal of Pharmaceutical and Clinical Research, 2009. **2**(1).